ABSORPTION BANDWIDTHS FOR

CARBON DIOXIDE

GAS

By

CHARLES ALFRED MORGAN, JR.

Bachelor of Science
Southern Methodist University
1961

Master of Science
Oklahoma State University
1963

Submitted to the
Faculty of the Graduate College of the
Oklahoma State University in partial
fulfillment of the requirements
for the degree of
DOCTOR OF PHILOSOPHY
May, 1966

ABSORPTION BANDWIDTHS FOR

CARBON DIOXIDE

GAS

Thesis Approved:

J. A. Wiebelt
Thesis Adviser

J. R. Haworth

E. K. McLaughlan

E. E. Koch

J. H. Boggs
Dean of the Graduate School

ACKNOWLEDGMENTS

The author wishes to acknowledge the assistance, support, and encouragement received during the course of his graduate studies.

For help in topic selection and encouragement to see the problem through to a solution, I wish to acknowledge the assistance of my committee chairman and thesis adviser, Dr. J. A. Wiebelt. To the rest of my thesis committee, Dr. D. R. Haworth, Dr. E. E. Kohnke, and Dr. E. K. McLachlan, I wish to express my appreciation of their guidance and constructive criticism.

I am appreciative of the influence on my graduate studies of many others: Dr. M. K. Jovanovic and Dr. J. P. Holman are two of the many who should be mentioned.

Finally, I wish to acknowledge the continuous support and encouragement of my wife, Nancy.

TABLE OF CONTENTS

TABLE OF CONTENTS (CONTINUED)

LIST OF TABLES

LIST OF FIGURES

LIST OF FIGURES (CONTINUED)

LIST OF FIGURES (CONTINUED)

CHAPTER I

INTRODUCTION

A need to calculate the surface heat transfer due to radiation exists in thermal analyses of furnaces, fuel combustion chambers, and other enclosures subjected to a high temperature environment. If the enclosure contains a gas which emits and absorbs radiant energy, the effect of the gas on the surface heat transfer must be considered.

In this thesis are presented the results of an analytical study of the variation of absorption bandwidths of carbon dioxide-nitrogen gas mixtures with gas properties. More specifically, correlations are presented of the band absorption and band absorption divided by absorption bandwidth for the 15.0, 4.3, 2.7,and 2.0 micron absorption bands of a gaseous mixture of carbon dioxide and nitrogen at various gas temperatures and gas pressures, and for various amounts of the mixture.

The two correlated quantities, band absorption and band absorption divided by absorption bandwidth, allow calculation of absorption bandwidth. That this property is

relevant to the calculation of radiant heat transfer is illustrated in this introductory chapter. This is done by briefly developing and presenting the equations of radiant energy transfer.

First, monochromatic equations are briefly developed and presented. Difficulties in the utilization of these monochromatic equations are known to be reduced if the equations are reformulated so as to apply to a band of frequencies, this band of frequencies being either the region of a gas absorption band, or, a region of frequencies wherein the gas is perfectly transmitting. Therefore, "band" equations are also briefly developed and presented, and, serve to indicate the utility of the absorption bandwidth correlations presented in this thesis.

Equations of Monochromatic Radiant Energy Transfer

Consider an enclosure composed of M distinct surfaces, as shown in Figure 1. Let the surfaces be numbered 1 through M. The enclosure is assumed to contain a gas which participates in radiative exchange, i.e., a participating gas. The monochromatic radiant heat transfer per unit area and per unit time to the j^{th} surface of the enclosure is given by Wiebelt (1)* as

*Single Arabic numbers in parentheses refer to references in Bibliography.

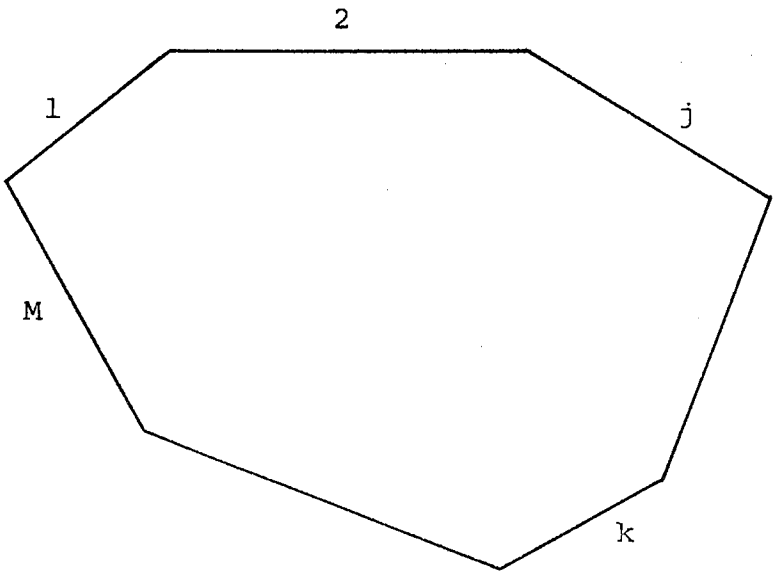

Figure 1. An Enclosure with M Surfaces

$$q_{j\nu} = \frac{\alpha_{j\nu} J_{j\nu} - \epsilon_{j\nu} E_{bj\nu}}{\rho_{j\nu}}, \quad j = 1,2, \ldots, M \qquad \text{(I-1)}$$

In Equation (I-1) the subscript ν, wavenumber, is used in place of f, frequency. The wavenumber of radiated energy is related to the frequency of radiated energy by the expression $\nu = f/c$ where c is the velocity of light. Wavenumber may also be related to the wavelength, λ, of radiated energy using the expression $c = \lambda f$. The result is

$$\nu = \frac{1}{c} \cdot \frac{c}{\lambda} = \frac{1}{\lambda}$$

The terms in Equation (I-1) may now be said to have values valid in the wavenumber region ν to $\nu + d\nu$, where $d\nu$ is a differential increment of wavenumber. The subscript j on each of the terms in Equation (I-1) indicates that each term applies to the $j^{\underline{th}}$ surface.

The terms in Equation (I-1) are:

$q_{j\nu}$ = monochromatic heat transfer per unit area to the $j^{\underline{th}}$ surface

$\alpha_{j\nu}$ = monochromatic absorptance of the $j^{\underline{th}}$ surface

$\epsilon_{j\nu}$ = monochromatic emittance of the $j^{\underline{th}}$ surface

$\rho_{j\nu}$ = monochromatic reflectance of the $j^{\underline{th}}$ surface

$J_{j\nu}$ = monochromatic radiosity of the $j^{\underline{th}}$ surface

$E_{bj\nu}$ = monochromatic black-body emissive power of the $j^{\underline{th}}$ surface.

The properties $\alpha_{j\nu}$ and $\rho_{j\nu}$, from their definitions, are related by the expression $\alpha_{j\nu} + \rho_{j\nu} = 1$, assuming the $j^{\underline{th}}$ surface is opaque. Also it is assumed that $\epsilon_{j\nu} = \alpha_{j\nu}$, i.e., radiative equilibrium, see Kourganoff (2) and Viskanta (3), of the $j^{\underline{th}}$ surface is assumed. The monochromatic radiosity of the $j^{\underline{th}}$ surface, $J_{j\nu}$, is defined as all of the monochromatic energy leaving the $j^{\underline{th}}$ surface per unit area and per unit time. Mathematically, this may be expressed as the sum of the reflected monochromatic energy plus the emitted monochromatic energy leaving surface j (1):

$$J_{j\nu} = \rho_{j\nu} G_{j\nu} + \epsilon_{j\nu} E_{bj\nu} \qquad \text{(I-2)}$$

In Equation (I-2), $G_{j\nu}$ is the monochromatic irradiation of the $j^{\underline{th}}$ surface, i.e., all the monochromatic energy per unit area and per unit time arriving at surface j. The monochromatic black-body emissive power of the $j^{\underline{th}}$ surface, $E_{bj\nu}$, is defined by Planck's equation,

$$E_{bj\nu} = \frac{c_1 \nu^3}{\left[\exp\left(\frac{c_2 \nu}{T}\right)\right] - 1}$$

$$c_1 = 1.1855 \times 10^{-8} \frac{\text{Btu}}{\text{hr} - \text{ft}^2 - (\text{cm}^{-1})^4} \qquad \text{(I-3)}$$

$$c_2 = 2.5884 \text{ cm} - {}^{\circ}\text{R},$$

where the units of the constants c_1 and c_2 indicate that the units of wavenumber, ν, are inverse centimeters, cm^{-1}, and the units of the temperature of the $j^{\underline{th}}$ surface, T_j,

are degrees Rankine.

In order to use Equation (I-1), surface radiative property data are required, as is $J_{j\nu}$ and $E_{bj\nu}$. It is assumed in this study that surface property data are available. If the surfaces of the enclosure are assumed to have known temperatures, T_j, $j = 1,2, \ldots, M$, then, Equation (I-3) may be used to evaluate $E_{bj\nu}$. The only remaining unknown in Equation (I-1), other than $q_{j\nu}$, is $J_{j\nu}$. Therefore, expressions allowing the determination of $J_{j\nu}$, $j = 1,2,\ldots,M$, must be developed.

Equation (I-2) may be used to calculate $J_{j\nu}$ if an expression for $G_{j\nu}$ is available. An expression for $G_{j\nu}$ may be derived from considerations of Figure 2. In Figure 2 are shown two surfaces, j and k, of the M surface enclosure. The surfaces have areas A_j and A_k and known temperatures T_j and T_k. The two differential areas, dA_j and dA_k, are located on surfaces j and k, respectively. These areas, dA_j and dA_k, are separated by the distance r_{jk} and have normals oriented at the angles φ_j and φ_k from r_{jk}, respectively. The two surfaces are also separated by the participating gas.

At this point two other assumptions must be mentioned. First, the gas is assumed to be at a known and constant temperature, T_g. In most real situations the gas is non-

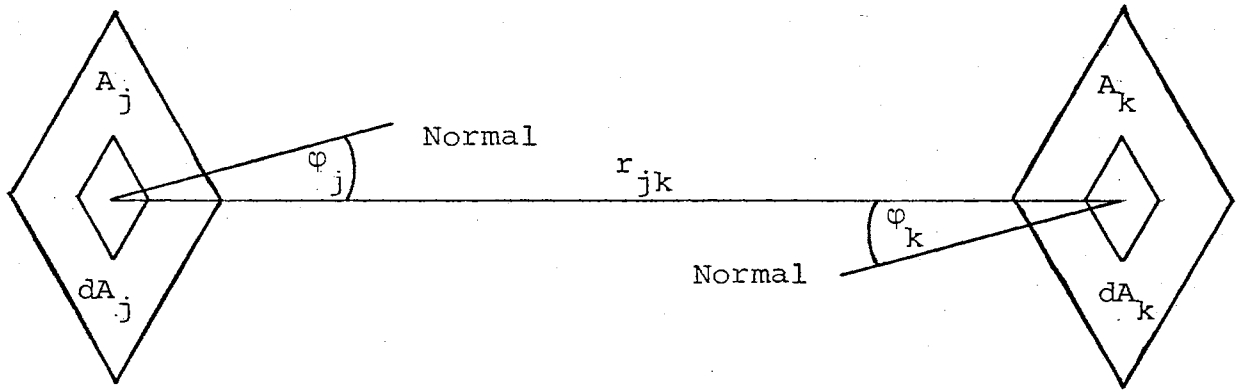

Figure 2. Geometry For Exchange of Thermal Radiation

isothermal. However, complexities in treating the radiative absorption and emission of the gas are reduced if the gas is assumed to be isothermal. This point is elaborated in Chapter II of this thesis. The second assumption is that the surfaces of the enclosure are diffuse emittors and reflectors. For many engineering materials, this second assumption is approximately realized. With the above assumptions in mind, the monochromatic irradiation of surface j due to energy coming from the direction of surface k is [Bevans, et al (4)]

$$G_{j\nu}A_j\Big|_{\text{From k}} = \int_{A_j}\int_{A_k} (\tau_{g\nu}J_{k\nu} + \alpha_{g\nu}E_{bg\nu}) \frac{\cos\varphi_j \cos\varphi_k}{\pi r_{jk}^2} dA_k dA_j \quad . \quad \text{(I-4)}$$

In Equation (I-4), $\tau_{g\nu}$ is the monochromatic transmittance of the gas between surfaces j and k. This property is formally defined in Chapter II of this thesis. The term $\frac{\cos\varphi_j \cos\varphi_k}{\pi r_{jk}^2}$ is a measure of the fraction of all energy leaving surface k that is directed toward surface j. Therefore, the term $\tau_{g\nu}J_{k\nu}\frac{\cos\varphi_j \cos\varphi_k}{\pi r_{jk}^2}$ is a measure of the energy arriving at surface j from surface k which was transmitted through the gas. The monochromatic absorptance of the gas between surface j and k is $\alpha_{g\nu}$. As will be shown in Chapter II, $\alpha_{g\nu} = 1 - \tau_{g\nu}$, and, for the conditions of radiative

equilibrium assumed in this study, $\alpha_{g\nu} = \epsilon_{g\nu}$, where $\epsilon_{g\nu}$ is the monochromatic emittance of the gas. The monochromatic black-body emissive power of the gas is $E_{bg\nu}$. It may be calculated from Planck's equation, Equation (I-3), by replacing T_j with T_g. The term $\alpha_{g\nu} E_{bg\nu} \frac{\cos\varphi_j \cos\varphi_k}{\pi r_{jk}^2}$ in Equation (I-4) is therefore a measure of the energy arriving at surface j which was emitted by the gas along the direction from surface k to surface j.

The total irradiation of surface j is due to the sum of the contributions from all surfaces, like the $k^{\underline{th}}$ surface, which form the M surface enclosure. Summing both sides of Equation (I-4) over k gives for the total monochromatic irradiation of surface j

$$G_{j\nu} A_j = \sum_{k=1}^{M} \int_{A_j} \int_{A_k} (\tau_{g\nu} J_{k\nu} + \alpha_{g\nu} E_{bg\nu}) \frac{\cos\varphi_j \cos\varphi_k}{\pi r_{jk}^2} dA_k dA_j \quad . \text{(I-5)}$$

Using Equation (I-2) in (I-5), a set of M simultaneous integral equations in $J_{j\nu}$ is obtained,

$$J_{j\nu} A_j = \epsilon_{j\nu} E_{bj\nu} A_j + \rho_j \sum_{k=1}^{M} \int_{A_j} \int_{A_k} (\tau_{g\nu} J_{k\nu} + \alpha_{g\nu} E_{bg\nu}) \frac{\cos\varphi_j \cos\varphi_k}{\pi r_{jk}^2} dA_k dA_j \qquad \text{(I-6)}$$

$$j = 1, 2, \ldots, M \quad .$$

In most real situations $\tau_{g\nu}$, $\alpha_{g\nu}$, and $J_{k\nu}$ vary with the spatial variables related to the enclosure geometry, e.g., A_j, A_k, r_{jk}, φ_j, and φ_k. In order to facilitate numerical computation the assumption is made that $\tau_{g\nu}$, $\alpha_{g\nu}$ and $J_{k\nu}$ do not vary with spatial variables. As applied to $\alpha_{g\nu}$ and $\tau_{g\nu}$, this approximation is made more feasible by considering them to vary with geometric mean beam length, discussed in Chapter II. In this way the spatial variation of $\alpha_{g\nu}$ and $\tau_{g\nu}$ are approximately accounted for. The approximation for many problems, as it applies to $J_{k\nu}$, does not result in large errors in heat transfer according to Sparrow, et al (5). With these approximations the following set of M simultaneous algebraic equations in the M unknown monochromatic radiosities may be written:

$$J_{j\nu}A_j = \epsilon_{j\nu}E_{bj\nu}A_j + \rho_{j\nu}\sum_{k=1}^{M}(\tau_{g\nu}J_{k\nu}+\alpha_{g\nu}E_{bg\nu})A_jF_{jk}$$

$$j = 1, 2, \ldots, M \quad , \tag{I-7}$$

or, cancelling A_j from each term,

$$J_{j\nu} = \epsilon_{j\nu}E_{bj\nu} + \rho_{j\nu}\sum_{k=1}^{M}(\tau_{g\nu}J_{k\nu}+\alpha_{g\nu}E_{bg\nu})F_{jk}$$

$$j = 1, 2, \ldots, M, \tag{I-8}$$

where F_{jk} is the configuration factor,

$$F_{jk} = \frac{1}{A_j} \int_{A_j} \int_{A_k} \frac{\cos\varphi_j \cos\varphi_k}{\pi r_{jk}^2} \, dA_k \, dA_j \quad .$$

Configuration factors for many geometries are available in the literature, e.g., Hamilton and Morgan (6). Therefore, if $\alpha_{g\nu}$ is available, Equation (I-8), in principle, may be used to calculate the M values of $J_{j\nu}$. Then, Equation (I-1) could be evaluated for the M values of $q_{j\nu}$. These calculations could be performed at various values of ν throughout the spectrum. The $q_{j\nu}$ results could then be numerically integrated to obtain the total radiant surface heat transfer to each of the M surfaces comprising the enclosure. Because lack of spectral property data and/or time limitations may prohibit the use of the above monochromatic method, the monochromatic heat transfer and radiative exchange equations are reformulated to apply to a band of wavenumbers instead of a single wavenumber.

Band Equations of Radiant Energy Transfer

It is known that polyatomic gases absorb monochromatic radiant energy in regions of wavenumber called absorption bands, Herzberg (7). Adjacent to these absorption bands are windows wherein the gas is nearly perfectly transmitting. Such a situation is illustrated in Figure 3 which shows a low

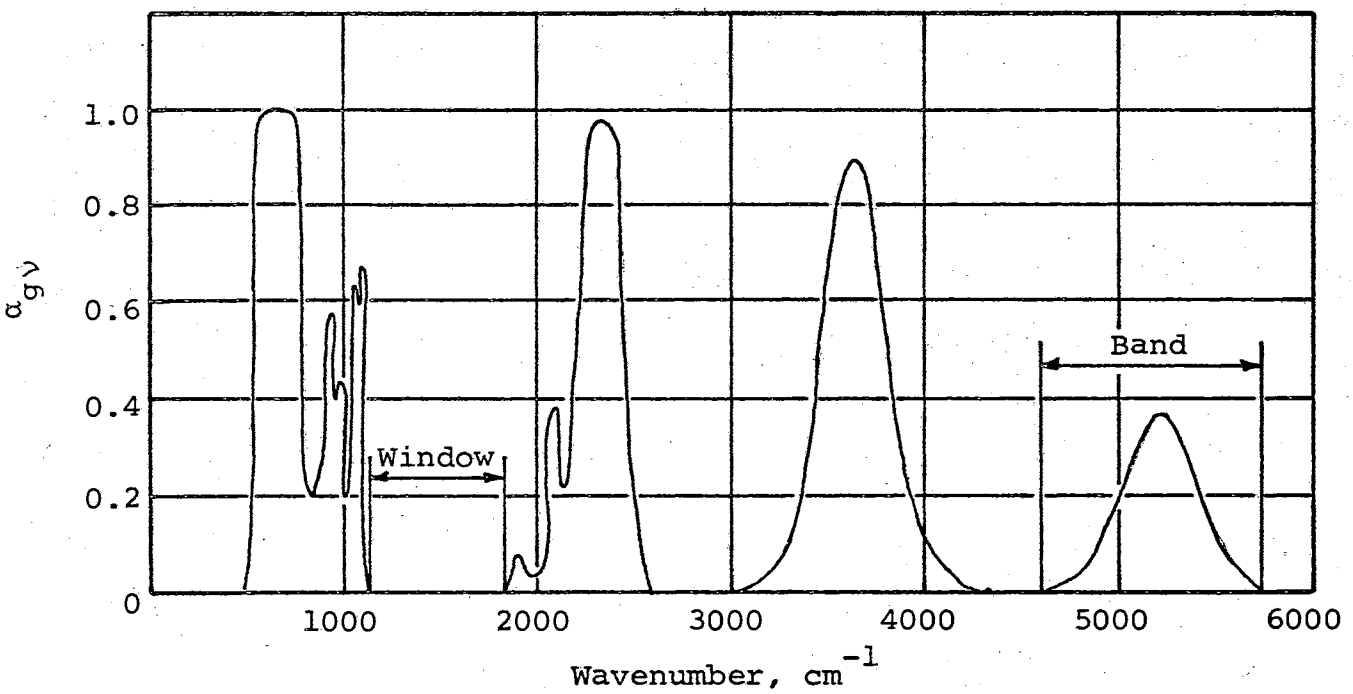

Figure 3. Gas Absorptance Versus Wavenumber
(Data from Edwards (23))

resolution plot of $\alpha_{g\nu}$ versus wavenumber for a mixture of carbon dioxide and nitrogen.

Strictly speaking, the band limits are not rigorously defined. That is, upper and lower limits above and below which, respectively, no absorption occurs may not exist for all bands under all conditions. The most obvious example of this occurs with band overlap. For such a situation it is difficult to say where one band begins and another ends. However, for purposes of the present study, visual inspection of each band allowed, in most cases, the determination of approximate band limits. These limits were dictated by the location of minimum, if not zero, values of spectral absorptance.

The monochromatic expressions presented in the last section are reformulated in this section to apply to a wavenumber band $\Delta\nu$. The bandwidth $\Delta\nu$ may be thought of as the width of an absorption band for purposes of reformulating the radiant transfer equations. However, these expressions will be seen to apply also to a window region.

The expression for surface heat transfer, Equation (I-1), in the band $\Delta\nu$ becomes (1)

$$q_{j\Delta\nu} = \frac{\bar{\alpha}_{j\Delta\nu} J_{j\Delta\nu} - \bar{\epsilon}_{j\Delta\nu} E_{bj\Delta\nu}}{\bar{\rho}_{j\Delta\nu}} , \quad j = 1, 2, \ldots, M , \qquad (I-9)$$

where:

$q_{j\Delta\nu}$ = the radiant heat transfer to surface j in the region $\Delta\nu$

$$\overline{\alpha}_{j\Delta\nu} = \frac{\int_{\Delta\nu} \alpha_{j\nu} G_{j\nu} d\nu}{\int_{\Delta\nu} G_{j\nu} d\nu}$$

$$\overline{\epsilon}_{j\nu} = \frac{\int_{\Delta\nu} \epsilon_{j\nu} E_{bj\nu} d\nu}{\int_{\Delta\nu} E_{bj\nu} d\nu}$$

$$\overline{\rho}_{j\Delta\nu} = 1 - \overline{\alpha}_{j\Delta\nu}$$

$$J_{j\Delta\nu} = \int_{\Delta\nu} J_{j\nu} d\nu$$

$$E_{bj\Delta\nu} = \int_{\Delta\nu} E_{bj\nu} d\nu$$

The definition of radiosity, Equation (I-2), in a band $\Delta\nu$ becomes (1)

$$J_{j\Delta\nu} = \overline{\rho}_{j\Delta\nu} G_{j\Delta\nu} + \overline{\epsilon}_{j\Delta\nu} E_{bj\Delta\nu} , \qquad \text{(I-10)}$$

where the irradiation of the $j^{\underline{th}}$ surface in $\Delta\nu$ is

$$G_{j\Delta\nu} = \int_{\Delta\nu} G_{j\nu} d\nu$$

Equation (I-4), when rewritten to apply to the region $\Delta\nu$, gives for the irradiation of the $j^{\underline{th}}$ surface due to energy in $\Delta\nu$ coming from the $k^{\underline{th}}$ surface (4)

$$G_{j\Delta\nu}A_j\Big|_{\text{From } k} = \int_{A_k}\int_{A_j}\int_{\Delta\nu}(\tau_{g\nu}J_{k\nu}+\alpha_{g\nu}E_{bg\nu})\frac{\cos\varphi_j\cos\varphi_k}{\pi r_{jk}^2}\,d\nu dA_k dA_j \qquad \text{(I-11)}$$

Summing the right side of Equation (I-11) over the M surfaces of the enclosure gives the total irradiation of the j^{th} surface in the band $\Delta\nu$,

$$G_{j\Delta\nu}A_j = \sum_{k=1}^{M}\int_{A_j}\int_{A_k}\int_{\Delta\nu}(\tau_{g\nu}J_{k\nu}+\alpha_{g\nu}E_{bg\nu})\frac{\cos\varphi_j\cos\varphi_k}{\pi r_{jk}^2}\,d\nu dA_k dA_j \; . \qquad \text{(I-12)}$$

Substituting for $G_{j\Delta\nu}$ in Equation (I-12) using Equation (I-10), the radiosity of the j^{th} surface in $\Delta\nu$ is obtained,

$$J_{j\Delta\nu}A_j = \bar{\epsilon}_{j\Delta\nu}E_{bj\Delta\nu}A_j + \bar{\rho}_{j\Delta\nu}\sum_{k=1}\int_{A_j}\int_{A_k}\int_{\Delta\nu}(\tau_{g\nu}J_{k\nu}+\alpha_{g\nu}E_{bg\nu})\frac{\cos\varphi_j\cos\varphi_k}{\pi r_{jk}^2}d\nu dA_k dA_j \; . \qquad \text{(I-13)}$$

As with the corresponding monochromatic expression, the unknown $J_{j\Delta\nu}$ values may not be evaluated without making several assumptions regarding Equation (I-13).

First, it is again assumed that $\tau_{j\nu}$, $\alpha_{g\nu}$, and $J_{k\nu}$ do not vary with spatial variables. As stated before, when mean beam lengths are used this assumption is not too unreasonable and it is discussed further in Chapter II. Secondly, it is assumed that $E_{bg\nu}$ does not vary appreciably with ν in band $\Delta\nu$. This is called by Edwards (8) the band-

absorption simplification. A poorer approximation than the band-absorption simplification is the band-energy approximation, Edwards (8). This is the assumption that $J_{k\nu}$ does not vary appreciably with ν in the region $\Delta\nu$. This is a poorer approximation because $J_{j\nu}$ consists of energy which has passed through the gas many times before reaching surface j. It therefore picks up the spectral variations from the gas (and reflecting enclosure surfaces) more than the emitted energy of the gas. The emitted energy has a spectral variation due to the gas resulting from only one passage through the gas.

With these three approximations in mind, Equation (I-13) becomes

$$J_{j\Delta\nu}A_j = \bar{\epsilon}_{j\Delta\nu}E_{bj\Delta\nu}A_j + \bar{\rho}_{j\Delta\nu}\sum_{k=1}^{M}(\bar{J}_{k\nu}\int_{\Delta\nu}\tau_{g\nu}d\nu + \bar{E}_{bg\nu}\int_{\Delta\nu}\alpha_{g\nu}d\nu)A_jF_{jk} \quad , \qquad \text{(I-14)}$$

where, for numerical computation, the average values of $J_{k\nu}$ and $E_{bg\nu}$ in $\Delta\nu$ are defined as follows:

$$\bar{J}_{k\nu} = \frac{1}{\Delta\nu}\int_{\Delta\nu}J_{k\nu}d\nu = \frac{J_{k\Delta\nu}}{\Delta\nu}$$

$$\bar{E}_{bg\nu} = \frac{1}{\Delta\nu}\int_{\Delta\nu}E_{bg\nu}d\nu = \frac{E_{bg\Delta\nu}}{\Delta\nu} \quad .$$

The term $\int_{\Delta\nu}\alpha_{g\nu}d\nu$ which appears in Equation (I-14) defines the band absorption, $\mathcal{A}$, Edwards (8),

$$a = \int_{\Delta\nu} \alpha_{g\nu} d\nu \quad . \tag{I-15}$$

The term $\int_{\Delta\nu} \tau_{g\nu} d\nu$ may be rewritten as

$$\int_{\Delta\nu} \tau_{g\nu} d\nu = \int_{\Delta\nu} (1 - \alpha_{g\nu}) d\nu = \Delta\nu - a \quad . \tag{I-16}$$

Substituting these last definitions into Equation (I-14), cancelling A_j from each term, and slightly rearranging, results in the following set of M simultaneous algebraic equations in the M unknown $J_{j\Delta\nu}$ values,

$$J_{j\Delta\nu} = \bar{\epsilon}_{j\Delta\nu} E_{bj\Delta\nu} + \bar{\rho}_{j\Delta\nu} \sum_{k=1}^{M} \left[\left(1 - \frac{a}{\Delta\nu}\right) J_{k\Delta\nu} + \frac{a}{\Delta\nu} E_{bg\Delta\nu} \right] F_{jk}$$

$$j = 1, 2, \ldots, M \quad . \tag{I-17}$$

In principle, the M values of $J_{j\Delta\nu}$ may be calculated from Equation (I-17). These results could then be substituted into Equation (I-9) allowing calculation of the M values of $q_{j\Delta\nu}$. In order to evaluate Equation (I-17) the terms other than $J_{j\Delta\nu}$, $j = 1, 2, \ldots, M$, must be available. In particular, the absorption bandwidth, $\Delta\nu$, must be known since it appears both explicitly and implicitly in Equation (I-17). It is required to evaluate $E_{bj\Delta\nu}$ and $E_{bg\Delta\nu}$ from, say, tabulations of Planck's functions. It is also required in the calculations of the surface properties, for instance, $\bar{\rho}_{j\Delta\nu}$, the average value of $\rho_{j\nu}$ in $\Delta\nu$.

Such values of absorption bandwidths, as depicted in Figure 3, for various gas conditions, do not exist in the literature. The work of this thesis was to correlate such absorption bandwidths of carbon dioxide and nitrogen gas mixtures with gas conditions. Correlation of $\mathcal{A}$ and $\mathcal{A}/\Delta\nu$ presented in Chapter III of this thesis allow one to calculate actual bandwidths, $\Delta\nu$, as a function of gas temperature, gas pressure, and amount of absorbing gas.

Effective bandwidths do exist in the literature (9), e.g., Edwards et al. However, they do not account for variation of bandwidth with gas conditions.

Using the correlations in Chapter III to obtain $\Delta\nu$ then, allows one to evaluate $E_{bg\Delta\nu}$ and $E_{bj\Delta\nu}$. If, as is assumed, surface spectral radiative property data are available, e.g., $\rho_{j\nu}$ versus ν, then $\overline{\rho}_{j\Delta\nu}$, $\overline{\alpha}_{j\Delta\nu}$, and $\overline{\epsilon}_{j\Delta\nu}$ may also be approximated in the region $\Delta\nu$. Extensive correlations of band absorption, $\mathcal{A}$, for various gas conditions do exist in the literature, e.g., Edwards (8) and Howard, et al (10). These values might be used in Equation (I-17), but, to be consistent, it is suggested that the correlations in Chapter III be used.

This essentially completes the formulation and discussion of the use of the band equations of radiant energy transfer. The importance of absorption bandwidth is

illustrated by its appearance, both explicitly and implicitly, in the band equations. In Chapter II, Literature Survey, further discussion of the effects of a participating gas on radiant heat transfer and documentation of related studies in the literature is presented.

CHAPTER II

LITERATURE SURVEY

This chapter consists of a survey of selected articles from the literature which pertain to gas absorptance and its use in radiant heat transfer calculations. In particular, monochromatic gas absorptance, from both theoretical and experimental viewpoints, is discussed. Then, theoretical and experimental band absorption is discussed. Finally, a brief discussion of selected previous work in the area of radiant heat transfer calculation methods involving an absorbing and emitting gas is presented.

Monochromatic Gas Absorptance

Consider a parallel beam of monochromatic radiation with intensity* $I_{\nu o}$ entering an absorbing gas with mass density ρ. If the gas is a mixture, such as carbon dioxide and nitrogen, let ρ be the mass density of the

---

*Intensity of radiation in a certain direction is defined as the radiant energy per unit area normal to the specified direction and per unit solid angle about the specified direction and per unit time.

active gas, carbon dioxide. Let the distance traveled through the gas be r, the path length, at which point the intensity is I_ν. Consider the change in intensity between r and r + dr where dr is a differential increment of r. The corresponding differential change in intensity is due to absorption and emission by the gas in the increment dr and according to Howard, et al (10) is defined by Lambert's law:

$$dI_\nu = k_\nu I_{bg\nu} \rho dr - k_\nu I_\nu \rho dr \quad . \qquad \text{(II-1)}$$

In this expression $I_{bg\nu}$ is the Planckian black-body intensity and k_ν is the absorption coefficient.

The absorption coefficient, k_ν, varies with gas temperature, gas pressure, and concentration of absorbing gas, Edwards (8). If the gas were non-isothermal, i.e., T_g varies with r, then k_ν and $I_{bg\nu}$ would vary with r in Equation (II-1). This type of situation results in a complex interpretation of gas absorptance, which has found application in problems of astrophysics, Kourganoff (2), but has not been studied extensively from the viewpoint of engineering application until recently, Edwards (11). For purposes of this study, an isothermal gas is assumed.

For the case of an isothermal gas, Equation (II-1) may be integrated from r = 0, where $I_\nu = I_{\nu o}$, to some arbitrary value of r, obtaining the intensity at r

$$I_\nu = I_{\nu o}[\exp(-k_\nu \rho r)] + I_{bg\nu}[1-\exp(-k_\nu \rho r)] \quad . \qquad \text{(II-2)}$$

The first term on the right side of Equation (II-2) is that part of $I_{\nu o}$ which is transmitted through the gas. The factor, $\exp(-k_\nu \rho r)$, may then be defined as the monochromatic transmittance of the gas, $\tau_{g\nu}$. The second term on the right side of Equation (II-2) is the energy emitted by the gas. The coefficient, $1 - \exp(-k_\nu \rho r)$, is therefore the monochromatic emittance, $\epsilon_{g\nu}$, of the gas. Since radiative equilibrium is assumed to exist, the monochromatic transmittance, absorptance, and emittance are seen to be related by the expression

$$\alpha_{g\nu} = \epsilon_{g\nu} = 1 - \exp(-k_\nu \rho r) = 1 - \tau_{g\nu} \quad . \qquad \text{(II-3)}$$

The product of the active gas mass density and path length, ρr, which appears in Equation (II-3) defines the mass path length, w,

$$w = \rho r \quad . \qquad \text{(II-4)}$$

Equation (II-3) may then be rewritten as

$$\alpha_{g\nu} = \epsilon_{g\nu} = 1 - \exp(-k_\nu w) = 1 - \tau_{g\nu} \quad . \qquad \text{(II-5)}$$

Since w is usually known from gas conditions and enclosure geometry, $\alpha_{g\nu}$ may be evaluated from Equation (II-5) if values of absorption coefficient, k_ν, are available. Microscopic descriptions of gas radiation which result in expressions for k_ν have been derived, e.g., Penner (12).

However, evaluation of these expressions is difficult, for example, see the work of Wyatt (13) and Stull (14), and therefore theoretical values of k_ν are not readily available for engineering use. A similar lack of experimental values of k_ν exists due to the high resolution required of instruments which might be used for this purpose, Edwards (8).

Even though theoretical values of $\alpha_{g\nu}$ are not generally available, it is possible to measure directly the monochromatic transmittance of a gas and from this to calculate $\alpha_{g\nu} = 1 - \tau_{g\nu}$. Edwards (8) has performed such measurements on various gases, and in particular, on mixtures of carbon dioxide and nitrogen. He combined his results with a theoretical expression for $\alpha_{g\nu}$ to obtain a semi-empirical correlation of monochromatic gas absorptance as a function of pressure and mass path length, w, with gas temperature a parameter, over large ranges of these variables, Edwards (11).

A description of the experimental apparatus used by Edwards may be found in Bevans, et al (15). Briefly, the method of measurement consists of placing the sample gas in a pressure vessel of known (optical) length having means for temperature and pressure regulation. Radiant energy from a suitable source is directed by appropriate

optics through the test cell and into a monochromatic detection system. The energy passed through the gas at various wavenumbers is detected and recorded. This completes the absorption run. A similar run, the transmission run, is performed without an absorbing gas in the test cell. The ratio of the energy transmitted during the absorption run at a particular wavenumber to the energy passed without absorption during the transmission run at the same wavenumber is a measure of the monochromatic gas transmittance.

Many other workers have measured the monochromatic gas absorptance of carbon dioxide, e.g., see References (16, 17, 18, 19, etc.). However, most of their measurements have been performed for selected absorption bands and over ranges of gas temperature, gas pressure, and mass path lengths sometimes too narrow to be of general utility.

Measurements of $\alpha_{g\nu}$ allow, by numerical integration, calculation of band absorption. The next section is concerned with band absorption theory and the correlation of band absorption with gas conditions.

Band Absorption

Consider a gas absorption band such as one shown in Figure 3 of Chapter I. Band absorption is strictly defined

as

$$\mathcal{A} = \int_{\nu_L}^{\nu_U} \alpha_{g\nu} d\nu \quad ,$$

where ν_L is the lower limit of the band, below which no absorption occurs, and, ν_U is the upper limit of the band, above which no absorption occurs.

Theoretical models of band absorption exist, e.g., Plass (20,21). These models make use of the fact that the infrared absorption bands, of concern in this study, are due to changes in the molecular vibrational and rotational energies. Changes in the vibrational energies of gas molecules may be accompanied by changes in the rotational energies of the molecules. This results in absorption by rotational lines located about the vibrational frequency. The band is then composed of many absorption lines which are discernable, experimentally, only with very high resolution instruments. Low resolution instruments "see" the absorption as in Figure 3 of Chapter I.

An absorption line is said to have an intensity, S,

$$S = \int_{\Delta\nu_\ell} k_\nu d\nu \quad ,$$

where $\Delta\nu_\ell$ is the finite width of the absorption line. This indicates that, strictly speaking, the lines are not lines at all. Actually they resemble very small absorption bands. The absorption line is said to have a half-width,

δ, which is one half the line width at half maximum intensity. It is generally believed, e.g., Bevans, et al (4), the line shape is defined by the Lorentz expression,

$$k_\nu = \frac{S}{\pi} \frac{\delta}{(\nu-\nu_o)^2 + \delta^2} \quad , \qquad \text{(II-6)}$$

where ν_o is the wavenumber at the center of the line. The above mentioned line properties are depicted in Figure 4.

Absorption band models postulate the arrangement, i.e., the line location and distribution of line intensities, of lines in a band. Four generally accepted band models which exist are:

a) the Elsasser model

b) the statistical (Goody) model

c) the random Elsasser model

d) the quasi-random model.

The Elsasser model assumes the lines are uniformly spaced and that each line has the same intensity. The statistical model assumes the lines are randomly located and that the line intensity varies in any manner such that a distribution function describes it. The random Elsasser model assumes the lines of a band may be represented by a superposition of Elsasser bands, Plass (20). The quasi-random model represents the lines more accurately than the other models

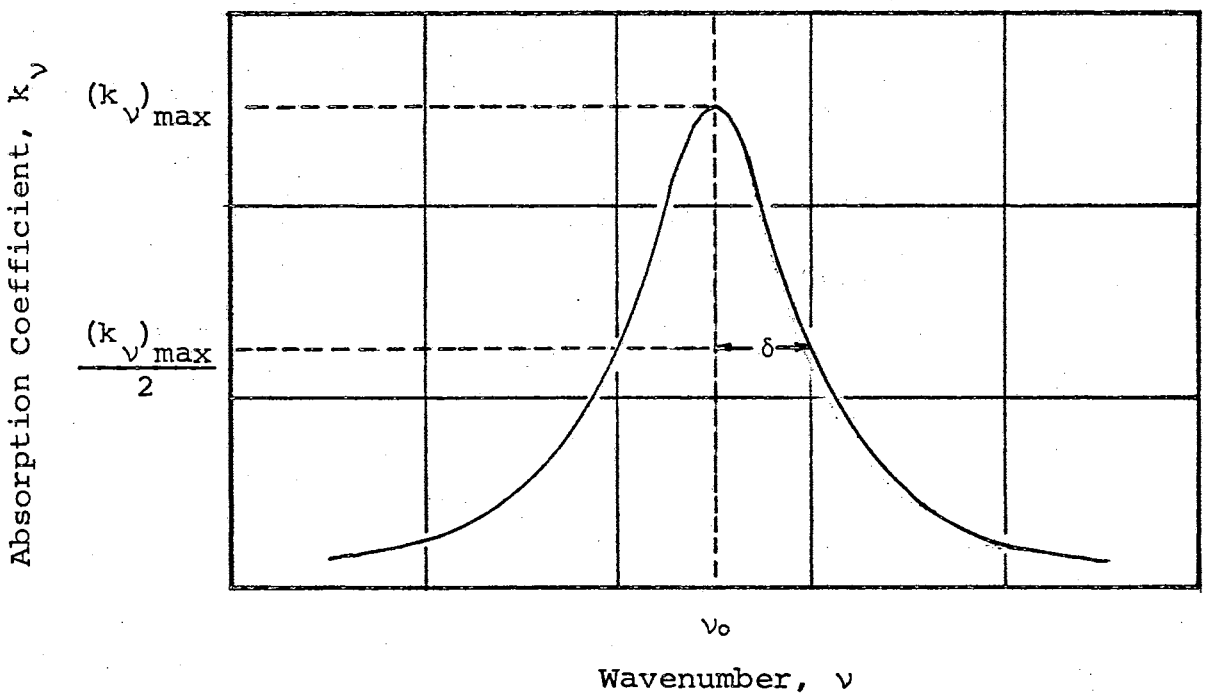

Figure 4. Lorentz Line

at a sacrifice in simplicity, and results in a band representation somewhere between the Elsasser and statistical models (21).

According to Plass (20) further classification of the band models may be made depending on whether the lines in the band are:

a) strong lines

b) weak lines

c) non-overlapping lines.

The strong line approximation is valid when there is complete absorption near the centers of the strongest lines in the band. The weak line approximation is valid when the absorption is small at all frequencies in the band. The non-overlapping line approximation is valid when the lines in the band do not overlap.

Mathematical expressions based on the various combinations of the above models indicate (20) band absorption, a, is a function of β and x, where

$$\beta = \frac{2\pi\delta}{d}$$

and

$$x = \frac{Sw}{2\pi\delta} \quad ,$$

where d is line spacing and δ, S, and w have been previously defined as line halfwidth, line intensity, and mass path

length, w. Variations of α with pressure are accounted for by β and x since both δ and w vary with pressure.

Reasoning from the band model theoretical results and complimenting this with experimental results, researchers, e.g., Howard, et al (10) have deduced two generally accepted correlation equations. These expressions correlate band absorption, with the two variables, mass path length and effective pressure, P_e , with temperature as a parameter. The two correlation equations differ depending on whether a band consists of weak lines or strong lines. For weak bands

$$\alpha = b_1 (w)^{m_1} (P_e)^{n_1} \quad , \qquad \text{(II-7)}$$

and for strong bands

$$\alpha = B_1 + M_1 \log w + N_1 \log P_e \quad . \qquad \text{(II-8)}$$

For mixtures of carbon dioxide and nitrogen Edwards (11) has found that the relation,

$$P_e = P_{N_2} + b\, P_{CO_2} \quad , \qquad \text{(II-9)}$$

where $b = 1.3$,

is the best choice for correlation of his data. The quantities P_{N_2} and P_{CO_2} in Equation (II-9) are the partial pressures of the nitrogen and the carbon dioxide, respectively.

Many researchers have experimentally determined the band absorption of carbon dioxide - nitrogen mixtures and correlated their results with gas conditions. Howard,

Burch, and Williams (10,22) studied the 15.0, 5.2, 4.8, 4.3, 2.7, 2.0, 1.6, and 1.4 micron absorption bands of carbon dioxide. Their work was performed at approximately room temperature. They allowed the amount* of absorbing gas, which is analogous to mass path length, w, to vary from 1 to 1000 atm-cm. Partial pressure of carbon dioxide was varied from zero to 50 mm Hg. Total pressures of the gas mixture up to 740 mm Hg were considered.

D. K. Edwards (23, 24, 8, 9) experimentally determined and correlated the 15.0, 10.5, 9.4, 7.5, 5.2, 4.8, 4.3, 2.7, 2.0, 1.6, and 1.4 micron bands of carbon dioxide-nitrogen gas mixtures. Total mixture pressure was allowed to vary from 0.5 to 10.0 atm, gas temperatures from 530° to 2500°R, carbon dioxide mole fractions from 0.05 to 1.00, and mass path lengths from approximately 0.00002 to 5.0 lbm/ft^2. This work is particularly notable for the wide ranges of gas conditions studied.

The studies of Howard, Burch, and Williams, (10,22) were supplemented in 1962 by the work of Burch, Gryvnak,

---

*Amount of absorbing gas, for constant temperature measurements, is defined as the product of active gas partial pressure times path length, e.g., $P_{CO_2}r$.

and Williams (25,26). These workers experimentally determined and correlated the band absorption of the 10.4, 9.4, 4.3, and 2.7 micron bands of carbon dioxide. They extended the older results of Howard, Burch, and Williams by employing improved experimental techniques, and by considering new ranges of pressure, amount of absorbing gas, and spectral frequencies. They also considered the effects of moderate temperature changes on some of the absorption bands.

In 1964, Edwards and Menard (27, 28) and Edwards and Sun (29) published improved correlations of the band absorption of the 15.0, 10.4, 9.4, 4.3, and 2.7 micron bands of carbon dioxide-nitrogen gas mixtures. The previous correlations of Edwards were improved by use of the statistical (Goody) model of band absorption to correlate experimentally determined band absorption with gas conditions. Further discussion of Edwards' use of the statistical model for purposes of band absorption calculations may be found in Edwards' reference (11).

Keeping in mind that the literature of gas absorption has by no means been exhaustively discussed, it is now possible to proceed to the next section of this chapter and consider works primarily concerned with the use of gas absorption data in radiant heat transfer calculations.

Gas Radiation Heat Transfer

This section might contain literally hundreds of references to the radiant heat exchange literature. Rather than take this approach and risk too shallow a discussion of these contributions, only those articles from the literature which are closely related to the use of the heat transfer expressions presented in Chapter I are discussed. For further references to current work in radiant heat transfer, the reader is directed to the literature review by Viskanta and Grosh (30). This section will confine itself to discussion of the concept of mean beam length and gray solutions to the enclosure problem as presented in Chapter I.

The concept of mean beam length may be introduced by considering Equation (I-13),

$$J_{j\Delta\nu}A_j = \bar{\varepsilon}_{j\Delta\nu}E_{bj\Delta\nu}A_j + \bar{\rho}_{j\Delta\nu}\sum_{k=1}^{M}\int_{A_j}\int_{A_k}\int_{\Delta\nu}(\tau_{g\nu}J_{k\nu}+\alpha_{g\nu}E_{bg\nu})\frac{\cos\varphi_j\cos\varphi_k}{\pi r_{jk}^2}\,d\nu dA_k dA_j .$$

From this expression, consider the term

$$\int_{A_j}\int_{A_k}\int_{\Delta\nu}(\tau_{g\nu}J_{k\nu}+\alpha_{g\nu}E_{bg\nu})\frac{\cos\varphi_j\cos\varphi_k}{\pi r_{jk}^2}\,d\nu dA_k dA_j .$$

Making use of the relation, $\tau_{g\nu} = 1 - \alpha_{g\nu}$, this last expression becomes

$$\int_{A_j}\int_{A_k}\int_{\Delta\nu}(1-\alpha_{g\nu})J_{k\nu}+\alpha_{g\nu}E_{bg\nu})\frac{\cos\varphi_j\cos\varphi_k}{\pi r_{jk}^2}\,d\nu dA_k dA_j .$$

From this expression consider the integrals

$$\int_{A_j}\int_{A_k}\int_{\Delta\nu} \alpha_{g\nu} J_{k\nu} \frac{\cos\varphi_j \cos\varphi_k}{\pi r_{jk}^2} \, d\nu dA_k dA_j$$

and

$$\int_{A_j}\int_{A_k}\int_{\Delta\nu} \alpha_{g\nu} E_{bg\nu} \frac{\cos\varphi_j \cos\varphi_k}{\pi r_{jk}^2} \, d\nu dA_k dA_j \quad .$$

As in Chapter I, assume $J_{k\nu}$ does not vary appreciably with ν in the region $\Delta\nu$(band energy simplification) and, $E_{bg\nu}$ does not vary appreciably with ν in the region $\Delta\nu$ (band absorption simplification). The last two expressions become in this case

$$\bar{J}_{k\nu} \int_{A_j}\int_{A_k}\int_{\Delta\nu} \alpha_{g\nu} \frac{\cos\varphi_j \cos\varphi_k}{\pi r_{jk}^2} \, d\nu dA_k dA_j$$

and

$$\bar{E}_{bg\nu} \int_{A_j}\int_{A_k}\int_{\Delta\nu} \alpha_{g\nu} \frac{\cos\varphi_j \cos\varphi_k}{\pi r_{jk}^2} \, d\nu dA_k dA_j \quad .$$

The common factor in these two expressions is

$$\int_{A_j}\int_{A_k}\int_{\Delta\nu} \alpha_{g\nu} \frac{\cos\varphi_j \cos\varphi_k}{\pi r_{jk}^2} \, d\nu dA_k dA_j \quad ,$$

which may be rearranged as

$$\int_{A_j}\int_{A_k} \left[\int_{\Delta\nu} \alpha_{g\nu} d\nu \right] \frac{\cos\varphi_j \cos\varphi_k}{\pi r_{jk}^2} \, dA_k dA_j \quad .$$

Making use of the definition of band absorption,

$$a = \int_{\Delta\nu} \alpha_{g\nu} d\nu \quad ,$$

this last expression becomes

$$\int_{A_j}\int_{A_k} \alpha \frac{\cos\varphi_j \cos\varphi_k}{\pi r_{jk}^2} \, dA_k dA_j \quad .$$

In the last section of this chapter it was shown that band absorption is typically correlated with expressions of the form,

$$\alpha = b_1 (w)^{m_1} (P_e)^{n_1} \qquad \text{(II-10)}$$

and

$$\alpha = B_1 + M_1 \log w + N_1 \log P_e \qquad \text{(II-11)}$$

for weak and strong bands, respectively. Since mass path length, w, is the product ρr_{jk}, then $\alpha = \alpha(r_{jk})$ indicates the functional dependency of band absorption on path length. The last double integral expression above may be written to show this functional dependency, defining, after Bevans, et al (4), at the same time the geometric absorption factor, $(FA\alpha)_{jk}$,

$$(FA\alpha)_{jk} = \int_{A_j}\int_{A_k} \alpha(r_{jk}) \frac{\cos\varphi_j \cos\varphi_k}{\pi r_{jk}^2} \, dA_k dA_j \quad . \qquad \text{(II-12)}$$

Although required in the band equations of radiant exchange, it is not practical to present geometrical absorption factors in simple graphical or tabular forms, Dunkle (31). This is due to the variety of band absorption expressions and enclosure geometries.

It is possible to simplify matters by defining a mean beam length, $\bar{r}'_{jk}$. First define the mean absorption as (31)

$$\overline{\alpha(r_{jk})} = \frac{(FA\alpha)_{jk}}{A_j F_{jk}} \quad . \tag{II-13}$$

Then define the mean beam length such that

$$\alpha(\bar{r}'_{jk}) = \overline{\alpha(r_{jk})} \quad , \tag{II-14}$$

i.e., the mean beam length is the path length such that the band absorption based on mean beam length is equal to the mean absorptance (31). Again, however, it is impractical to evaluate $(FA\alpha)_{jk}$ in Equation (II-13) so, further simplification is required.

R. V. Dunkle (31) defines a geometric mean beam length, $\bar{r}_{jk}$, using Equation (II-14) and assuming a linear absorption law. By linear absorption law it is meant α varies directly with r_{jk}. This is equivalent to assuming the exponent m_1 is one in Equation (II-7),

$$\alpha = b_1 (w)^{1.0} (P_e)^{n_1} \quad ,$$

where w is pr_{jk}. Accepting the linear approximation for the moment, and combining it with Equations (II-12, 13, 14), results in Dunkle's (31) definition of geometric mean beam length,

$$\bar{r}_{jk} = \frac{1}{A_j F_{jk}} \int_{A_j A_k} \int \frac{\cos\varphi_j \cos\varphi_k}{\pi r_{jk}} \, dA_k \, dA_j \quad . \tag{II-15}$$

Dunkle (31) has evaluated Equation (II-15) for parallel rectangles, perpendicular rectangles, and small sphere to rectangle geometries and presented his results in tabular and graphical form.

Geometric mean beam lengths are used in the band equations of radiant exchange, rather than actual path lengths, in the evaluation of band absorption, α. This is the basis of the assumption that gas absorptance does not vary with spatial variables. In reality, gas absorptance varies with path length, but this functional dependency is approximately accounted for by calculating gas absorptance as a function of geometric mean beam length between two surfaces.

J. A. Wiebelt (32) has compared the use of geometric mean beam lengths to the use of geometric absorption factors for the case of weak band absorption, i.e., Equation (II-7), and perpendicular rectangles. He found that errors in α were typically 10 percent, and 20 percent in the most extreme cases considered

Before proceeding to Chapter III, one more approach to the problem of radiative exchange in an enclosure containing a participating gas should be considered. This is the gray approach.

If the gas and enclosure radiative properties are assumed not to vary with frequency, then the system is called gray. Essentially, this means the radiative exchange equations are formulated so as to apply to the entire spectrum rather than to a single frequency or to a band of frequencies. The radiative properties used in this formulation are total values, that is integrated monochromatic values.

The same enclosure-gas system treated in Chapter I is still appropriate. The radiant heat transfer to the j^{th} surface is

$$q_j = \frac{\alpha_j J_j - \epsilon_j E_{bj}}{\rho_j} \quad , \qquad \text{(II-16)}$$

where:

q_j = radiant energy to the j^{th} surface per unit area per unit time

α_j = absorptance of the j^{th} surface

ϵ_j = emittance of the j^{th} surface

ρ_j = transmittance of the j^{th} surface

J_j = radiosity of the j^{th} surface

E_{bj} = black-body emissive power of the j^{th} surface.

Again it is assumed the surface properties are available, i.e., ρ_j is known, $\alpha_j = 1 - \rho_j$ by definition and, although not strictly true, $\epsilon_j = \alpha_j$. The black-body emissive power may be calculated from

$$E_{bj} = \sigma T_j^4 \quad , \qquad \text{(II-17)}$$

where σ is the Stefan-Boltzmann constant and is equal to 0.1713×10^{-8} Btu/hr - ft^2 - $^\circ$R^4. An expression for the only unknown on the right side of Equation (II-16), J_j, may be determined from consideration of Equation (I-13), rewritten to apply to the wavenumber region zero to infinity, rather than $\Delta\nu$,

$$J_j A_j = \epsilon_j E_{bj} A_j + \rho_j \sum_{k=1}^{M} \int_{A_j} \int_{A_k} \int_{\nu=o} (\tau_{g\nu} J_{k\nu} + \epsilon_{g\nu} E_{bg\nu}) \frac{\cos\varphi_j \cos\varphi_k}{\pi r_{jk}^2} \, d\nu dA_k dA_j \quad . \text{(II-18)}$$

Notice that $\alpha_{g\nu}$ is replaced with $\epsilon_{g\nu}$ in this expression. This is necessary because of the assumptions required to allow the integrations indicated in Equation (II-18). As in Chapter I, assume $J_{k\nu}$ does not vary with spatial variables. Also as in Chapter I, assume $\tau_{g\nu}$ and $\epsilon_{g\nu}$ spatial variations are accounted for by geometric mean beam lengths. Assuming in addition the gas is gray, i.e., $\tau_{g\nu}$ and $\alpha_{g\nu}$ do not vary with ν, the indicated integrations may be performed, resulting in

$$J_j A_j = \epsilon_j E_{bj} A_j + \rho_j \sum_{k=1}^{M} (\tau_g J_k + \epsilon_g E_{bg}) A_j F_{jk} \quad , \qquad \text{(II-19)}$$

or, cancelling A_j from each term,

$$J_j = \epsilon_j E_{bj} + \rho_j \sum_{k=1}^{M} (\tau_g J_k + \epsilon_g E_{bg}) F_{jk} \qquad \text{(II-20)}$$

The total gas transmittance is defined as

$$\tau_g = \frac{\int_{\nu=0}^{\infty} \tau_{g\nu} J_{k\nu} d\nu}{\int_{\nu=0}^{\infty} J_{k\nu} d\nu} = \frac{\int_{\nu=0}^{\infty} \tau_{g\nu} J_{k\nu} d\nu}{J_k} ,$$

which may not be evaluated since $J_{k\nu}$ is unknown. The total gas emittance is defined as

$$\epsilon_g = \frac{\int_{\nu=0}^{\infty} \epsilon_{g\nu} E_{bg\nu} d\nu}{\int_{\nu=0}^{\infty} E_{bg\nu} d\nu} = \frac{\int_{\nu=0}^{\infty} \epsilon_{g\nu} E_{bg\nu} d\nu}{E_{bg}} = \frac{\int_{\nu=0}^{\infty} \epsilon_{g\nu} E_{bg\nu} d\nu}{\sigma T_g^4} .$$

Values of ϵ_g may be calculated if sufficient spectral gas emittance data are available, Edwards (23). However, Hottel (33) has graphically presented experimentally determined values of ϵ_g for carbon dioxide as a function of mixture total pressure, gas temperature, and product of carbon dioxide partial pressure, P_{CO_2}, times a mean beam length, L.

The total gas absorptance may also be determined from Hottel's curves using the empirical expression,

$$\alpha_g = \epsilon_{go} \left(\frac{T_g}{T_o} \right)^{0.65} , \qquad \text{(II-21)}$$

where α_g is the gas absorptance to radiation from a source at temperature T_o, ε_{go} is gas emittance, evaluated at temperature T_o rather than T_g and evaluated at P_{CO_2} L T_o/T_g rather than P_{CO_2} L. The corresponding total transmittance is, by definition,

$$\tau_g = 1 - \alpha_g \quad . \qquad \text{(II-22)}$$

Strictly speaking, the values of ε_g plotted by Hottel are valid for gases in black or near black enclosures. For such an enclosure, interreflections are not appreciable. In the gray formulation, as presented in this chapter, interreflections are accounted for. Therefore, the values of ε_g and α_g from Hottel's plots are only approximately valid when used with the gray approach presented above.

Having Hottel's total gas emittance graphs and assuming that configuration factor values and surface property data are available, one can evaluate Equation (II-20) for the M values of J_j. With these values Equation (II-16) can, in principle, be evaluated, thereby completing the problem of calculation of the M values of q_j.

In Chapter I of this thesis equations of radiative exchange for an enclosure containing a participating gas were briefly discussed and presented. Assumptions required for the numerical evaluation of these equations were briefly discussed in Chapter I and further elaborated in

this chapter. Also in this chapter, background information related to the use of the radiative exchange equations was presented, documenting at the same time a small but major part of the literature which pertains to radiative exchange including the effects of a participating gas. It was established that a need exists for absorption bandwidths such that the radiative exchange equations may be evaluated. For this purpose, effective absorption bandwidths of carbon dioxide-nitrogen gas mixtures exist in the literature, e.g., Edwards, et al (9). Actual absorption bandwidths as pictured in Figure 3 were not found in the literature. In Chapter III of this thesis are presented correlations of band absorption and band absorption divided by such absorption bandwidths for mixtures of gaseous carbon dioxide and nitrogen, as a function of equivalent pressure and mass path length, for various gas temperatures. Such correlations allow the calculation of absorption bandwidths of the four bands considered.

CHAPTER III

DISCUSSION AND PRESENTATION OF RESULTS

It has been shown in Chapters I and II that absorption bandwidths are required to evaluate the band equations of radiant energy exchange in an enclosure containing a participating gas. The lack of actual bandwidth data in the literature raised several questions. First, can actual absorption bandwidths, as opposed to effective bandwidths (which do exist in the literature) be determined? Second, if actual bandwidths can be determined, can they be correlated in a manner such that they can be easily used in the band equations of radiant exchange? Third, if actual bandwidths can be easily used, will their use result in satisfactory values of radiant heat transfer? This chapter represents an attempt to affirmatively answer the first two questions. The third question is answered in Chapter IV.

Source of Spectral Data

In order to ascertain if actual absorption bandwidths may be determined, spectral data in the form of mono-

chromatic gas absorptance versus frequency are required. For this type of data to indicate how absorption bandwidths vary with gas conditions, the spectral data for various absorption bands at various gas temperatures, pressures, and mass path lengths are required. Such a source of data was found in a report by D. K. Edwards (11).

As mentioned previously, Edwards has correlated experimental spectral absorptance data with a theoretical expression. Strictly speaking his correlation gives average absorptance in narrow frequency ranges which, for purposes of heat transfer calculation, may be considered an approximation to monochromatic absorptance. Edwards correlated this narrow band absorptance for isothermal carbon dioxide, water vapor, and methane at five temperatures from 500 to 2500 degrees Rankine and pressures from 0.1 to 10 atmospheres. For purposes of this study, only the carbon dioxide correlation was used.

Edwards correlated spectral absorptance with the statistical (Goody) model of narrow band absorptance,

$$\alpha_{g\nu} = 1 - \exp\left\{\frac{-C^2 w}{\sqrt{1 + \frac{C^2 w}{B^2 P_e n}}}\right\} , \qquad \text{(III-1)}$$

where w and P_e have been previously defined as mass path length and equivalent pressure, respectively. The constants

C^2, B^2, and n are empirically determined constants with n = 0.8 for carbon dioxide. For carbon dioxide-nitrogen mixtures Edwards gives values of B^2, C^2, and BC as a function of wavenumber for five temperatures. The five temperatures are 535, 1000, 1500, 2000, and 2500 degrees Rankine. The wavenumber region extends approximately from 500 to 6000 inverse centimeters. The mass path lengths considered varied approximately from 0.00002 to 5.0 pounds mass per square foot. Equivalent pressures varied over the approximate range of from 0.3 to 13.5 atmospheres. The wavenumber region considered was sufficient to define the 15.0, 4.3, 2.7, and 2.0 micron absorption bands.

Values of the empirical spectral constants B^2, C^2, and BC are tabulated in Appendix A. There it will be noticed that some entries are C^2 = L, for large, B^2 = S, for small, and the product BC is given numerically. This product is used to evaluate Equation (III-1) for gas conditions where C^2 is very large and B^2 is very small, for then Equation (III-1) reduces to

$$\alpha_{g\nu} = 1 - \exp\left\{ - BC \sqrt{wP_e^{\,n}} \right\} \quad . \qquad \text{(III-2)}$$

Equations (III-1,2) were evaluated for all frequencies for which values of B^2 and C^2 or BC were available, and for the range of gas conditions mentioned above. Computation

was performed on an electronic computer. Typical results are illustrated in Figure 5. The programs used to calculate the approximately 150 curves typified by Figure 5 are listed in Appendix B.

Examination of these curves indicated the approximate absorption bandwidths of the 15.0, 4.3, 2.7, and 2.0 micron absorption bands could, in most cases, be defined. For some conditions, overlap of absorption bands occurred such that the absorptance was not zero at the boundary of a band. In this situation it was difficult to say where one band ended and another began. Therefore, it was necessary to either estimate the band limit, if possible, or consider the band limit undefined. In some other cases values of B^2 and C^2 or BC were not available at enough frequency points to define a band. In this situation, where practical, the band was defined by extrapolation or by assuming the band was symmetrical in shape. Otherwise the band was considered undefined.

From the above mentioned plots, measurements of absorption bandwidths of the 15.0, 4.3, 2.7, and 2.0 micron bands of carbon dioxide were made. This represents an affirmative answer to the first question raised in the introductory paragraph. Actual bandwidths of carbon dioxide at various gas conditions were determined.

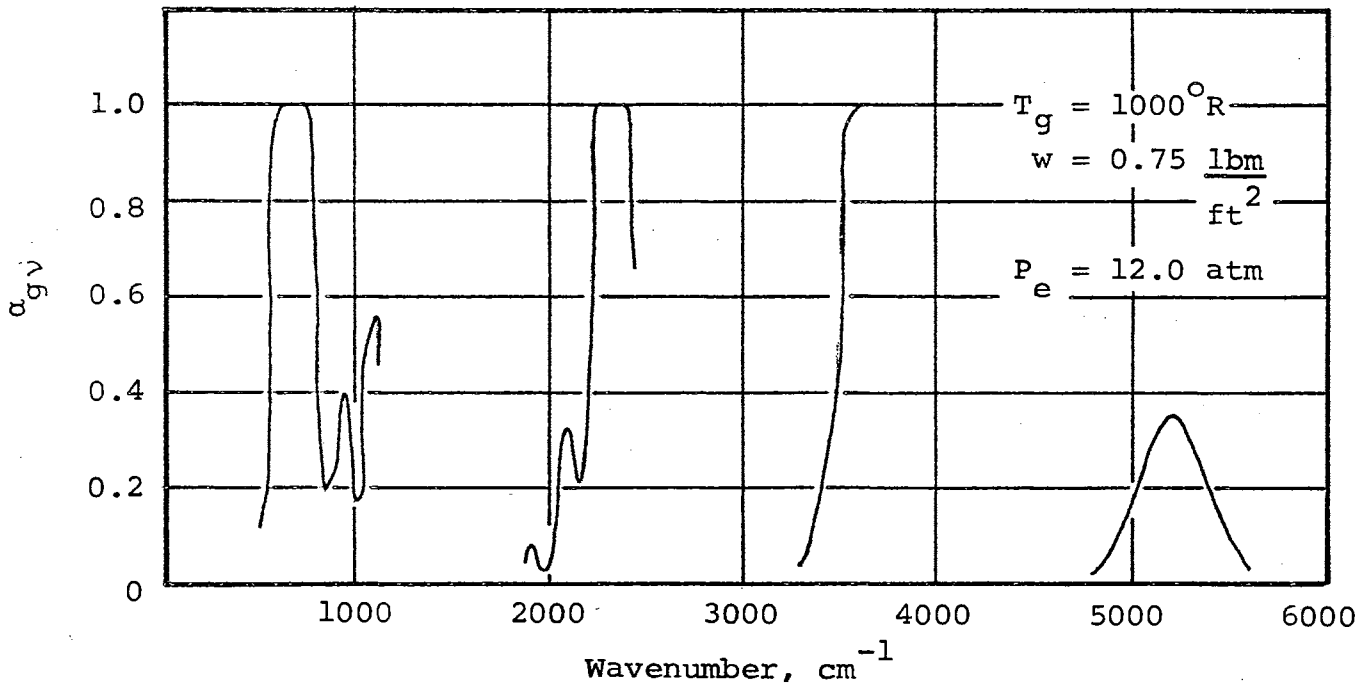

Figure 5. Spectral Absorptance of Carbon Dioxide Using Equation (III-1)

Correlation of Actual Bandwidths

The second question raised in the introductory paragraph of this chapter deals with the possibility of correlating the bandwidths of various carbon dioxide absorption bands with gas conditions. No attempt to correlate bandwidths directly with gas conditions was made, for several reasons. It has been shown that band absorption, $\mathcal{A}$, may be correlated with gas conditions using the weak and strong band correlation expressions. One might hope that average band absorption, $\mathcal{A}/\Delta\nu$, where $\Delta\nu$ is actual absorption bandwidth, might also be correlated in a manner similar to the correlation of $\mathcal{A}$. If such a correlation is possible, not only would values of $\mathcal{A}/\Delta\nu$ be directly available for use in the band equations of radiant exchange, but actual bandwidths could be calculated from the expression

$$\Delta\nu = \frac{\mathcal{A}}{(\mathcal{A}/\Delta\nu)} \quad . \qquad \text{(III-3)}$$

From plots of computer calculated spectral absorptance, actual absorption bandwidths were measured. From the corresponding computer calculated output listings of spectral absorptance, band absorption was calculated by numerical integration. A combination of Simpson's rule and the trapezoidal rule was used in the numerical integrations. From these results, values of $\mathcal{A}/\Delta\nu$ were calculated.

An attempt to correlate $a/\Delta\nu$ with weak and strong band expressions was made. The attempt results in correlations of the form

$$\frac{a}{\Delta\nu} = b_2 (w)^{m_2} \ (P_e)^{n_2} \qquad \text{(III-4)}$$

and

$$\frac{a}{\Delta\nu} = B_2 + M_2 \log w + N_2 \log P_e \quad , \qquad \text{(III-5)}$$

where, as previously defined,

$$P_e = P_{N_2} + 1.3 \ P_{CO_2} \quad , \qquad \text{(III-6)}$$

and b_2, m_2, n_2, B_2, M_2, and N_2 are correlation constants.

The method of correlation was that suggested in the report by Howard, Burch, and Williams (10). Values of $a/\Delta\nu$ for individual bands were plotted versus w on log-log scales with P_e as a parameter, for five temperatures from 535 to 2500 degrees Rankine. A typical plot is shown in Figure 6. All similar plots are presented in Appendix C. On the typical plot, Figure 6, at lower values of $a/\Delta\nu$, is indicated the weak band region. At higher values of $a/\Delta\nu$ the strong band region is indicated.

The weak band region, on log-log scales, shows the lines of $a/\Delta\nu$ versus w to be approximately linear, each with approximately the same slope, m_2. This indicates $a/\Delta\nu$ varies as w^{m_2}. Therefore, the ratio $(a/\Delta\nu)/w^{m_2}$ should not vary appreciably with w. This ratio when

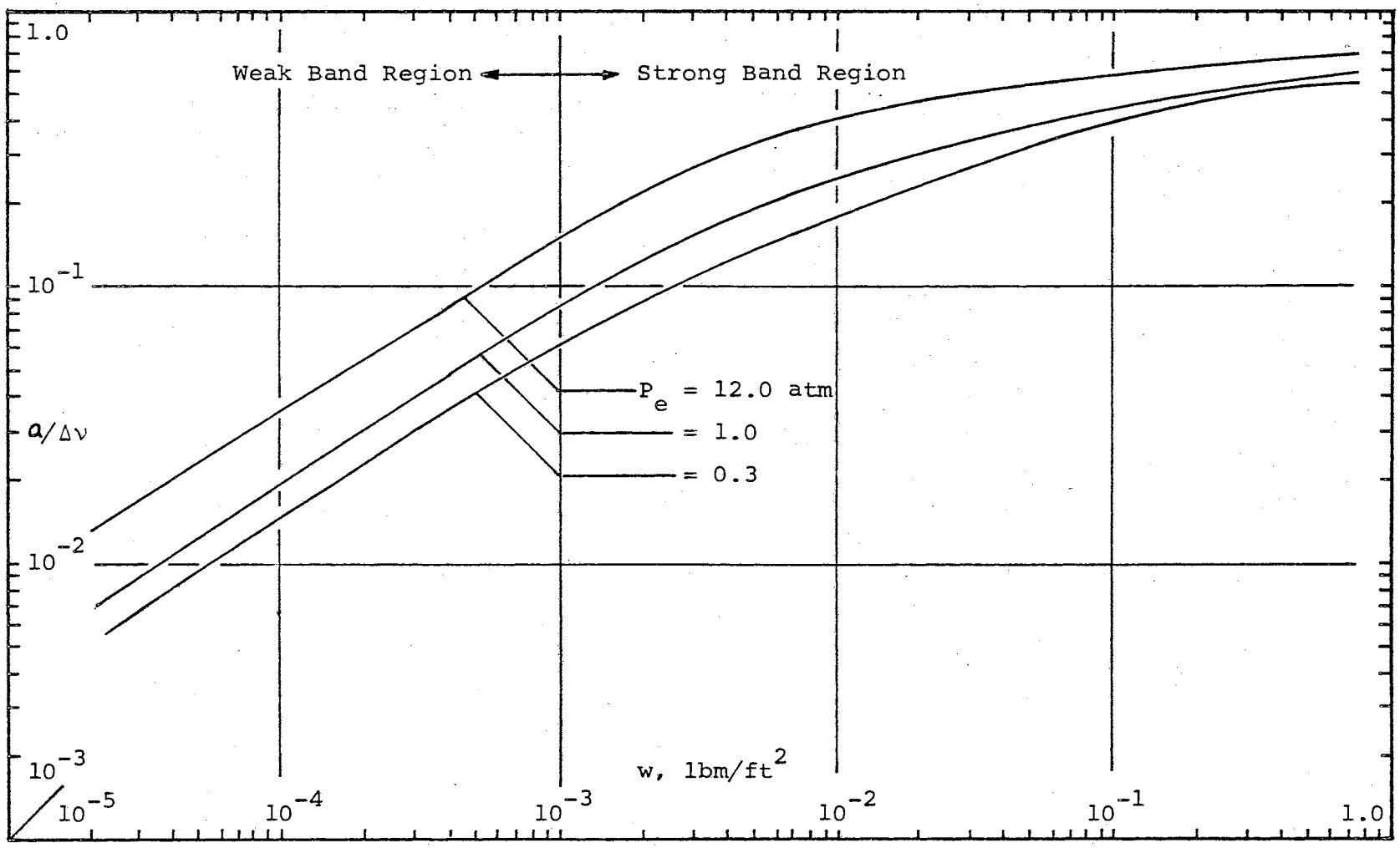

Figure 6. Variation of $a/\Delta\nu$ with Mass Path Length and Equivalent Pressure, 15.0μ - 1000°R

plotted against P_e on log-log scales, see Figure 7, results in a scatter of points which may be approximately represented by a single straight line, for all values of w, with a slope of n_2 and an intercept b_2. Therefore $(a/\Delta\nu)/w^{m_2}$ varies as $P_e^{n_2}$ and the weak band fit is

$$\frac{a}{\Delta\nu} = b_2 \ (w)^{m_2} \ (P_e)^{n_2} \quad .$$

To arrive at the strong band fit the strong band region values of $a/\Delta\nu$ are plotted versus w on semi-log scales, with P_e as a parameter, as shown in Figure 8. The lines of $a/\Delta\nu$ versus w are seen to be approximately linear, each with approximately the same slope, M_2. This indicates that $a/\Delta\nu$ is a function of M_2 log w. Therefore, $a/\Delta\nu - M_2$ log w should not vary appreciably with w. Figure 9 shows a plot of $a/\Delta\nu - M_2$ log w versus P_e on semi-log scales. For all values of w a single straight line with slope N_2 and intercept B_2 approximately represents the scatter of points. Therefore $a/\Delta\nu - M_2$ log w varies with N_2 log P_e and the strong band fit is

$$\frac{a}{\Delta\nu} = B_2 + M_2 \log w + N_2 \log P_e \quad .$$

By the above outlined correlation methods, values of the correlation constants b_2, m_2, n_2, B_2, M_2, and N_2 were determined. The results are tabulated in Table I . The band and temperature as well as the range of w and P_e

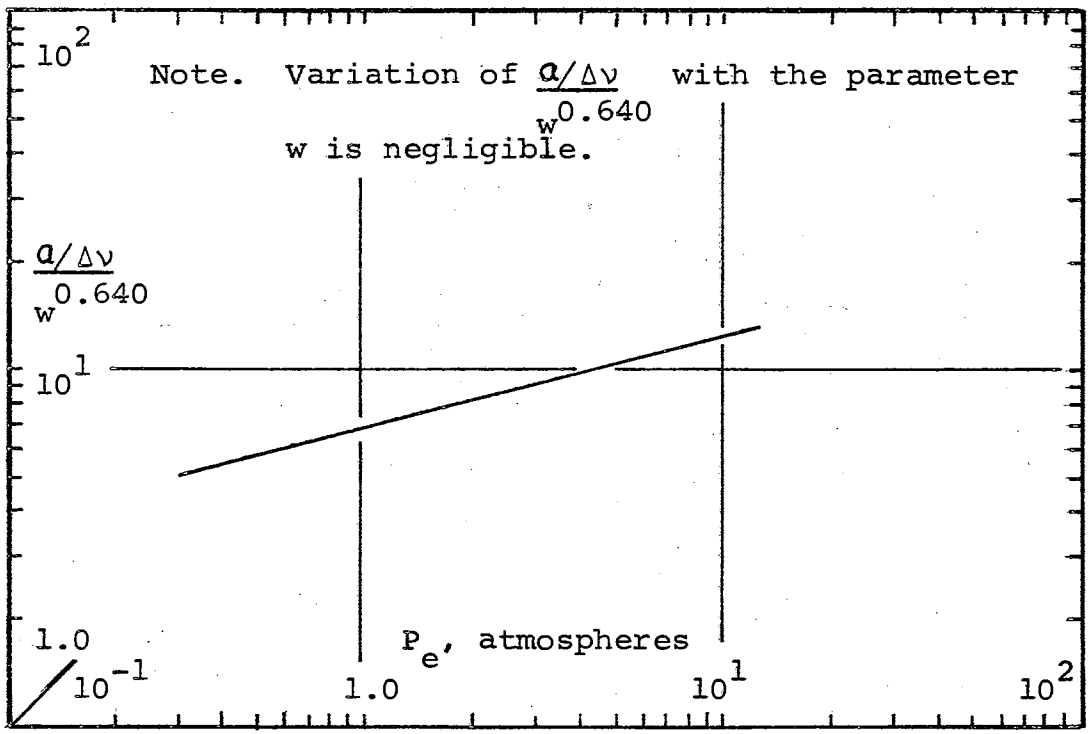

Figure 7. Weak Band Variation of $\frac{a/\Delta\nu}{w^{m_2}}$ with Mass Path Length and Equivalent Pressure, 15.0μ - 1000°R

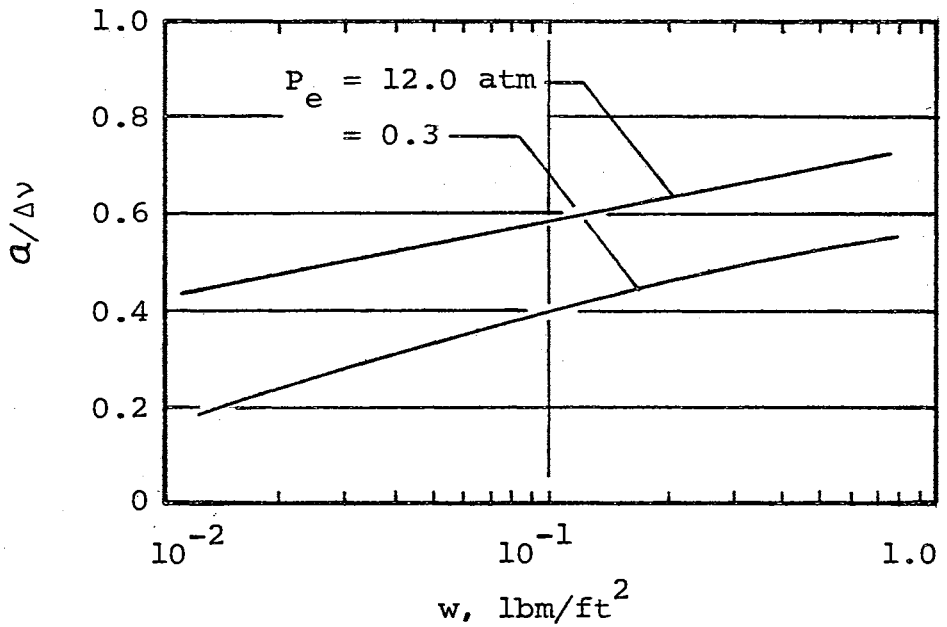

Figure 8. Variation of $\alpha/\Delta\nu$ with Mass Path Length and Equivalent Pressure, 15.0μ - 1000°R

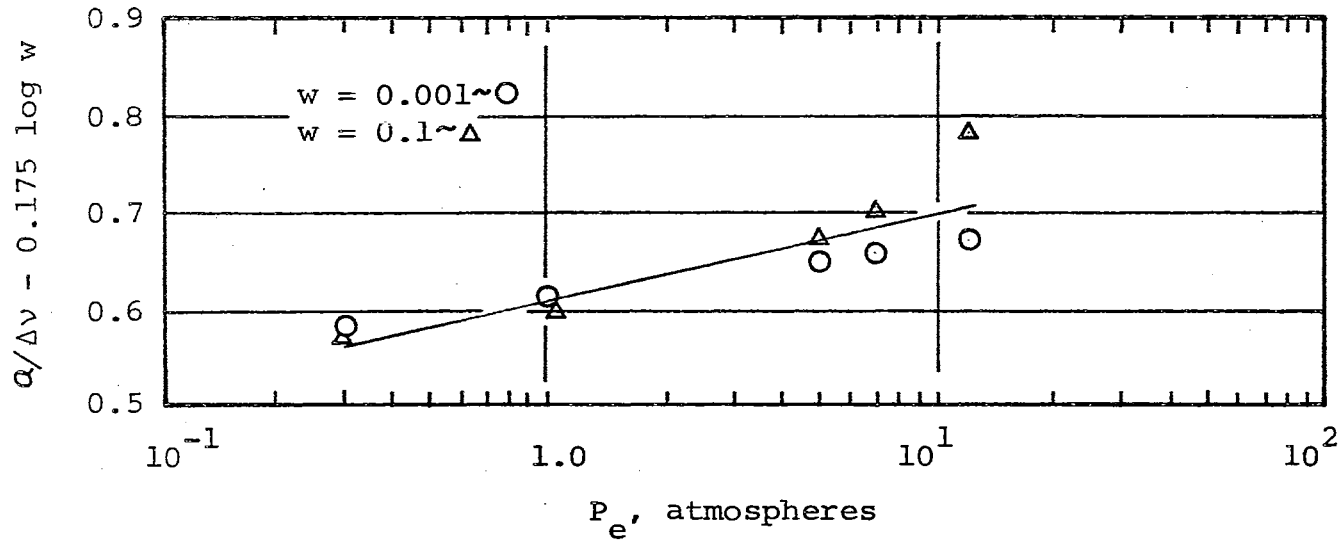

Figure 9. Strong Band Variation of $\alpha/\Delta\nu - M_2 \log w$ with Mass Path Length and Equivalent Pressure, 15.0μ - 1000°R

TABLE I

$a/\Delta\nu$ CORRELATION CONSTANTS

Band μ	T_g °R	w_L lbm/ft^2	w_U lbm/ft^2	Pe_L atm	Pe_U atm	Weak Fit b_2	Weak Fit m_2	Weak Fit n_2	Strong Fit B_2	Strong Fit M_2	Strong Fit N_2
	535	.00004	.001	.3	13.5	7.75	.631	.252			
	535	.001	5.	.3	13.5				.520	.142	.075
	1000	.00002	.001	.3	12.	6.90	.640	.261			
	1000	.001	.75	.3	12.				.612	.175	.092
15.0	1500	.0001	.001	.3	12.	17.2	.721	.0346			
	1500	.001	.5	.3	12.				.755	.203	.092
	2000	.0001	.001	.3	12.	21.0	.721	.0360			
	2000	.001	.387	.3	12.				.833	.225	.100
	2500	.0017	.3	.65	12.				.842	.217	.095
	535	.00004	5.	.3	13.5				.755	.15	.094
	1000	.00002	.001	.3	12.	2.25	.315	.306			
	1000	.001	.75	.3	12.				.75	.15	.095
	1500	.0001	.001	.3	12.	4.9	.482	.229			
4.3	1500	.001	.5	.3	12.				.56	.115	.075
	2000	.0001	.01	.3	12.	2.75	.360	.0135			
	2000	.01	.387	.3	12.				.621	.069	.046
	2500	.0017	.01	.65	12.	1.14	.329	.0852			
	2500	.01	.3	.65	12.				.630	.199	.084
	535	.00004	.01	.3	13.5	.800	.360	.369			
	535	.01	5.	.3	13.5				.45	.110	.115
	1000	.00002	.02	.3	12.	.705	.360	.297			
	1000	.02	.75	.3	12.				.470	.150	.125
	1500	.0001	.01	.3	12.	1.53	.495	.221			
2.7	1500	.01	.5	.3	12.				.545	.185	.129
	2000	.001	.01	.3	12.	3.51	.604	.116			
	2000	.01	.387	.3	12.				.610	.190	.086
	2500	.0017	.01	.65	12.	3.41	.586	.176			
	2500	.01	.3	.65	12.				.727	.234	.120
	535	.1	1.	.3	13.5	.091	.523	.252			
	535	1.	5.	.3	13.5	.090	.378	.297			
	1000	.01	.1	.3	12.	.124	.617	.212			
2.0	1000	.1	.75	.3	12.	.103	.545	.230			
	1500	.001	.5	.3	12.	.094	.414	.342			
	2000	.01	.387	.3	12.	.117	.464	.345			
	2500	.01	.3	.65	12.	.143	.568	.243			

for the weak and strong band fits are indicated.

In order to calculate $\Delta\nu$ from Equation (III-3) correlations of α are required. Correlations of α, for example those of Edwards (8, 9, 28, 29), exist in the literature. One could use these correlations of α in Equation (III-3) to calculate $\Delta\nu$. This is not completely satisfactory, however, because of the possibility of Edwards assigning band limits different than the band limits assigned in this study to the same band at the same conditions. As mentioned before, this can occur because of band overlap, poorly defined bands, or can result from differences in experimentally determined spectral absorptance compared to the semi-empirical curves used in this study. Therefore, to be consistent, band absorption was correlated in a manner similar to the $\alpha/\Delta\nu$ correlations. The results are tabulated in Table II. Correlation constants b_1, m_1, n_1, B_1, M_1, and N_1 are presented for use with the expressions

$$\alpha = b_1 \ (w)^{m_1} \ (P_e)^{n_1} \qquad \text{(III-7)}$$

and

$$\alpha = B_1 + M_1 \log w + N_1 \log P_e \ . \qquad \text{(III-8)}$$

The correlation constants are presented for the 15.0, 4.3, 2.7, and 2.0 micron bands for the same range of conditions as the $\alpha/\Delta\nu$ correlations. Plots of α versus w on log-log scales, with P_e as parameter, are presented in Appendix D.

TABLE II

α CORRELATION CONSTANTS

Band μ	T_g °R	w_L lbm/ft^2	w_U lbm/ft^2	P_{e_L} atm	P_{e_U} atm	Weak Fit b_1	Weak Fit m_1	Weak Fit n_1	Strong Fit B_1	Strong Fit M_1	Strong Fit N_1
15.0	535	.00004	.0025	.3	13.5	1150.	.622	.266			
	535	.0025	5.	.3	13.5				167.	52.	25.
	1000	.00002	.003	.3	12.	1540.	.622	.243			
	1000	.003	.75	.3	12.				258.	83.	31.
	1500	.0001	.002	.3	12.	20800.	.923	.0333			
	1500	.002	.5	.3	12.				310.	93.	34.
	2000	.0001	.0015	.3	12.	25500.	.928	.0315			
	2000	.0015	.387	.3	12.				343.	98.	38.
	2500	.0017	.01	.65	12.	1900.	.523	.0405			
	2500	.01	.3	.65	12.				377.	108.	36.
4.3	535	.00004	.0001	.3	13.5	1470.	.432	.288			
	535	.0001	5.	.3	13.5				169.	33.	24.
	1000	.000025	.001	.3	12.				198.	39.	24.
	1000	.001	.75	.3	12.				222.	46.	30.
	1500	.0007	.5	.3	12.				315.	79.	32.
	2000	.0001	.001	.3	12.	8600.	.662	.0315			
	2000	.001	.387	.3	12.				513.	138.	56.
	2500	.004	.3	.65	12.				217.	77.	38.
2.7	535	.00004	.01	.3	13.5	460.	.450	.378			
	535	.01	5.	.3	13.5				245.	91.	73.
	1000	.00002	.01	.3	12.	970.	.495	.360			
	1000	.01	.75	.3	12.				423.	160.	122.
	1500	.0001	.01	.3	12.	2190.	.635	.284			
	1500	.01	.5	.3	12.				508.	194.	113.
	2000	.001	.01	.3	12.	3300.	.734	.135			
	2000	.01	.387	.3	12.				520.	212.	107.
	2500	.0017	.01	.65	12.	3200.	.649	.176			
	2500	.01	.3	.65	12.				585.	212.	138.
2.0	535	.1	5.	.3	13.5	73.	.536	.302			
	1000	.01	.75	.3	12.	96.	.743	.320			
	1500	.001	.5	.3	12.	89.	.518	.378			
	2000	.01	.387	.3	12.	108.	.518	.374			
	2500	.01	.3	.65	12.	212.	.748	.243			

From these curves the correlation constants were determined.

Validity of Correlation Expressions

The curves of $\alpha/\Delta\nu$ in Appendix C and α in Appendix D were obtained by fairing through raw data determined from computer-calculated results. To these faired curves, the correlation expressions for α and $\alpha/\Delta\nu$ were fitted, as discussed previously in this chapter. The correlation expressions only approximately fit the α and $\alpha/\Delta\nu$ curves. For some conditions of mass path length and equivalent pressure the correlation expressions fit the curves better than for other conditions. This is illustrated in Figure 10 where, for the 15 micron band at a gas temperature of 535 degrees Rankine, the correlation expressions for $\alpha/\Delta\nu$ at the lowest and highest equivalent pressures are plotted along with the computer-determined curves of $\alpha/\Delta\nu$. Figure 10 is typical of similar curves, plotted for all bands and gas temperatures considered, which are presented in Appendix C. Band absorption comparisons, similar to Figure 10, are presented in Appendix D.

Figure 10 indicates the largest percent deviation of correlation expression value from the computer-determined value occurs at the value of mass path length where transition of weak band to strong band fit takes place,

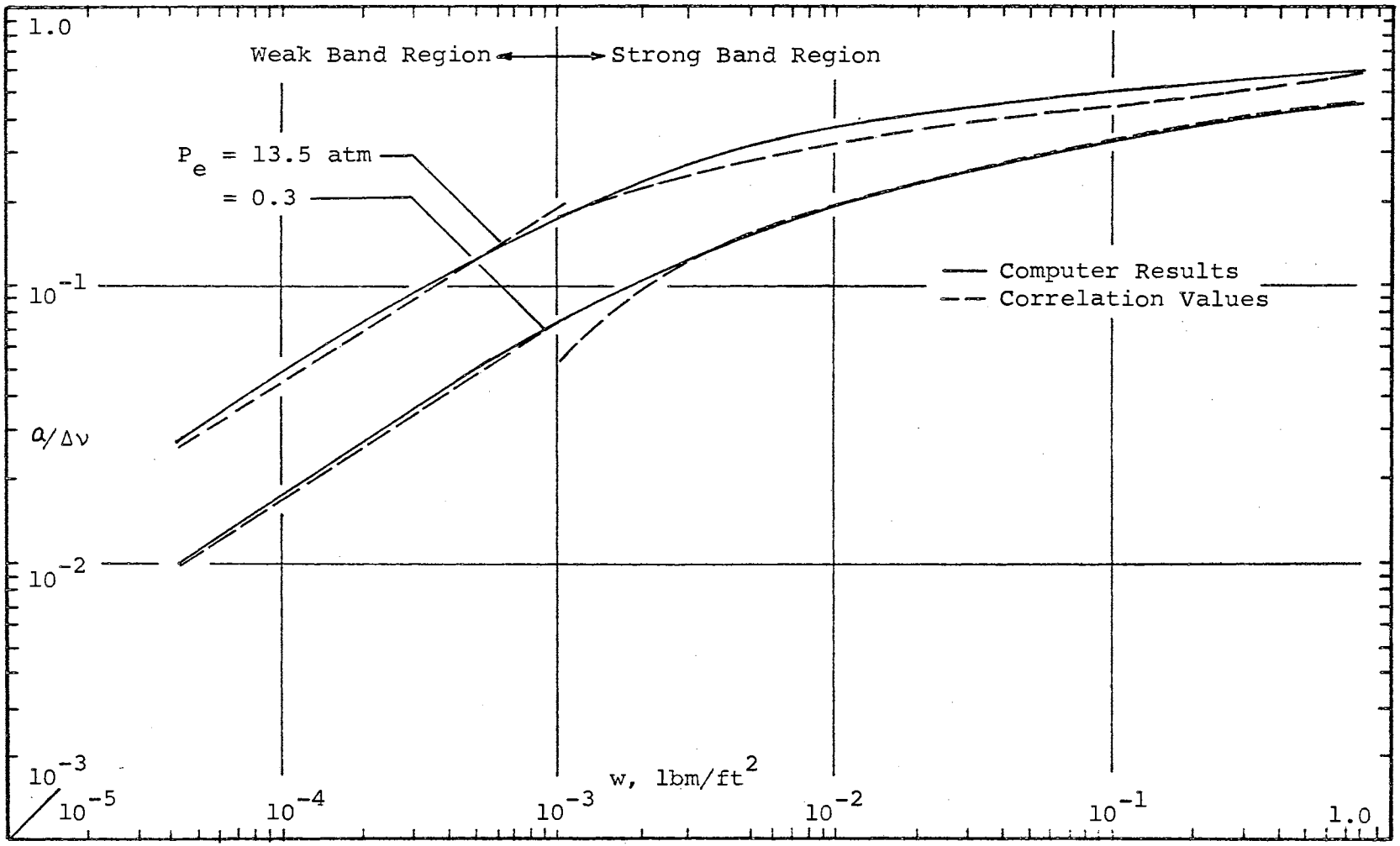

Figure 10. Comparison of Correlation Expressions with Computer Determined Values, 15.0μ - 535°R

and for the lowest value of equivalent pressure at this point. In Figure 10 a deviation of -26 percent occurs at this point for the strong band fit. Inspection of Appendices C and D indicates this maximum deviation to range as high as 70 percent.

At mass path lengths not too close to the transition value, Figure 10 indicates both the weak and strong band expressions fit the computer-determined curves well. Examination of Appendices C and D reveals typical deviations within ± 20 percent.

The real test of the validity of the correlations of α and $\alpha/\Delta\nu$ presented in Tables I and II occurs when they are used in heat transfer calculations. In Chapter IV a radiant heat transfer problem is posed and solved using the correlation expressions in the band equations of radiative exchange.

CHAPTER IV

AN APPLICATION OF RESULTS

In this chapter an example problem of radiative exchange in an enclosure is posed and surface radiant heat transfer calculated. The band equations of radiant exchange are used with the correlations of a and $a/\Delta\nu$ to solve the problem.

In order to assess the worth of the a and $a/\Delta\nu$ correlations as used in the band equations, a standard of comparison is required. Therefore, the solution of the problem using the band equations is compared to a solution resulting from use of the more exact monochromatic equations of radiative exchange. For further comparison, the results using the band method are compared to results calculated from application of the less exact gray method discussed in Chapter II.

Definition of Problem

Consider an infinitely long square duct containing a mixture of carbon dioxide and nitrogen gases. It is desired to calculate the radiant heat transfer per unit area and

per unit time to the surfaces of the duct.

The square duct is depicted in Figure 11. The cross-sectional area of the duct is assumed to be one square foot. Since the duct is assumed infinitely long, no net longitudinal heat exchange takes place. Therefore, the heat transfer to each of the four surfaces indicated in Figure 11 need only be calculated on a per-square-foot basis. The surface temperatures are assumed to be:

$$T_1 = 1000^\circ R$$

$$T_2 = 800^\circ R$$

$$T_3 = 800^\circ R$$

$$T_4 = 1000^\circ R$$

The surfaces are assumed to be of the same material: Type 321 corrosion-resistant stainless steel, sample number 18, as listed in Chapter 2 of the text by Kreith (34). Kreith gives tabulated values of spectral reflectance for this material and this property is plotted in Figure 12.

The duct is assumed to contain an isothermal ideal gas mixture of carbon dioxide and nitrogen. The assumed gas conditions are:

$$T_g = 1000^\circ R$$

$$P_{TOT} = 1.0 \text{ atm}$$

$$x_{CO_2} = 0.2,$$

where T_g is gas temperature, P_{TOT} is the total mixture

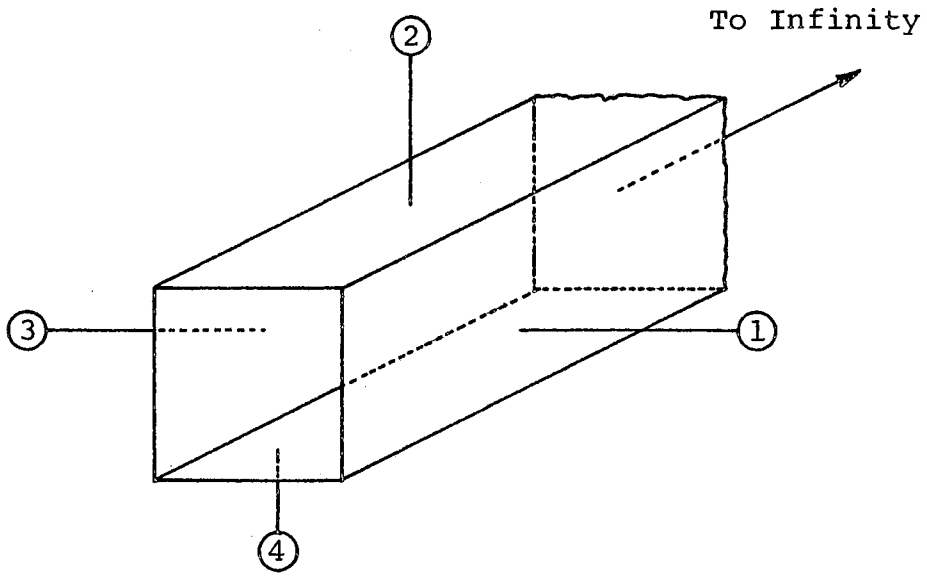

Figure 11. Infinitely Long Square Duct

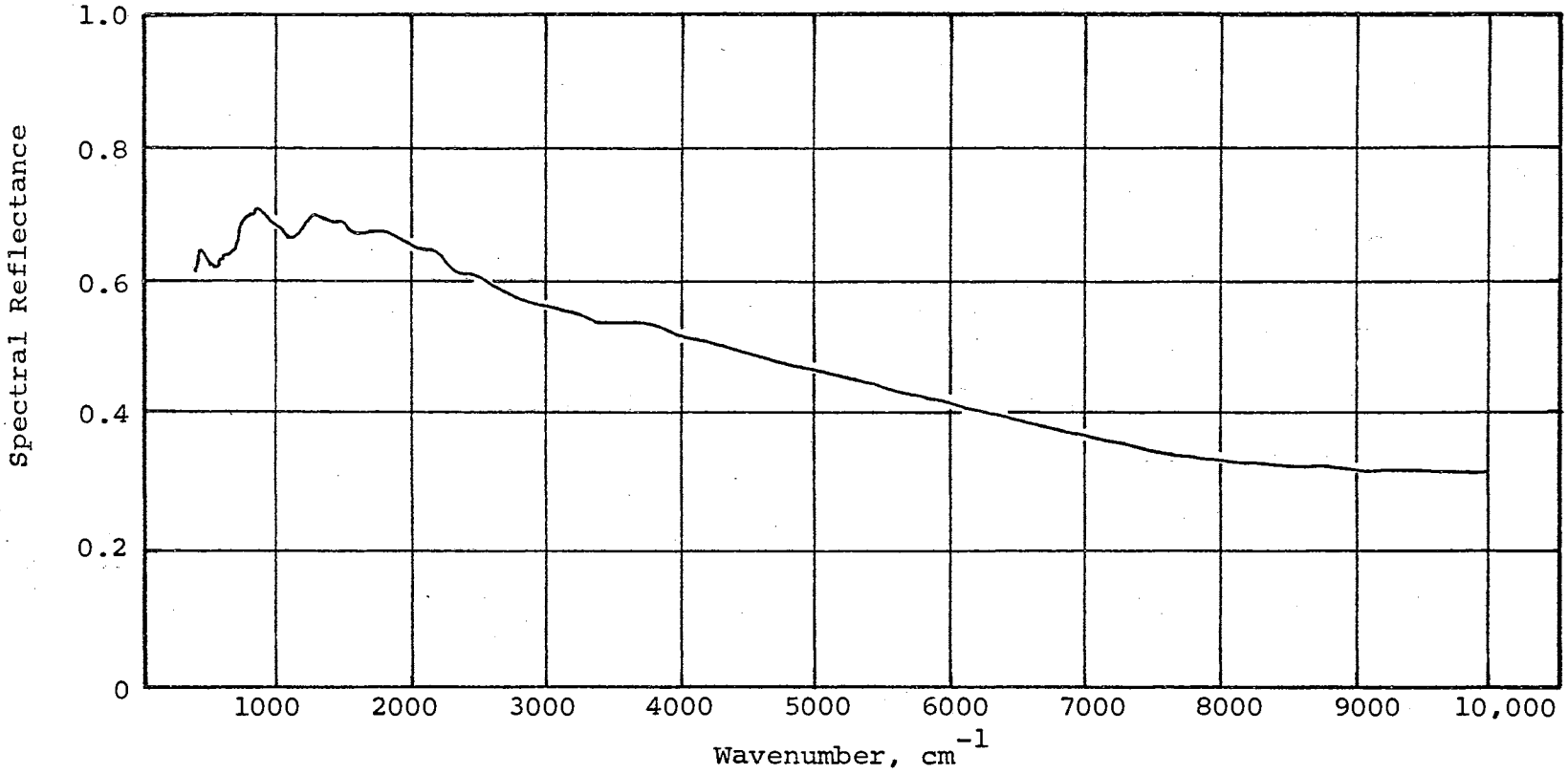

Figure 12. Spectral Reflectance of Duct Wall

pressure, and x_{CO_2} is the mole fraction of carbon dioxide.

For the geometry of this problem, any pair of surfaces of the duct are distinguished as either equal, parallel, opposed rectangles, or equal, perpendicular, adjacent rectangles. For these cases, the paper by R. V. Dunkle (31) may be used to obtain configuration factors and geometric mean beam lengths. The values are tabulated in Tables III and IV. These two tables indicate the configuration factor for the opposed surfaces is, $F_{opp} = 0.414$, and for the adjacent surfaces is $F_{adj} = 0.293$; the geometric mean beam length for the opposed surfaces is, $\bar{r}_{opp} = 1.35$ feet and, for the adjacent surfaces is, $\bar{r}_{adj} = 0.75$ feet. Values of zero are entered in Table III and IV for the configuration factors and geometric mean beam lengths of each surface to itself. This indicates the surfaces cannot "see" themselves.

Solution of Problem Using Band Equations

Values of $\mathcal{A}$ and $\mathcal{A}/\Delta\nu$ may be calculated from the correlation expressions presented in Chapter III, Equations (III-4, 5, 7, 8). To use these expressions and to read the correlation constants from Tables I and II of Chapter III, mass path lengths and equivalent pressure are required.

TABLE III

CONFIGURATION FACTOR, F_{jk}

j \ k	1	2	3	4
1	0	.293	.414	.293
2	.293	0	.293	.414
3	.414	.293	0	.293
4	.293	.414	.293	0

TABLE IV

GEOMETRIC MEAN BEAM LENGTH, $\bar{r}_{jk}$

j \ k	1	2	3	4
1	0	.75	1.35	.75
2	.75	0	.75	1.35
3	1.35	.75	0	.75
4	.75	1.35	.75	0

Mass path length is the product, $\rho_{CO_2}\bar{r}_{jk}$. Since ideal gases are assumed,

$$\rho_{CO_2} = \frac{P_{CO_2}}{R_{CO_2}T_g} \quad , \tag{IV-1}$$

where P_{CO_2} is the partial pressure of carbon dioxide and R_{CO_2} is the carbon dioxide gas constant which has the value, 35.12 ft-lbf/lbm-°R. Therefore, mass path length may be calculated from

$$w_{jk} = \rho_{CO_2}\bar{r}_{jk} = \frac{P_{CO_2}}{R_{CO_2}T_g}\bar{r}_{jk} \quad . \tag{IV-2}$$

Since $P_{CO_2} = x_{CO_2}P_{TOT}$, Equation (IV-2) may be rewritten as

$$w_{jk} = \frac{x_{CO_2}P_{TOT}}{R_{CO_2}T_g}\bar{r}_{jk} \quad . \tag{IV-3}$$

Substituting the values:

$$x_{CO_2} = 0.2$$

$$P_{TOT} = 1.0 \text{ atm}$$

$$R_{CO_2} = 35.12 \text{ ft-lbf/lbm-°R}$$

$$T_g = 1000°R$$

$$\bar{r}_{adj} = 0.75 \text{ ft}$$

$$\bar{r}_{opp} = 1.35 \text{ ft} \quad ,$$

into Equation (IV-3) results in mass path lengths of $w_{adj} = 0.00904$ lbm/ft^2, for adjacent rectangles, and $w_{opp} = 0.0163$ lbm/ft^2, for opposed rectangles.

The equivalent pressure has been previously defined, Equation (II-9), and may be calculated as follows:

$$P_e = P_{N_2} + b\, P_{CO_2}$$

$$= x_{N_2}\, P_{TOT} + 1.3\, x_{CO_2}\, P_{TOT}$$

$$= (1 - x_{CO_2})\, P_{TOT} + 1.3\, x_{CO_2}\, P_{TOT}$$

$$= (1 - 0.2)(1.0) + (1.3)(0.2)(1.0)$$

$$= 1.06 \text{ atm},$$

where the relations* $P_{N_2} = x_{N_2}\, P_{TOT}$, $P_{CO_2} = x_{CO_2}\, P_{TOT}$, and $x_{N_2} = 1 - x_{CO_2}$ and the value b = 1.3 have been used.

Tables I and II of Chapter III may now be entered for purposes of calculating values of α and $\alpha/\Delta\nu$. Since two nonzero values of w_{jk} appear in the example problem, two nonzero values each for α and $\alpha/\Delta\nu$, for each band, may be calculated. These values are tabulated in Table V under the headings α_{opp} and $(\alpha/\Delta\nu)_{opp}$ for opposed rectangles and α_{adj} and $(\alpha/\Delta\nu)_{adj}$ for adjacent rectangles. Also listed in Table V are values of $\Delta\nu_{opp}$, where

$$\Delta\nu_{opp} = \frac{\alpha_{opp}}{(\alpha/\Delta\nu)_{opp}} \quad ,$$

---

* The nitrogen partial pressure is P_{N_2} and x_{N_2} is the nitrogen mole fraction.

TABLE V

BAND ABSORPTION DATA

Band	$\mathcal{A}_{opp}$ cm^{-1}	$\mathcal{A}_{adj}$ cm^{-1}	$(\mathcal{A}/\Delta\nu)_{opp}$	$(\mathcal{A}/\Delta\nu)_{adj}$	$\mathcal{A}_{adj}/\Delta\nu_{opp}$	$\Delta\nu_{opp}$ cm^{-1}	$\Delta\nu_{adj}$ cm^{-1}
15.0μ	110.4	89.1	0.301	0.257	0.243	367.	347.
4.3μ	140.5	128.7	0.484	0.446	0.444	290.	289.
2.7μ	129.0	96.4	0.163	0.132	0.122	791.	730.
2.0μ	4.6	3.0	0.010	0.007	0.006	464.	430.

and $\Delta\nu_{adj}$, where

$$\Delta\nu_{adj} = \frac{a_{adj}}{(a/\Delta\nu)_{adj}} \quad .$$

Table V, in addition, contains values of $a_{adj}/\Delta\nu_{opp}$, the use of which in the band equations is indicated later in this section.

For each absorption band in Table V, two bandwidths are listed. In order that the solution of the exchange equations for each band be valid over only one bandwidth, the equations are solved for the widest bandwidth, $\Delta\nu_{opp}$, although $\Delta\nu_{adj}$ is incorporated in the band equations.

Actual band and window limits may now be defined from values of $\Delta\nu_{opp}$. Since values of $\Delta\nu_{adj}$ are incorporated in the band equations, corresponding band and window limits are also required. It is assumed that band limits may be calculated from the expressions

$$\nu_L = \nu_C - \frac{\Delta\nu}{2} \qquad \text{(IV-4)}$$

and

$$\nu_U = \nu_C + \frac{\Delta\nu}{2} \quad , \qquad \text{(IV-5)}$$

where ν_L and ν_U are the lower and upper band limits, respectively, and ν_C is approximately the center wavenumber of the band. The center wavenumber may be approximately calculated from the wavelength band designation, e.g.,

$$\nu_C = \frac{10{,}000}{\lambda_C} = [\mathrm{cm}^{-1}] \quad ,$$

where λ_c is 15.0, 4.3, 2.7, and 2.0 microns for the four bands considered in this study. Calculation of band limits from Equation (IV-4, 5) involves the assumption that the absorption band is symmetrical about the center wavenumber. This is an approximation which is not too unrealistic in some cases. The approximation is justified by simplicity and because heat transfer results are not drastically affected. The opposed and adjacent band and window limits are schematically illustrated in Figure 13.

The spectrum is seen in Figure 13 to be divided into nine regions composed of five windows and four bands. For each of the opposed regions it is possible to obtain an average reflectance using the expression

$$\bar{\rho}_{\Delta\nu_{opp}} = \frac{\int_{\Delta\nu_{opp}} \rho_\nu d\nu}{\Delta\nu_{opp}} \quad .$$

This expression was evaluated for each opposed region using numerical integration of the spectral reflectance data plotted in Figure 12. The results are tabulated in Table VI. Also tabulated in Table VI is average emittance of each of the nine opposed regions. This average emittance was calculated from the approximate relation

$$\bar{\epsilon}_{\Delta\nu_{opp}} = 1 - \bar{\rho}_{\Delta\nu_{opp}} \quad .$$

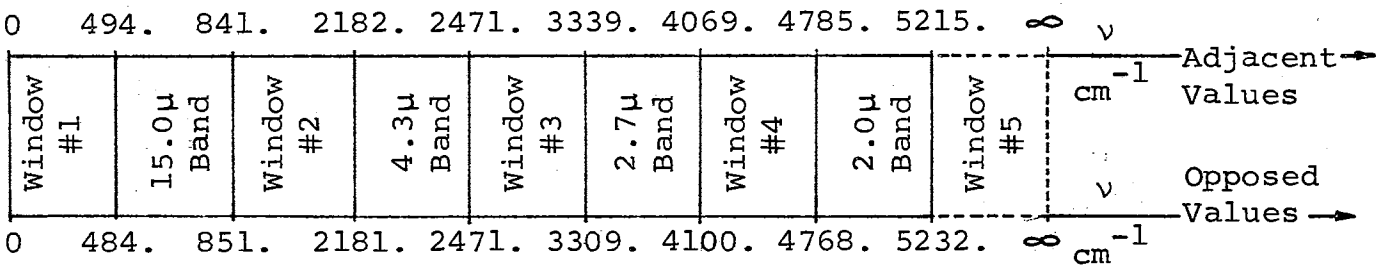

Figure 13. Band And Window Limits

TABLE VI

BAND AND WINDOW AVERAGE REFLECTANCE AND EMITTANCE

Region	$\bar{\rho}_{\Delta\nu_{opp}}$	$\bar{\varepsilon}_{\Delta\nu_{opp}}$
Window #1	0.64	0.36
15.0 μ Band	0.65	0.35
Window # 2	0.68	0.32
4.3 μ Band	0.62	0.38
Window # 3	0.57	0.43
2.7 μ Band	0.54	0.46
Window # 4	0.50	0.50
2.0 μ Band	0.47	0.53
Window # 5	0.39	0.61

Knowing the band limits allows one to enter tabulations of Planck's functions such as those in Wiebelt's text (1), and obtain values of black-body emissive power for the four surfaces of the enclosure and for the gas, for each of the nine regions. These values are required for the opposed regions. In addition, the adjacent region values of gas black-body emissive power are required, as is shown later in this section. These values are listed in Table VII.

The input values required to use Equation (I-17) for evaluation of surface radiosity are now collected. Equation (I-17) is rewritten below with several changes in notation,

$$J_{j\Delta\nu_{opp}} = \bar{\epsilon}_{j\Delta\nu_{opp}} E_{bj\Delta\nu_{opp}} + \bar{\rho}_{j\Delta\nu_{opp}} \sum_{k=1}^{4} \left[\left(1 - \frac{a_{jk}}{\Delta\nu_{opp}}\right) J_{k\Delta\nu_{opp}} + \frac{a_{jk}}{\Delta\nu_{jk}} E_{bg\Delta\nu_{jk}} \right] F_{jk} ,$$

$$j = 1, 2, 3, 4 . \qquad \text{(IV-8)}$$

In Equation (IV-8) band absorption has been given the subscript jk to indicate it varies with $\bar{r}_{jk}$. The emission term, $\left(\frac{a_{jk}}{\Delta\nu_{jk}}\right) E_{bg\Delta\nu_{jk}}$, implies that the emission of the gas may be calculated as if it occurred partially over $\Delta\nu_{opp}$ and partially over $\Delta\nu_{adj}$ even though the required quantity is the emission over the largest (opposed) bandwidth, $\Delta\nu_{opp}$. That these viewpoints are equivalent when jk refers

TABLE VII

REGION VALUES OF BLACK-BODY EMISSIVE POWER

Region	$E_{b1\Delta\nu_{opp}} = E_{b4\Delta\nu_{opp}} = E_{bg\Delta\nu_{opp}}$ Btu/hr-ft^2	$E_{b2\Delta\nu_{opp}} = E_{b3\Delta\nu_{opp}}$ Btu/hr-ft^2	$E_{bg\Delta\nu_{adj}}$ Btu/hr-ft^2
Window # 1	105.0	76.6	111.0
15.0 μ Band	275.0	161.4	260.0
Window # 2	1038.7	412.4	1048.7
4.3 μ Band	105.4	23.6	104.7
Window # 3	143.3	23.7	145.5
2.7 μ Band	35.1	3.4	31.8
Window # 4	7.6	.5	8.4
2.0 μ Band	3.0	.1	1.7
Window # 5	0	0	1.2

to opposed rectangles follows from definition of terms. One may reason that they are also equivalent when jk refers to adjacent rectangles. The emission in the wide band, $\Delta\nu_{opp}$, is equal to the sum of the emission over three spectral regions. The three regions are schematically indicated in Figure 14. The emittance in regions one and three is zero for adjacent rectangles, which implies the emission is zero in these regions. Therefore, the emission in $\Delta\nu_{opp}$ is equal to the emission in $\Delta\nu_{adj}$ for adjacent rectangles.

One may expand the sum over k in Equation (IV-8) and write the resulting expression four times for the four values of j. These four expressions may each be rearranged to collect coefficients of the four unknowns, $J_{j\Delta\nu_{opp}}$, $j = 1, 2, 3, 4$. These last four expressions may be represented in matrix notation as shown in Equation (IV-9).

Expression (IV-9) represents four equations in the four unknown surface radiosities. From inspection of the duct geometry and surface temperature distribution and since the surfaces are all of the same material, one may deduce the $J_{4\Delta\nu_{opp}} = J_{1\Delta\nu_{opp}}$ and $J_{3\Delta\nu_{opp}} = J_{2\Delta\nu_{opp}}$. Making these substitutions, only the first two equation in Expression(IV-9) need be solved for the two unknowns, $J_{1\Delta\nu_{opp}}$ and $J_{2\Delta\nu_{opp}}$. Rewiting the first two equations of Expression (IV-9) with

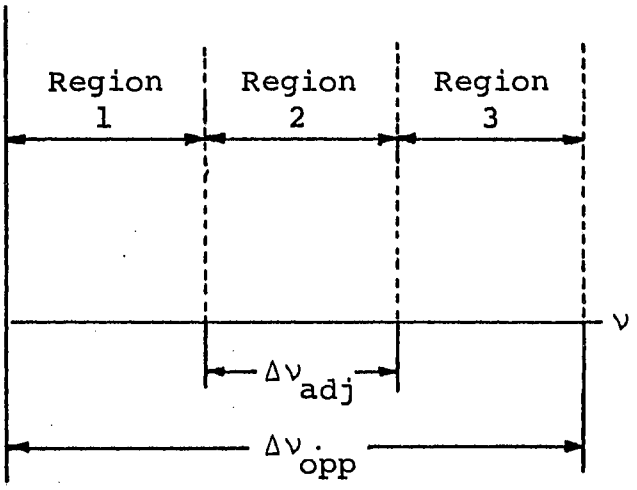

Figure 14. Emission from $\Delta\nu_{opp}$

$$
\begin{pmatrix}
1 & -\bar{\rho}_{1\Delta\nu_{opp}}\left(1-\frac{a_{12}}{\Delta\nu_{opp}}\right)F_{12} & -\bar{\rho}_{1\Delta\nu_{opp}}\left(1-\frac{a_{13}}{\Delta\nu_{opp}}\right)F_{13} & -\bar{\rho}_{1\Delta\nu_{opp}}\left(1-\frac{a_{14}}{\Delta\nu_{opp}}\right)F_{14} \\
-\bar{\rho}_{2\Delta\nu_{opp}}\left(1-\frac{a_{21}}{\Delta\nu_{opp}}\right)F_{21} & 1 & -\bar{\rho}_{2\Delta\nu_{opp}}\left(1-\frac{a_{23}}{\Delta\nu_{opp}}\right)F_{23} & -\bar{\rho}_{2\Delta\nu_{opp}}\left(1-\frac{a_{24}}{\Delta\nu_{opp}}\right)F_{24} \\
-\bar{\rho}_{3\Delta\nu_{opp}}\left(1-\frac{a_{31}}{\Delta\nu_{opp}}\right)F_{31} & -\bar{\rho}_{3\Delta\nu_{opp}}\left(1-\frac{a_{32}}{\Delta\nu_{opp}}\right)F_{32} & 1 & -\bar{\rho}_{3\Delta\nu_{opp}}\left(1-\frac{a_{34}}{\Delta\nu_{opp}}\right)F_{34} \\
-\bar{\rho}_{4\Delta\nu_{opp}}\left(1-\frac{a_{41}}{\Delta\nu_{opp}}\right)F_{41} & -\bar{\rho}_{4\Delta\nu_{opp}}\left(1-\frac{a_{42}}{\Delta\nu_{opp}}\right)F_{42} & -\bar{\rho}_{4\Delta\nu_{opp}}\left(1-\frac{a_{43}}{\Delta\nu_{opp}}\right)F_{43} & 1
\end{pmatrix}
$$

(IV-9)

$$
=
\begin{pmatrix}
\bar{\rho}_{1\Delta\nu_{opp}}\left[\frac{a_{12}}{\Delta\nu_{12}}F_{12}E_{bg\Delta\nu_{12}}+\frac{a_{13}}{\Delta\nu_{13}}F_{13}E_{bg\Delta\nu_{13}}+\frac{a_{14}}{\Delta\nu_{14}}F_{14}E_{bg\Delta\nu_{14}}\right]+\bar{\epsilon}_{1\Delta\nu_{opp}}E_{b1\Delta\nu_{opp}} \\
\bar{\rho}_{2\Delta\nu_{opp}}\left[\frac{a_{21}}{\Delta\nu_{21}}F_{21}E_{bg\Delta\nu_{21}}+\frac{a_{23}}{\Delta\nu_{23}}F_{23}E_{bg\Delta\nu_{23}}+\frac{a_{24}}{\Delta\nu_{24}}F_{24}E_{bg\Delta\nu_{24}}\right]+\bar{\epsilon}_{2\Delta\nu_{opp}}E_{b2\Delta\nu_{opp}} \\
\bar{\rho}_{3\Delta\nu_{opp}}\left[\frac{a_{31}}{\Delta\nu_{31}}F_{31}E_{bg\Delta\nu_{31}}+\frac{a_{32}}{\Delta\nu_{32}}F_{32}E_{bg\Delta\nu_{32}}+\frac{a_{34}}{\Delta\nu_{34}}F_{34}E_{bg\Delta\nu_{34}}\right]+\bar{\epsilon}_{3\Delta\nu_{opp}}E_{b3\Delta\nu_{opp}} \\
\bar{\rho}_{4\Delta\nu_{opp}}\left[\frac{a_{41}}{\Delta\nu_{41}}F_{41}E_{bg\Delta\nu_{41}}+\frac{a_{42}}{\Delta\nu_{42}}F_{42}E_{bg\Delta\nu_{42}}+\frac{a_{43}}{\Delta\nu_{43}}F_{43}E_{bg\Delta\nu_{43}}\right]+\bar{\epsilon}_{4\Delta\nu_{opp}}E_{b4\Delta\nu_{opp}}
\end{pmatrix}
$$

the indicated substitutions, and replacing the subscript jk with either adj or opp, whichever is appropriate, results in Equation (IV-10). Note that no subscript is required on $\bar{\rho}_{\Delta\nu_{opp}}$ or $\bar{\epsilon}_{\Delta\nu_{opp}}$ since the surfaces are all of the same material. These last two equations may be solved for each band by substituting values from Tables (III, V, VI, VII). For a window region the equations may be evaluated using Tables (II, VI, VII), and substituting zero for all values of band absorption.

Once the surface radiosities are calculated, the surface heat transfer values may be calculated for each region from Equation (I-9). Equation (I-9) is rewritten below with the assumption, $\bar{\epsilon}_{\Delta\nu_{opp}} = \bar{\alpha}_{\Delta\nu_{opp}}$,

$$q_{j\Delta\nu_{opp}} = \frac{\bar{\alpha}_{j\Delta\nu_{opp}}}{\bar{\rho}_{j\Delta\nu_{opp}}} \left(J_{j\Delta\nu_{opp}} - E_{bj\Delta\nu_{opp}}\right) \qquad \text{(IV-11)}$$

$$j = 1, 2, 3, 4.$$

As a check on the computations which follow, one may make energy balances on the surfaces and on the gas. The net energy gained by the surfaces must equal the net energy lost by the gas. Or, saying this in another way, the sum of the net surface gain of energy minus the sum of the net gain of energy of the gas must be zero. The radiant energy gain of the gas is the sum of the energy from the surfaces

$$\begin{pmatrix} 1 & -\bar{\rho}_{\Delta\nu_{opp}}\left(1-\frac{a_{adj}}{\Delta\nu_{opp}}\right)F_{adj} & -\bar{\rho}_{\Delta\nu_{opp}}\left(1-\frac{a_{opp}}{\Delta\nu_{opp}}\right)F_{opp} & -\bar{\rho}_{\Delta\nu_{opp}}\left(1-\frac{a_{adj}}{\Delta\nu_{opp}}\right)F_{adj} \\ -\bar{\rho}_{\Delta\nu_{opp}}\left(1-\frac{a_{adj}}{\Delta\nu_{opp}}\right)F_{adj} & 1 & -\bar{\rho}_{\Delta\nu_{opp}}\left(1-\frac{a_{adj}}{\Delta\nu_{opp}}\right)F_{adj} & -\bar{\rho}_{\Delta\nu_{opp}}\left(1-\frac{a_{opp}}{\Delta\nu_{opp}}\right)F_{opp} \end{pmatrix}$$

(IV-10)

$$= \begin{pmatrix} \bar{\rho}_{\Delta\nu_{opp}}\left[2 \times \frac{a_{adj}}{\Delta\nu_{adj}}F_{adj}E_{bg\Delta\nu_{adj}} + \frac{a_{opp}}{\Delta\nu_{opp}}F_{opp}E_{bg\Delta\nu_{opp}}\right] + \bar{\epsilon}_{\Delta\nu_{opp}}E_{b1\Delta\nu_{opp}} \\ \bar{\rho}_{\Delta\nu_{opp}}\left[2 \times \frac{a_{adj}}{\Delta\nu_{adj}}F_{adj}E_{bg\Delta\nu_{adj}} + \frac{a_{opp}}{\Delta\nu_{opp}}F_{opp}E_{bg\Delta\nu_{opp}}\right] + \bar{\epsilon}_{\Delta\nu_{opp}}E_{b2\Delta\nu_{opp}} \end{pmatrix}$$

which is absorbed by the gas minus the energy emitted by the gas. Specifically, the net energy gain of the gas due to absorption of energy from the j^{th} surface and due to emission of the gas towards the j^{th} surface, in any region $\Delta\nu$, is

$$q_{j\text{-gas},\Delta\nu} = \sum_{k=1}^{M} \left(\frac{a_{jk}}{\Delta\nu} F_{jk} J_{j\Delta\nu} - \frac{a_{jk}}{\Delta\nu_{jk}} F_{jk} E_{bg\Delta\nu_{jk}} \right). \qquad \text{(IV-12)}$$

The net energy gain of the gas due to the presence of all M surfaces is

$$q_{g,net,\Delta\nu} = \sum_{j=1}^{M} q_{j\text{-gas},\Delta\nu} \quad . \qquad \text{(IV-13)}$$

For an energy balance to exist, $-q_{g,net,\Delta\nu}$ must be equal to $\sum_{j=1}^{M} q_{j\Delta\nu}$.

In terms of the example problem, Equation (IV-12) becomes

$$q_{j\text{-gas},\Delta\nu_{opp}} = J_{j\Delta\nu_{opp}} \left[2 \times \frac{a_{adj}}{\Delta\nu_{opp}} F_{adj} + \frac{a_{opp}}{\Delta\nu_{opp}} F_{opp} \right]$$

$$- \left[2 \times \frac{a_{adj}}{\Delta\nu_{adj}} F_{adj} E_{bg\Delta\nu_{adj}} + \frac{a_{opp}}{\Delta\nu_{opp}} F_{opp} E_{bg\Delta\nu_{opp}} \right] \qquad \text{(IV-14)}$$

Also for the particular example problem under consideration, the symmetry makes possible an energy balance verification

by comparing the sum $-\sum_{j=1}^{2} q_{j\text{-gas},\Delta\nu_{opp}}$ to $\sum_{j=1}^{2} q_{j\Delta\nu_{opp}}$. These two quantities are equal when an energy balance prevails.

The values of $q_{j\Delta\nu}$ may now be calculated. The results, along with $-q_{g,net,\Delta\nu_{opp}}$, are presented in Table VIII.

In Table VIII an energy balance for the entire spectrum, as well as for each of the nine regions, is indicated. This completes the solution of the problem using the band method.

Comparison of Results

In Appendix E, the heat transfer problem posed in the first section of this chapter is solved using the monochromatic method. In Appendix F, the problem is again solved, but using the gray method. In Table IX are tabulated the results of these two calculations along with the results of the band method. The results tabulated are values of total surface radiant heat transfer to each surface.

The most accurate results are those calculated using the monochromatic method. The band method results compare exceptionally well to the monochromatic method results. The band method results in a 2.8 percent error in q_1 and a 0.5 percent error in q_2, when compared to the monochromatic method results. This close agreement should not in general

TABLE VIII

BAND METHOD HEAT TRANSFER RESULTS

Region	$q_{1\Delta\nu_{opp}} = q_{4\Delta\nu_{opp}}$ Btu/hr-ft^2	$q_{2\Delta\nu_{opp}} = q_{3\Delta\nu_{opp}}$ Btu/hr-ft^2	$-q_{g,net,\Delta\nu_{opp}}$ Btu/hr-ft^2
Window # 1	- 5.71	5.71	0
15.0 μ Band	- 11.44	31.71	20.27
Window # 2	-110.57	110.57	0
4.3 μ Band	- 5.94	27.39	21.45
Window # 3	- 29.43	29.40	0
2.7 μ Band	- 6.40	10.10	3.70
Window # 4	- 2.09	2.09	0
2.0 μ Band	- .90	0.91	0.01
Window # 5	0	0	0
TOTALS	-172.5	+217.9	+45.4

TOTAL . . . . . 45.4 — ENERGY BALANCE

TABLE IX

COMPARISON OF SOLUTIONS

Method	$q_1 = q_4$ Btu/hr-ft^2	$q_2 = q_3$ Btu/hr-ft^2
Monochromatic	-177.5	219.0
Band	-172.5	217.9
Gray	-139.9	238.4

be expected. The gray method results in a 21.0 percent and a 9.0 percent error in q_1 and q_2, respectively, when compared to the monochromatic method.

This completes the application of the α and $\alpha/\Delta\nu$ correlations of Chapter III to an example heat transfer problem. The heat transfer results as calculated by the band method compare favorably to results calculated from the monochromatic method. This indicates that actual bandwidths do have application to engineering radiant heat transfer problems.

Many problems in the subject area of this thesis remain unsolved. Therefore, part of the next chapter is devoted to suggestions for future work.

CHAPTER V

SUMMARY, CONCLUSIONS, AND RECOMMENDATIONS

Summary

The design of high temperature enclosures containing a radiating gas usually involves a thermal analysis. The purpose of this thermal analysis might be the calculation of heat transfer to the surfaces of the enclosure. The energy is transferred to the surfaces by coupled radiative and convective exchange. Even though the convection and radiation modes of transfer are coupled, a common practice is to calculate the two quantities individually.

In the present study only the radiative surface heat transfer was considered. Several methods exist for the calculation of the radiant exchange. The method of interest for purposes of the present study is the band method. The band equations of radiant exchange were presented in Chapter I. The "band" is usually taken to be either the bandwidth of an absorption band of the gas in the enclosure or a window region of this gas. The bandwidth appears both explicitly and implicitly in the band equations. Therefore,

numerical values of bandwidths are required before the band equations may be numerically evaluated.

In the present study, plots of semi-empirical spectral absorptance were used to determine band absorption and absorption bandwidths of four major absorption bands of carbon dioxide-nitrogen gas mixtures. These quantities were determined for a wide range of the gas conditions: mass path length, effective pressure, and gas temperatures. The band absorption and the ratio of band absorption to bandwidth were each correlated with mass path length and effective pressure, for five gas temperatures. Therefore, actual absorption bandwidths may be calculated from the correlations with the expression,

$$\Delta\nu = \frac{a}{(a/\Delta\nu)} \quad .$$

The bandwidths calculated from this expression may be used in the numerical evaluation of the band equations.

Conclusions

Tables I and II of Chapter III indicate a and $a/\Delta\nu$ may be correlated with gas conditions. Such correlations of a are not new, but similar correlations of $a/\Delta\nu$ were not found in the literature. Also, the use of a and $a/\Delta\nu$ correlations to obtain absorption bandwidths as functions of gas conditions was not found to exist in the

literature.

The applicability of actual absorption bandwidths to the solution of the band equations has been illustrated in Chapter IV. There, an example problem was solved using the band method and the a and $a/\Delta\nu$ correlations of Tables I and II. The results for that example were satisfactory, indicating the correlations, yielding actual bandwidth, do have utility.

Limitations of the correlations do exist. These limitations were brought out in Chapter III. There it was shown that discontinuities in the correlation expressions exist in the transition region of the weak band fit to the strong band fit. For most gas conditions, however, the fit of the correlation expressions to the raw computer calculated data is satisfactory.

Recommendations

Extensions of the work presented in this thesis are possible. Correlations of a and $a/\Delta\nu$, as determined in the present study, may be attempted for other gases. In particular, water vapor and methane may be studied using Edwards' (11) semi-empirical expression as a source of spectral gas absorptance.

The correlations presented in this thesis may be redetermined using experimental spectral data rather than a semi-empirical expression for spectral gas absorptance. This would allow more bands to be considered and would guarantee that all bands could be completely defined.

If experimental determination of spectral absorptance is possible, one might also extend the ranges of gas conditions considered. Gas conditions could be varied such that absorption would vary from negligibly small values to saturation values.

Gas temperature has been left as a parameter in the correlations of $\mathcal{A}$ and $\mathcal{A}/\Delta\nu$ determined in the present study. Recent work by Edwards and Menard (27,28) and Edwards and Sun (29) indicates the possibility of incorporating gas temperature more explicitly in the correlation expressions. Studies of the variation of $\mathcal{A}$ and $\mathcal{A}/\Delta\nu$ with gas temperature could result in inclusion of gas temperature in the correlation expressions. Also, such studies should prove to have application in radiant transfer through a non-isothermal gas.

A SELECTED BIBLIOGRAPHY

1. Wiebelt, J. A. Engineering Radiation Heat Transfer. New York: Holt, Rinehart, and Winston, Inc., 1966 (In Press).

2. Kourganoff, V. Basic Methods In Transfer Problems. New York: Dover Publications, Inc., 1963.

3. Viskanta, Raymond. "Heat Transfer in Thermal Radiation Absorbing and Scattering Media." Argonne National Laboratory Report ANL - 6170, Argonne, Illinois, May, 1960.

4. Bevans, J. T., and Dunkle, R. V. "Radiant Interchange Within an Enclosure." Journal of Heat Transfer, February, 1960, pp. 1-19.

5. Sparrow, E. M., Gregg, J. L., Szel, J. V., and Manos, P. "Analysis, Results, and Interpretation for Radiation Between Some Simply-arranged Gray Surfaces." Journal of Heat Transfer, May, 1961, pp. 207-214.

6. Hamilton, D. C., and Morgan, W. R. "Radiant-Interchange Configuration Factors." National Advisory Committee for Aeronautics Technical Note TN 2836, Washington, December ,1952.

7. Herzberg, Gerhard. Molecular Spectra and Molecular Structure II. Infrared and Raman Spectra of Polyatomic Molecules. New York: D. Van Nostrand Company, Inc., 1945.

8. Edwards, D. K. "Radiation Interchange in a Nongray Enclosure Containing an Isothermal Carbon Dioxide-Nitrogen Gas Misture." Journal of Heat Transfer, Transactions American Society of Mechanical Engineers, Vol. 84, Series C, 1962, pp. 1-11.

9. Edwards, D. K., and Nelson, K. E. "Rapid Calculation of Radiant Energy Transfer Between Nongray Walls and Isothermal H_2O or CO_2 Gas." Journal of Heat Transfer, Transactions American Society of Mechanical Engineers, Vol. 84, Series C, 1962, pp. 273-278.

10. Howard, J. N., Burch, D. C., and Williams, D. "Near Infrared Transmission Through Synthetic Atmospheres, Parts I, II, and III." Air Force Cambridge Research Center, Geophysical Research Papers Number 40, 1953.

11. Edwards, D. K. "Studies of Infrared Radiation in Gases." University of California, Los Angeles, Department of Engineering Report Number 62-65, January, 1963.

12. Penner, S. S. Quantitative Molecular Spectroscopy and Gas Emissivities. Reading, Massachusetts: Addison-Wesley Publishing Company, Inc., 1959.

13. Wyatt, Philip J., Stull, V. Robert, and Plass, Gilbert N. "Quasi-Random Model of Band Absorption." Journal of the Optical Society of America, Vol. 52, No. 11, November, 1962, pp. 1209-1217.

14. Stull, V. Robert, Wyatt, Philip J., and Plass, G. N. "The Infrared Transmittance of Carbon Dioxide." Applied Optics, Vol. 3, No. 2, February, 1964, pp. 243-254.

15. Bevans, J. T., Dunkle, R. V., Edwards, D. K., Gier, J.T., Levenson, L. L., and Oppenheim, A. K. "Apparatus for the Determination of the Band Absorption of Gases at Elevated Pressures and Temperatures." Journal of the Optical Society of America, Vol. 50, No. 2, February, 1960, pp. 120-136.

16. Davies, William O. "Emissivity of Carbon Dioxide at 4.3μ." Journal of the Optical Society of America, Vol. 54, No. 4, April, 1964, pp. 467-471.

17. Plyler, Earle K., and Tidwell, Eugene D. "Absorption Bands of Carbon Dioxide from 2.8-4.2μ." Journal of the Optical Society of America, Vol. 52, No. 9, September, 1962, pp. 1017-1022.

18. Tourin, Richard H. "Measurements of Infrared Spectral Emissivities of Hot Carbon Dioxide in the 4.3μ Region." Journal of the Optical Society of America, Vol. 51, No. 2, February, 1961, pp. 175-183.

19. Tourin, R. H. "Infrared Spectral Emissivities of CO_2 in the 2.7 Micron Region." Infrared Physics, Vol.1, 1961, pp. 105-110.

20. Plass, Gilbert N. "Useful Representations for Measurements of Spectral Band Absorption." Journal of the Optical Society of America, Vol. 50, No. 9, September, 1960, pp. 868-875.

21. Jamison, John A., et al. Infrared Physics and Engineering. New York: McGraw-Hill Book Company, Inc., 1963.

22. Howard, J. N., Burch, D. E., and Williams, Dudley. "Infrared Transmission of Synthetic Atmospheres." Journal of the Optical Society of America, Vol. 46, 1956, pp. 186-190, 237-241, 242-245, 334-338.

23. Edwards, D. K. Experimental Determination of the Band Absorptivities of Carbon Dioxide Gas at Elevated Pressures and Temperatures. Ph.D. Thesis, Department of Mechanical Engineering, University of California, Berkeley, 1959.

24. Edwards, D. K."Absorption by Infrared Bands of Carbon Dioxide Gas at Elevated Pressures and Temperatures." Journal of the Optical Society of America, Vol. 50, No. 6, June, 1960, pp. 617-626.

25. Burch, Darrell, E., Gryvnak, David A., and Williams, Dudley. "Total Absorptance of Carbon Dioxide in the Infrared." Applied Optics, Vol. 1, No. 6, November, 1962, pp. 759-765.

26. Burch, D. E., Gryvnak, D., Singleton, E. B., France, W. L., and Williams, D. "Infrared Absorption by Carbon Dioxide, Water Vapor, and Minor Atmospheric Constituents." Air Force Cambridge Research Labs, Geophysics Research Directorate, Bedford, Massachusetts, 1960.

27. Edwards, D. K., and Menard, W. A. "Comparison of Models for Correlation of Total Band Absorption." Applied Optics, Vol. 3, No. 5, May, 1964, pp. 621-625.

28. Edwards, D. K., and Menard, W. A. "Correlations for Absorption by Methane and Carbon Dioxide Gases." Applied Optics, Vol. 3, No. 7, July, 1964, pp. 847-852.

29. Edwards, D. K., and Sun, W. "Correlations for Absorption by the 9.4-μ and 10.4-μ CO_2 Bands." Applied Optics, Vol. 3, No. 12, December, 1964, pp. 1501-1502.

30. Viskanta, R., and Grosh, R. J. "Recent Advances in Radiant Heat Transfer." Applied Mechanics Reviews, Vol. 17, No. 2, February, 1964, pp. 91-100.

31. Dunkle, R. V. "Geometric Mean Beam Lengths for Radiant Heat-Transfer Calculations." American Society of Mechanical Engineers Paper No. 62-WA-120, 1962.

32. Wiebelt, J. A. "Comparison of Geometric Absorption Factors with Geometric Mean Beam Lengths." Journal of Heat Transfer, August, 1963, pp. 287-288.

33. McAdams, W. H. Heat Transmission. New York: McGraw-Hill Book Company, Inc., 1954, Chapter 4 by Hoyt C. Hottel.

34. Kreith, Frank. "Radiation Heat Transfer and Thermal Control of Spacecraft." Oklahoma Engineering Experiment Station Publication No. 112, Oklahoma State University, Stillwater, Oklahoma, April, 1960.

APPENDIX A

CORRELATION CONSTANTS, C^2, B^2, AND BC VERSUS WAVENUMBER

CORRELATION CONSTANTS C^2, B^2, AND BC
VERSUS WAVENUMBER

ν cm^{-1}	Gas Temperature														
	535°R			1000°R			1500°R			2000°R			2500°R		
	C^2	B^2	BC	C^2	B^2	BC	C^2	B^2	BC	C^2	B^2	BC	C^2	B^2	BC
490										L	S	.113	L	S	.243
510				L	S	.0529	1.06	.0344		9.20	.0227		4.36	.0963	
530	.151	.002		L	S	.119	2.43	.079		7.90	.125		9.43	.235	
550	L*	S**	.043	3.43	.0552		9.20	.264		20.6	.297		24.6	.317	
570	.503	.159		10.0	.160		27.0	.310		40.2	.502		41.9	.516	
590	5.12	.099		39.6	.196		64.6	.458		69.6	.819		86.9	.669	
610	L	S	1.77	79.9	.373		125.	.669		156.	.900		160.	.892	
630	28.3	6.59		L	S	4.74	220.	1.19		247.	1.46		236.	1.47	
650	343.	11.3		L	S	6.30	326.	1.46		463.	.857		432.	1.02	
670	543.	.148		952.	.105		661.	.821		311.	.378		646.	.970	
690	L	S	8.23	594.	.0918		356.	1.86		475.	1.08		501.	1.12	
710	96.8	.172		183.	.294		261.	1.25		432.	.727		368.	1.02	
730	23.9	.178		71.7	.498		148.	.727		248.	.822		238.	1.10	
750	5.56	.222		38.1	.283		72.6	.525		111.	.736		129.	.868	
770	1.54	.0473		14.8	.238		32.3	.392		57.5	.555		77.2	.532	
790	.574	.0117		6.38	.0510		14.1	.257		L	S	2.36	36.1	.370	
810	L	S	.0415	3.16	.0281		7.23	.127		18.7	.174		20.5	.222	
830	L	S	.020	L	S	.131	3.72	.0868		9.12	.128		9.67	.197	
850				L	S	.0919	2.29	.0566		8.79	.0780		6.13	.176	
910	L	S	.0038	.625	.0428		3.46	.0643		4.57	.105		5.70	.130	
930	L	S	.0172	1.03	.0553		3.28	.0841		4.22	.115		5.08	.130	
950	.0803	.0206		1.17	.0589		2.95	.118		4.40	.107		5.61	.118	
960				.607	2.66										
970	.0745	.0250		1.02	.0534		1.94	.168		3.34	.0891		5.12	.0881	
990	L	S	.0187	.587	.0557		2.28	.0905		4.05	.119		6.27	.149	

APPENDIX A (CONTINUED)

ν cm^{-1}	Gas Temperature														
	535°R			1000°R			1500°R			2000°R			2500°R		
	C^2	B^2	BC	C^2	B^2	BC	C^2	B^2	BC	C^2	B^2	BC	C^2	B^2	BC
1010	L	S	.00495	L	S	.0796	3.21	.0274		4.28	.119		6.17	.172	
1030	.0332	.0226		1.09	.0421		3.89	.0997		5.73	.180		8.06	.135	
1050	.0692	.0365		1.38	.0784		3.74	.175		5.54	.207		7.65	.180	
1070	.0986	.0237		L	S	.274	3.84	.143		6.40	.161		9.96	.121	
1090	.0678	.0471		1.47	.165		5.84	.157		8.88	.222		11.5	.214	
1100	.102	.00156		L	S	.260									
1110							2.22	.050		4.04	.0804		3.20	.251	
1830													L	S	.0325
1870	L	S	.0159	L	S	.0183	L	S	.0285	L	S	.0293	L	S	.0385
1910	.113	.0163		L	S	.0345	L	S	.0268	L	S	.0263	L	S	.0385
1950	L	S	.0283	L	S	.0123	L	S	.0176	L	S	.0174	L	S	.0384
1990	.0934	.00174		L	S	.0122	L	S	.0215	L	S	.0309	L	S	.0772
2030	L	S	.0447	L	S	.0438	L	S	.0699	.834	.0189		1.74	.0399	
2070	.592	.0337		L	S	.166	L	S	.222	2.54	.0498		5.00	.118	
2110	.456	.0362		L	S	.160	2.82	.0326		3.99	.116		18.4	.247	
2150	.156	.0491		L	S	.0943	3.40	.0478		30.3	.495		61.8	.685	
2190	L	S	.0305	L	S	.165	22.4	.0886		220.	1.69		284.	.938	
2230	L	S	.238	66.5	.148		279.	.988		891.	2.88		120.	.195	
2270	131.	.185		193.	.211		2080.	.419		3050.	1.97		L	S	.458
2310	L	S	26.7	L	S	37.6	278.	1.12		739.	1.96		L	S	.0286
2350	L	S	53.8	L	S	51.0	381.	.566		425.	.745		L	S	.0286
2390	401.	.0358		L	S	12.0	476.	.0710		L	S	16.3	L	S	26.1
2430	L	S	.0738	L	S	.616	L	S	.987				L	S	6.01
2470							L	S	.209						
2510							L	S	.0561						
3225										L	S	.0234	L	S	.0744

APPENDIX A (CONTINUED)

ν cm^{-1}	Gas Temperature														
	535°R			1000°R			1500°R			2000°R			2500°R		
	C^2	B^2	BC	C^2	B^2	BC	C^2	B^2	BC	C^2	B^2	BC	C^2	B^2	BC
3285				L	S	.0131	L	S	.0171	L	S	.0791	L	S	.219
3345	L	S	.00949	L	S	.0402	1.99	.00555		3.01	.0478		16.5	.0258	
3405	L	S	.0332	L	S	.124	2.66	.0493		11.0	.0546		24.4	.102	
3465	.764	.0320		L	S	.405	14.4	.0835		37.4	.124		39.8	.290	
3525	65.6	.0104		56.5	.0430		31.0	.299		66.7	.263		65.9	.361	
3585	L	S	2.72	L	S	2.57	56.6	.409		75.7	.474		94.5	.455	
3645	L	S	3.67	L	S	3.35	88.5	.347					133.	.384	
3705	L	S	3.99	L	S	3.37	110.	.285		129.	.316		148.	.326	
3765	L	S	.722	L	S	3.79	L	S	3.57	29.6	.238		L	S	3.22
3825							L	S	2.06				L	S	1.98
3885							L	S	1.13						
3945							L	S	.532						
4005							L	S	.265						
4065							L	S	.177						
4800				L	S	.00768				L	S	.0344	L	S	.0454
4900	L	S	.0221	L	S	.0324	L	S	.0461	L	S	.0771	1.04	.00813	
5000	.654	.00767		.666	.00933		.569	.0221		L	S	.161	1.38	.0230	
5100	.860	.0209		1.09	.0223		L	S	.175	L	S	.228	2.25	.0227	
5200	.863	.0763		1.69	.0227		L	S	.220	1.64	.0394		2.25	.0263	
5300	.565	.117		.924	.0313		L	S	.187	1.62	.0269				
5400	.641	.0208		.517	.0214		L	S	.122	L	S	.139			
5500	L	S	.0420	L	S	.0460	L	S	.0655	L	S	.0759			
5600	L	S	.0178	L	S	.0149	L	S	.0310	L	S	.0372			
5700	.0700	.00106													

*L indicates a very large value.

**S indicates a very small value.

APPENDIX B

MONOCHROMATIC GAS ABSORPTANCE PROGRAM LISTINGS

Since the spectral correlation constants of Appendix A vary with gas temperature, six programs are presented below. These correspond with all the gas temperatures considered.

The following input and output notation is used in the programs:

GNU(I) = ν, cm^{-1}

CSQ(I) = value of C^2 at ν

BSQ(I) = value of B^2 at ν

BC(I) = value of BC at ν

W = w

PE = P_e

EN = n

TG = T_g

ALFAG(I) = $\alpha_{g\nu}$.

SPECTRAL GAS ABSORPTANCE, T_g = 535°R

```
      DIMENSIONGNU(63),ALFAG(63),CSQ(63),BSQ(63),BC(63),AGNU(63)
      DIMENSIONGNU1(63),GNU2(63),GNU3(63),GNU4(63),ALFAG1(63),ALFAG2(63)
     1,ALFAG3(63),ALFAG4(63)
      EQUIVALENCE(GNU(1),GNU1(1)),(GNU(28),GNU2(1)),(GNU(43),GNU3(1)),(G
     1NU(51),GNU4(1)),(ALFAG(1),ALFAG1(1)),(ALFAG(28),ALFAG2(1)),(ALFAG(
     243),ALFAG3(1)),(ALFAG(51),ALFAG4(1))
  100 FORMAT(4F10.5)
  101 FORMAT(1HL,2HW=,1PE20.7,5X,3HPE=,1PE20.7,5X,3HEN=,1PE20.7,5X,3HTG=
     1,1PE20.7)
  102 FORMAT(1HJ,4HGNU=,1PE20.7,5X,6HALFAG=,1PE20.7)
      DO10I=1,59
      READ(1,100)GNU(I),CSQ(I),BSQ(I),BC(I)
   10 AGNU(I)=GNU(I)
    1 READ(1,100)W,PE,EN,TG
      WRITE(3,101)W,PE,EN,TG
   11 DO30I=1,59
      IF(BC(I).NE.0.)GOTO20
      ALFAG(I)=1.-EXP(-(CSQ(I)*W)/(SQRT(1.+(CSQ(I)*W)/(BSQ(I)*(PE**EN)))
     1))
      GOTO30
   20 ALFAG(I)=1.-EXP(-BC(I)*SQRT(W*(PE**EN)))
   30 WRITE(3,102)GNU(I),ALFAG(I)
   40 CALLPLOT(GNU1,400.,1200.,0,ALFAG1,0.,1.,0,0.,0.,0.,0,27,1,1,3,2)
      CALLPLOT(GNU2,1800.,2600.,0,ALFAG2,0.,1.,0,0.,0.,0.,0,15,1,1,3,2)
      CALLPLOT(GNU3,3200.,4200.,0,ALFAG3,0.,1.,0,0.,0.,0.,0,8,1,1,3,2)
      CALLPLOT(GNU4,4600.,5800.,0,ALFAG4,0.,1.,0,0.,0.,0.,0,9,1,1,3,2)
      DO45I=1,59
   45 GNU(I)=AGNU(I)
      GOTO1
      END
```

SPECTRAL GAS ABSORPTANCE, T_g = 1000°R

```
      DIMENSIONGNU(63),ALFAG(63),CSQ(63),BSQ(63),BC(63),AGNU(63)
      DIMENSIONGNU1(63),GNU2(63),GNU3(63),GNU4(63),ALFAG1(63),ALFAG2(63)
     1,ALFAG3(63),ALFAG4(63)
      EQUIVALENCE(GNU(1),GNU1(1)),(GNU(31),GNU2(1)),(GNU(46),GNU3(1)),(G
     1NU(55),GNU4(1)),(ALFAG(1),ALFAG1(1)),(ALFAG(31),ALFAG2(1)),(ALFAG(
     246),ALFAG3(1)),(ALFAG(55),ALFAG4(1))
  100 FORMAT(4F10.5)
  101 FORMAT(1HL,2HW=,1PE20.7,5X,3HPE=,1PE20.7,5X,3HEN=,1PE20.7,5X,3HTG=
     1,1PE20.7)
  102 FORMAT(1HJ,4HGNU=,1PE20.7,5X,6HALFAG=,1PE20.7)
      DO10I=1,63
      READ(1,100)GNU(I),CSQ(I),BSQ(I),BC(I)
   10 AGNU(I)=GNU(I)
    1 READ(1,100)W,PE,EN,TG
      WRITE(3,101)W,PE,EN,TG
   11 DO30I=1,63
      IF(BC(I).NE.0.)GOTO20
      ALFAG(I)=1.-EXP(-(CSQ(I)*W)/(SQRT(1.+(CSQ(I)*W)/(BSQ(I)*(PE**EN)))
     1))
      GOTO30
   20 ALFAG(I)=1.-EXP(-BC(I)*SQRT(W*(PE**EN)))
   30 WRITE(3,102)GNU(I),ALFAG(I)
   40 CALLPLOT(GNU1,400.,1200.,0,ALFAG1,0.,1.,0,0.,0.,0.,0.,30,1,1,3,2)
      CALLPLOT(GNU2,1800.,2500.,0,ALFAG2,0.,1.,0,0.,0.,0.,0.,15,1,1,3,2)
      CALLPLOT(GNU3,3200.,4200.,0,ALFAG3,0.,1.,0,0.,0.,0.,0.,9,1,1,3,2)
      CALLPLOT(GNU4,4600.,5800.,0,ALFAG4,0.,1.,0,0.,0.,0.,0.,9,1,1,3,2)
      DO45I=1,63
   45 GNU(I)=AGNU(I)
      GOTO1
      END
```

SPECTRAL GAS ABSORPTANCE, T_g = 1500°R - PART 1

```
      DIMENSIONGNU(46),ALFAG(46),CSQ(46),BSQ(46),BC(46),AGNU(46)
      DIMENSIONGNU1(46),GNU2(46),ALFAG1(46),ALFAG2(46)
      EQUIVALENCE(GNU(1),GNU1(1)),(GNU(30),GNU2(1)),(ALFAG(1),ALFAG1(1))
     1,(ALFAG(30),ALFAG2(1))
  100 FORMAT(4F10.5)
  101 FORMAT(1HL,2HW=,1PE20.7,5X,3HPE=,1PE20.7,5X,3HEN=,1PE20.7,5X,3HTG=
     1,1PE20.7)
  102 FORMAT(1HJ,4HGNU=,1PE20.7,5X,6HALFAG=,1PE20.7)
      DO101I=1,46
      READ(1,100)GNU(I),CSQ(I),BSQ(I),BC(I)
   10 AGNU(I)=GNU(I)
    1 READ(1,100)W,PE,EN,TG
      WRITE(3,101)W,PE,EN,TG
   11 DO30I=1,46
      IF(BC(I).NE.0.)GOTO20
      ALFAG(I)=1.-EXP(-(CSQ(I)*W)/(SQRT(1.+(CSQ(I)*W)/(BSQ(I)*(PE**EN)))
     1))
      GOTO30
   20 ALFAG(I)=1.-EXP(-BC(I)*SQRT(W*(PE**EN)))
   30 WRITE(3,102)GNU(I),ALFAG(I)
   40 CALLPLOT(GNU1,400.,1200.,0,ALFAG1,0.,1.,0,0.,0.,0.,0.,29,1,1,3,2)
      CALLPLOT(GNU2,1800.,2600.,0,ALFAG2,0.,1.,0,0.,0.,0.,0.,17,1,1,3,2)
      DO45I=1,46
   45 GNU(I)=AGNU(I)
      GOTO1
      END
```

SPECTRAL GAS ABSORPTANCE, T_g = 1500°R - PART 2

```
      DIMENSIONGNU(22),ALFAG(22),CSQ(22),BSQ(22),BC(22),AGNU(22)
      DIMENSIONGNU1(22),GNU2(22),ALFAG1(22),ALFAG2(22)
      EQUIVALENCE(GNU(1),GNU1(1)),(GNU(15),GNU2(1)),(ALFAG(1),ALFAG1(1))
     1,(ALFAG(15),ALFAG2(1))
  100 FORMAT(4F10.5)
  101 FORMAT(1HL,2HW=,1PE20.7,5X,3HPE=,1PE20.7,5X,3HEN=,1PE20.7,5X,3HTG=
     1,1PE20.7)
  102 FORMAT(1HJ,4HGNU=,1PE20.7,5X,6HALFAG=,1PE20.7)
      DO10I=1,22
      READ(1,100)GNU(I),CSQ(I),BSQ(I),BC(I)
   10 AGNU(I)=GNU(I)
    1 READ(1,100)W,PE,EN,TG
      WRITE(3,101)W,PE,EN,TG
   11 DO30I=1,22
      IF(BC(I).NE.0.)GOTO20
      ALFAG(I)=1.-EXP(-(CSQ(I)*W)/(SQRT(1.+(CSQ(I)*W)/(BSQ(I)*(PE**EN)))
     1))
      GOTO30
   20 ALFAG(I)=1.-EXP(-BC(I)*SQRT(W*(PE**EN)))
   30 WRITE(3,102)GNU(I),ALFAG(I)
   40 CALLPLOT(GNU1,3200.,4200.,0,ALFAG1,0.,1.,0,0.,0.,0.,0.,14,1,1,3,2)
      CALLPLOT(GNU2,4600.,5800.,0,ALFAG2,0.,1.,0,0.,0.,0.,0.,8,1,1,3,2)
      DO45I=1,22
   45 GNU(I)=AGNU(I)
      GOTO1
      END
```

SPECTRAL GAS ABSORPTANCE, T_g = 2000°R

```
      DIMENSIONGNU(63),ALFAG(63),CSQ(63),BSQ(63),BC(63),AGNU(63)
      DIMENSIONGNU1(63),GNU2(63),GNU3(63),GNU4(63),ALFAG1(63),ALFAG2(63)
     1,ALFAG3(63),ALFAG4(63)
      EQUIVALENCE(GNU(1),GNU1(1)),(GNU(31),GNU2(1)),(GNU(45),GNU3(1)),(G
     1NU(54),GNU4(1)),(ALFAG(1),ALFAG1(1)),(ALFAG(31),ALFAG2(1)),(ALFAG(
     245),ALFAG3(1)),(ALFAG(54),ALFAG4(1))
  100 FORMAT(4F10.5)
  101 FORMAT(1HL,2HW=,1PE20.7,5X,3HPE=,1PE20.7,5X,3HEN=,1PE20.7,5X,3HTG=
     1,1PE20.7)
  102 FORMAT(1HJ,4HGNU=,1PE20.7,5X,6HALFAG=,1PE20.7)
      DO10I=1,62
      READ(1,100)GNU(I),CSQ(I),BSQ(I),BC(I)
   10 AGNU(I)=GNU(I)
    1 READ(1,100)W,PE,EN,TG
      WRITE(3,101)W,PE,EN,TG
   11 DO30I=1,62
      IF(BC(I).NE.0.)GOTO20
      ALFAG(I)=1.-EXP(-(CSQ(I)*W)/(SQRT(1.+(CSQ(I)*W)/(BSQ(I)*(PE**EN)))
     1))
      GOTO30
   20 ALFAG(I)=1.-EXP(-BC(I)*SQRT(W*(PE**EN)))
   30 WRITE(3,102)GNU(I),ALFAG(I)
   40 CALLPLOT(GNU1,400.,1200.,0,ALFAG1,0.,1.,0,0.,0.,0.,0.,30,1,1,3,2)
      CALLPLOT(GNU2,1800.,2600.,0,ALFAG2,0.,1.,0,0.,0.,0.,0.,14,1,1,3,2)
      CALLPLOT(GNU3,3200.,4200.,0,ALFAG3,0.,1.,0,0.,0.,0.,0.,9,1,1,3,2)
      CALLPLOT(GNU4,4600.,5800.,0,ALFAG4,0.,1.,0,0.,0.,0.,0.,9,1,1,3,2)
      DO45I=1,62
   45 GNU(I)=AGNU(I)
      GOTO1
      END
```

SPECTRAL GAS ABSORPTANCE, $T_g = 2500°R$

```
      DIMENSIONGNU(63),ALFAG(63),CSQ(63),BSQ(63),BC(63),AGNU(63)
      DIMENSIONGNU1(63),GNU2(63),GNU3(63),GNU4(63),ALFAG1(63),ALFAG2(63)
     1,ALFAG3(63),ALFAG4(63)
      EQUIVALENCE(GNU(1),GNU1(1)),(GNU(31),GNU2(1)),(GNU(47),GNU3(1)),(G
     1NU(58),GNU4(1)),(ALFAG(1),ALFAG1(1)),(ALFAG(31),ALFAG2(1)),(ALFAG(
     247),ALFAG3(1)),(ALFAG(58),ALFAG4(1))
  100 FORMAT(4F10.5)
  101 FORMAT(1HL,2HW=,1PE20.7,5X,3HPE=,1PE20.7,5X,3HEN=,1PE20.7,5X,3HTG=
     1,1PE20.7)
  102 FORMAT(1HJ,4HGNU=,1PE20.7,5X,6HALFAG=,1PE20.7)
      DO10I=1,62
      READ(1,100)GNU(I),CSQ(I),BSQ(I),BC(I)
   10 AGNU(I)=GNU(I)
    1 READ(1,100)W,PE,EN,TG
      WRITE(3,101)W,PE,EN,TG
   11 DO30I=1,62
      IF(BC(I).NE.0.)GOTO20
      ALFAG(I)=1.-EXP(-(CSQ(I)*W)/(SQRT(1.+(CSQ(I)*W)/(BSQ(I)*(PE**EN)))
     1))
      GOTO30
   20 ALFAG(I)=1.-EXP(-BC(I)*SQRT(W*(PE**EN)))
   30 WRITE(3,102)GNU(I),ALFAG(I)
   40 CALLPLOT(GNU1,400.,1200.,0,ALFAG1,0.,1.,0,0.,0.,0.,0.,36,1,1,3,2)
      CALLPLOT(GNU2,1800.,2600.,0,ALFAG2,0.,1.,0,0.,0.,0.,0.,16,1,1,3,2)
      CALLPLOT(GNU3,3200.,4200.,0,ALFAG3,0.,1.,0,0.,0.,0.,0.,11,1,1,3,2)
      CALLPLOT(GNU4,4600.,5800.,0,ALFAG4,0.,1.,0,0.,0.,0.,0.,5,1,1,3,2)
      DO45I=1,62
   45 GNU(I)=AGNU(I)
      GOTO1
      END
```

APPENDIX C

CURVES OF $a/\Delta\nu$ VERSUS w

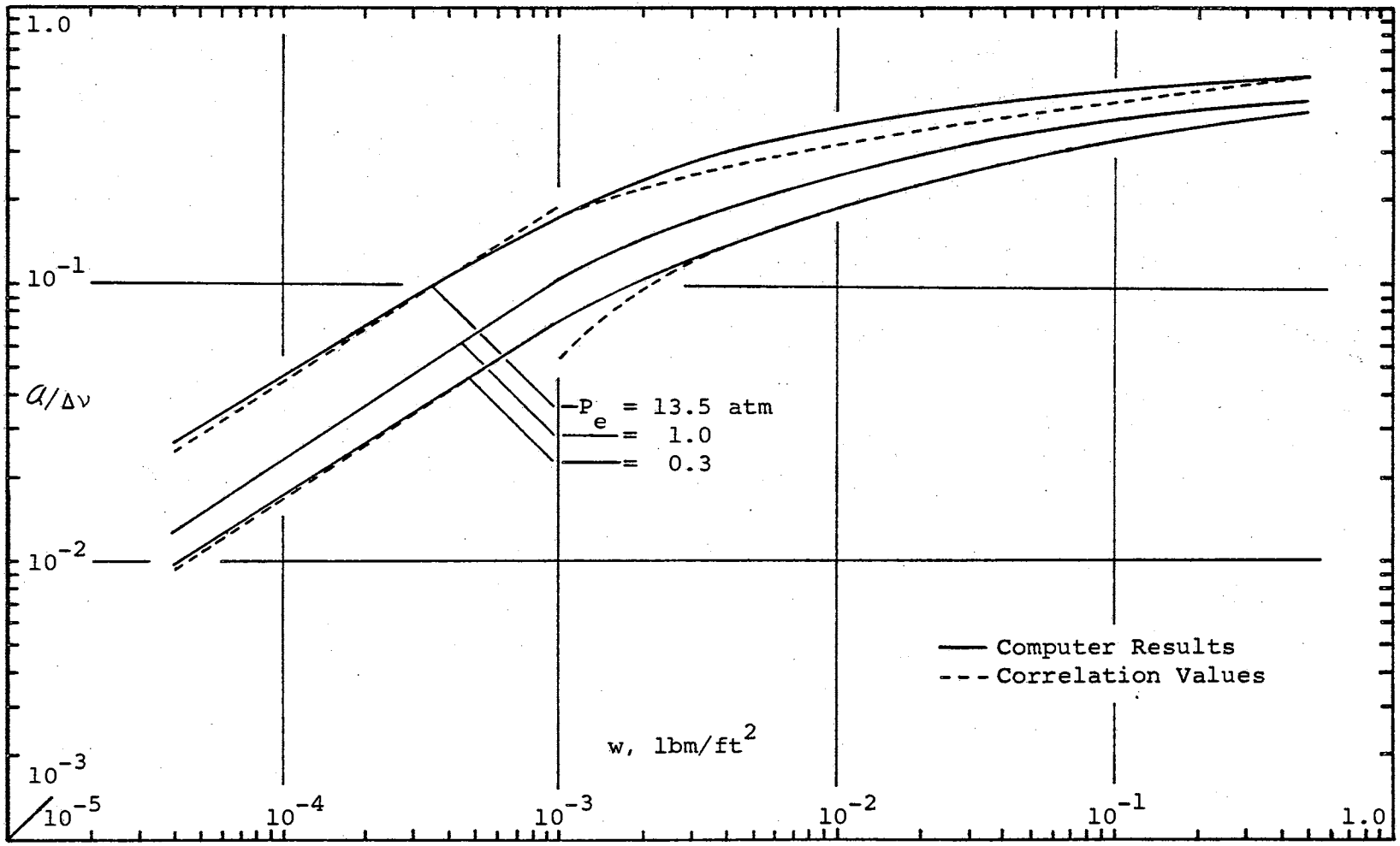

Figure 15. Variation of $a/\Delta\nu$ with Mass Path Length and Equivalent Pressure, 15.0μ - 535°R

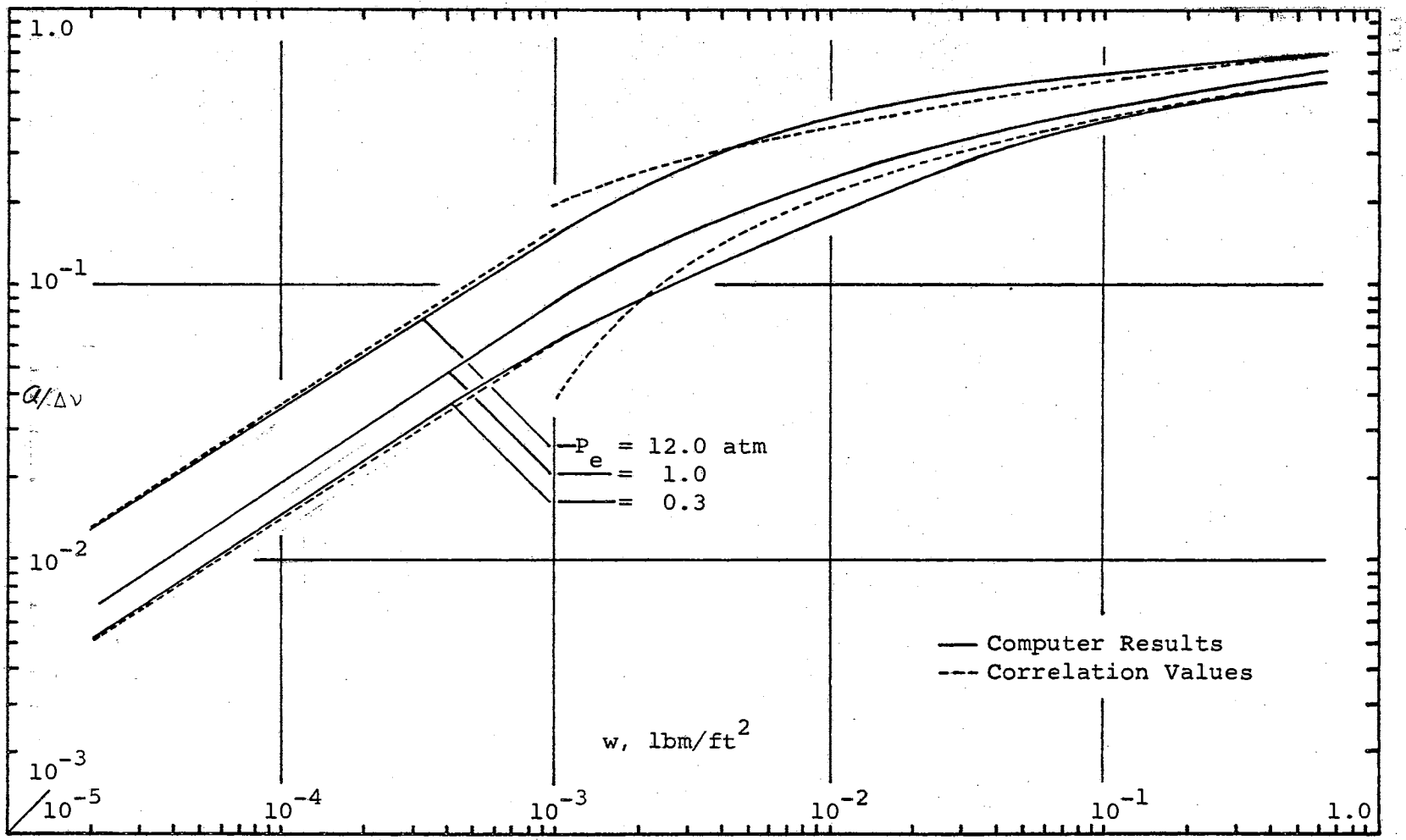

Figure 16. Variation of $a/\Delta\nu$ with Mass Path Length and Equivalent Pressure, 15.0μ - 1000°R

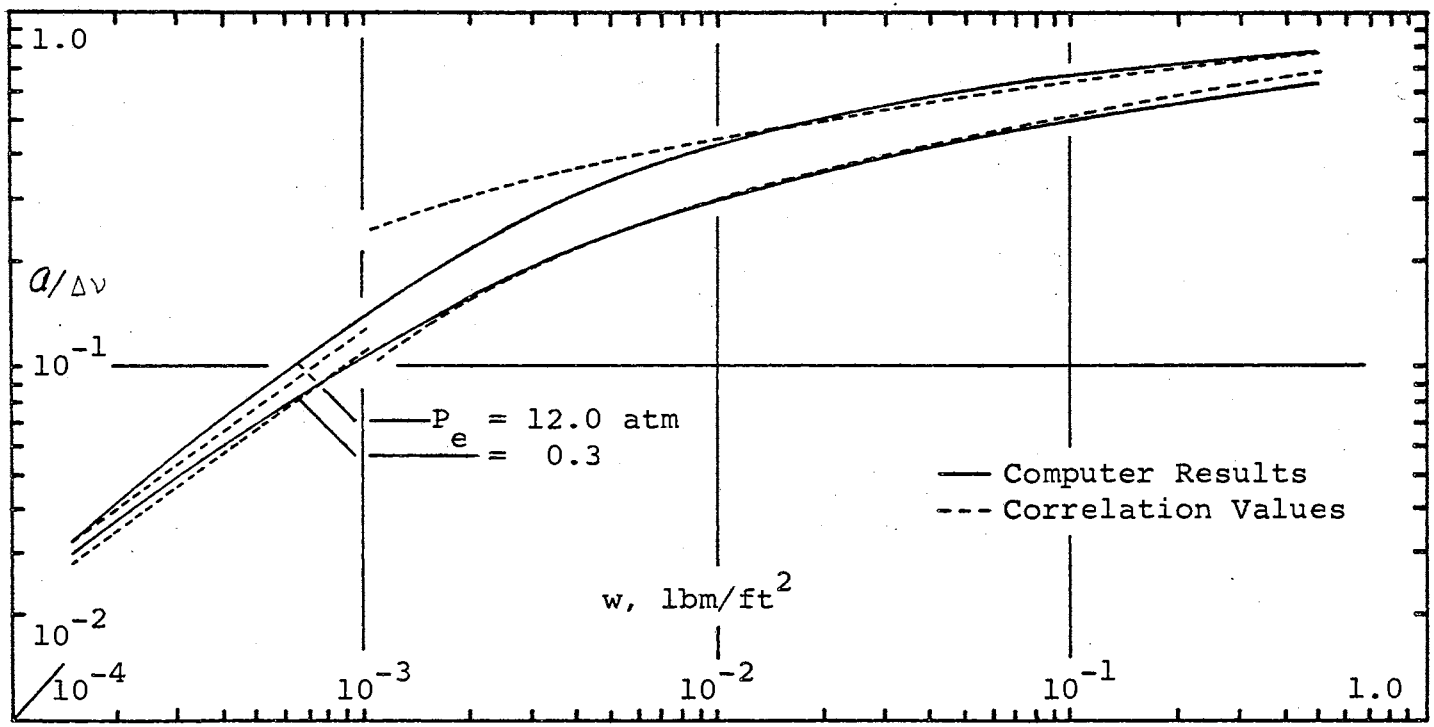

Figure 17. Variation of $a/\Delta\nu$ with Mass Path Length and Equivalent Pressure, 15.0μ - 1500°R

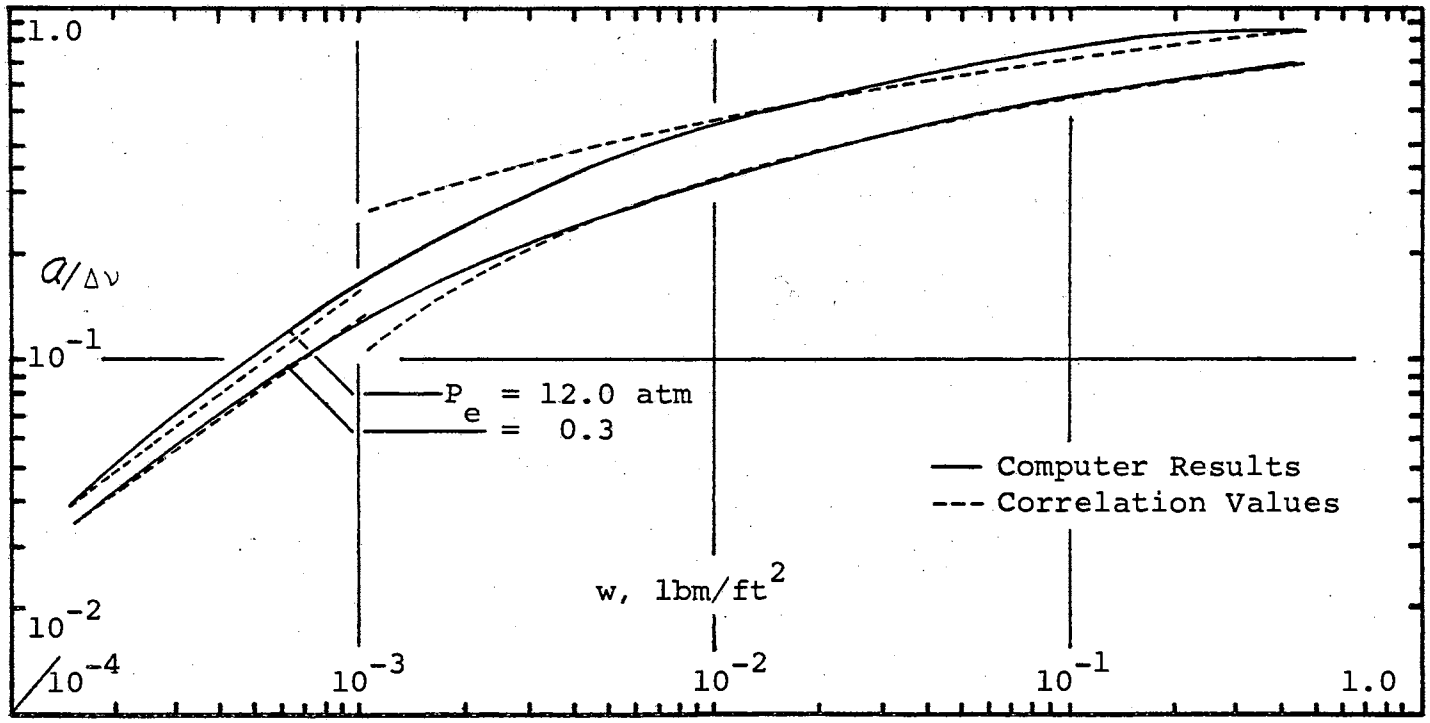

Figure 18. Variation of $a/\Delta\nu$ with Mass Path Length and Equivalent Pressure, 15.0μ - 2000°R

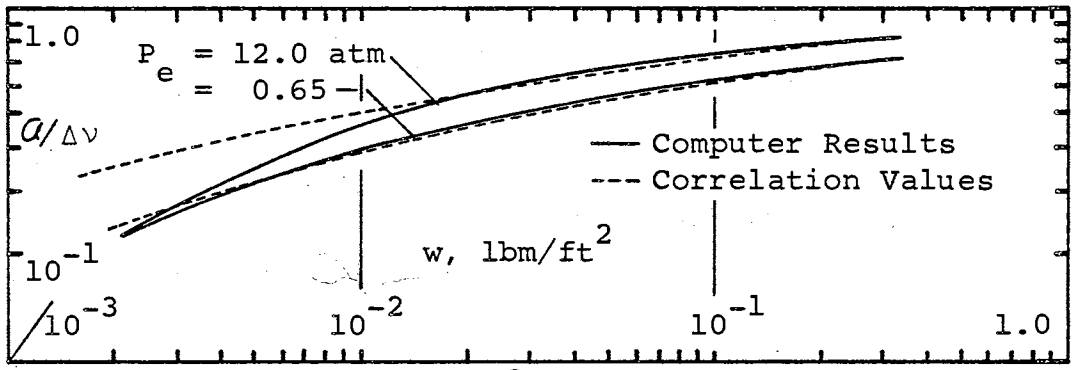

Figure 19. Variation of $a/\Delta\nu$ with Mass Path Length and Equivalent Pressure, 15.0μ - 2500°R

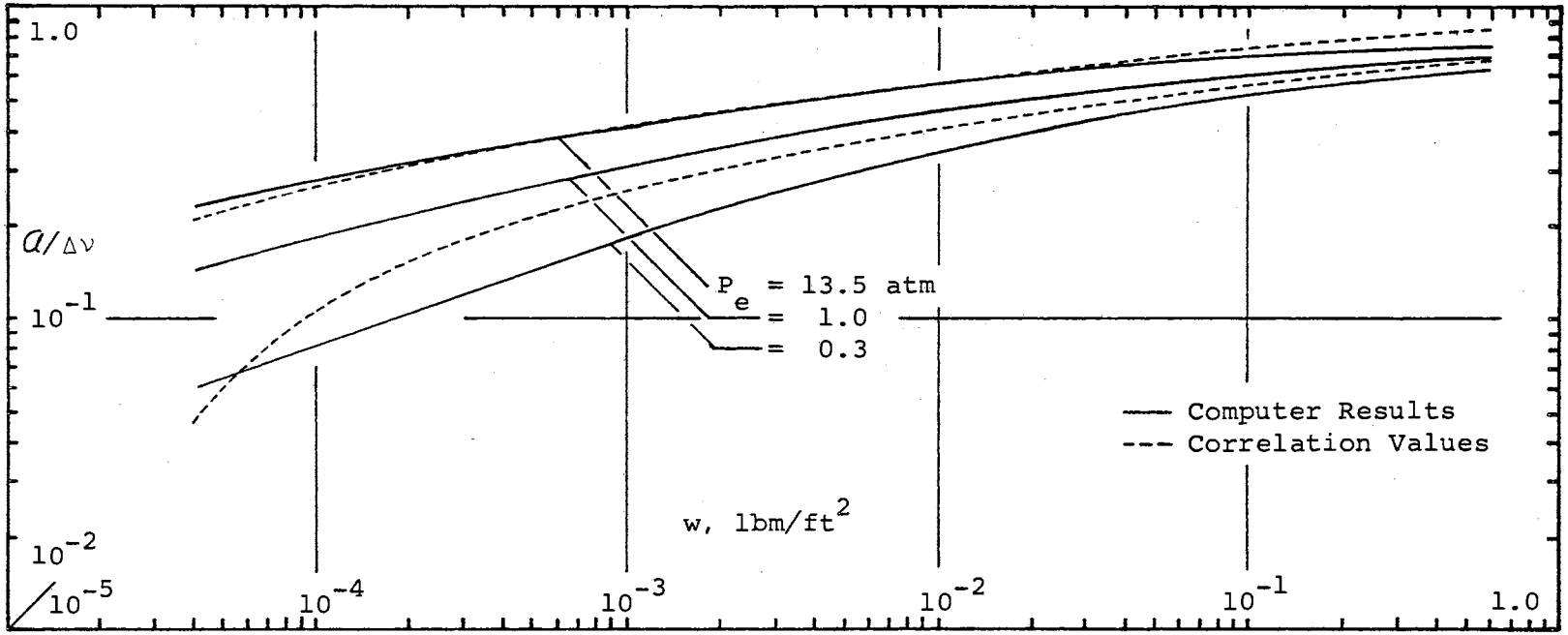

Figure 20. Variation of $a/\Delta\nu$ with Mass Path Length and Equivalent Pressure, 4.3μ - 535°R

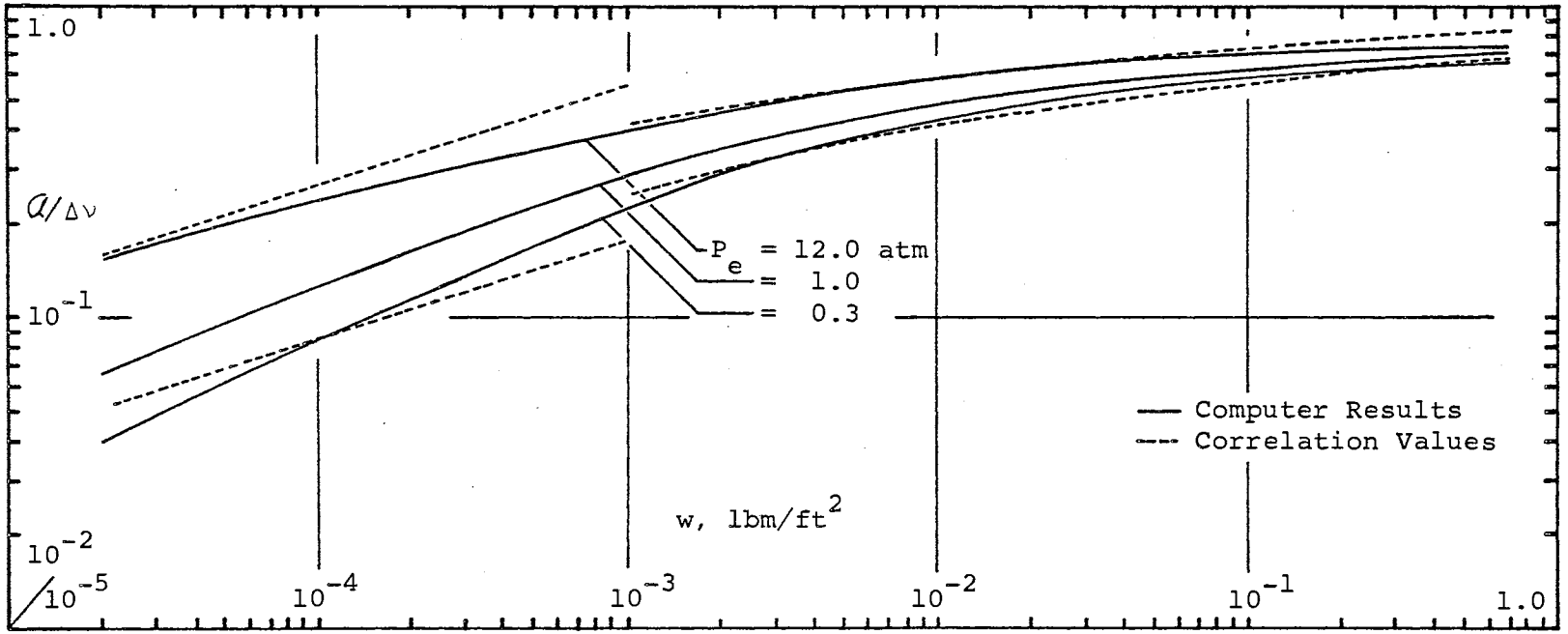

Figure 21. Variation of $a/\Delta\nu$ with Mass Path Length and Equivalent Pressure, 4.3μ - 1000°R

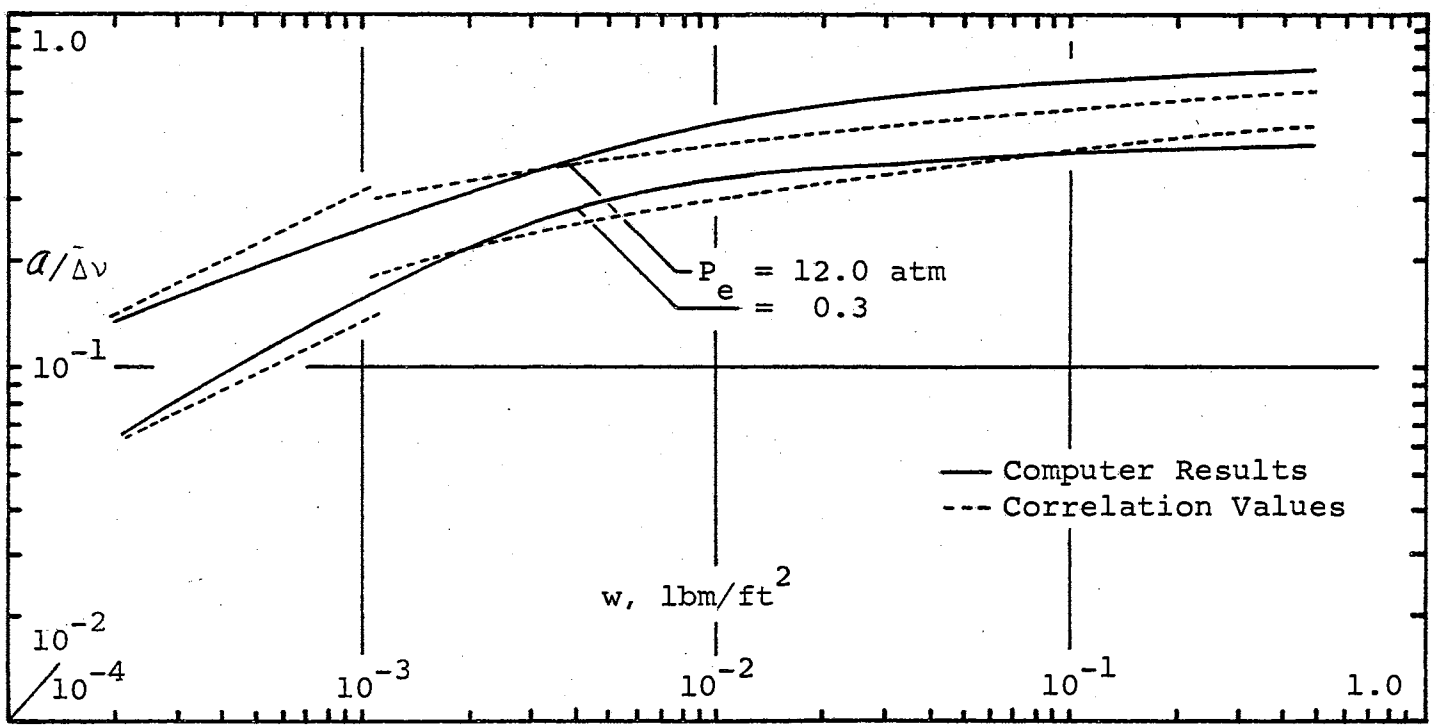

Figure 22. Variation of $a/\Delta\nu$ with Mass Path Length and Equivalent Pressure, 4.3μ - 1500°R

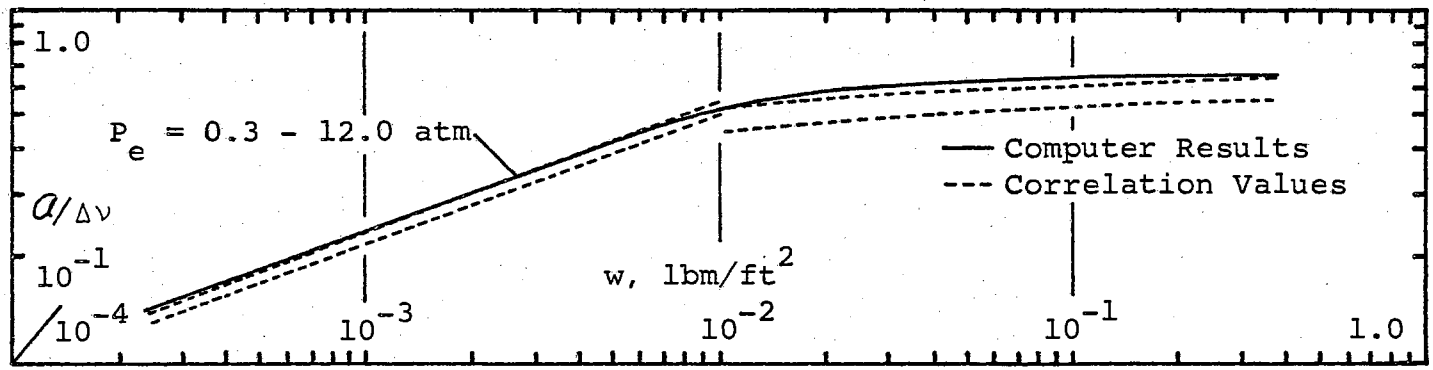

Figure 23. Variation of $a/\Delta\nu$ with Mass Path Length and Equivalent Pressure, 4.3μ - 2000°R

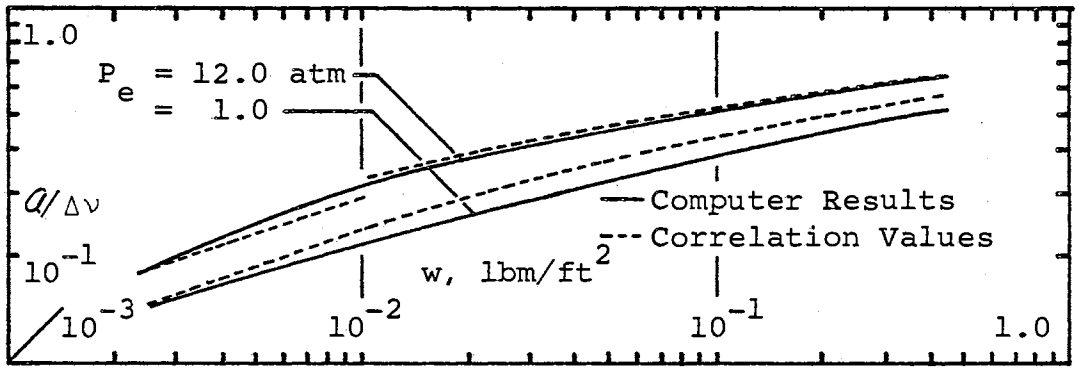

Figure 24. Variation of $a/\Delta\nu$ with Mass Path Length and Equivalent Pressure, 4.3μ - 2500°R

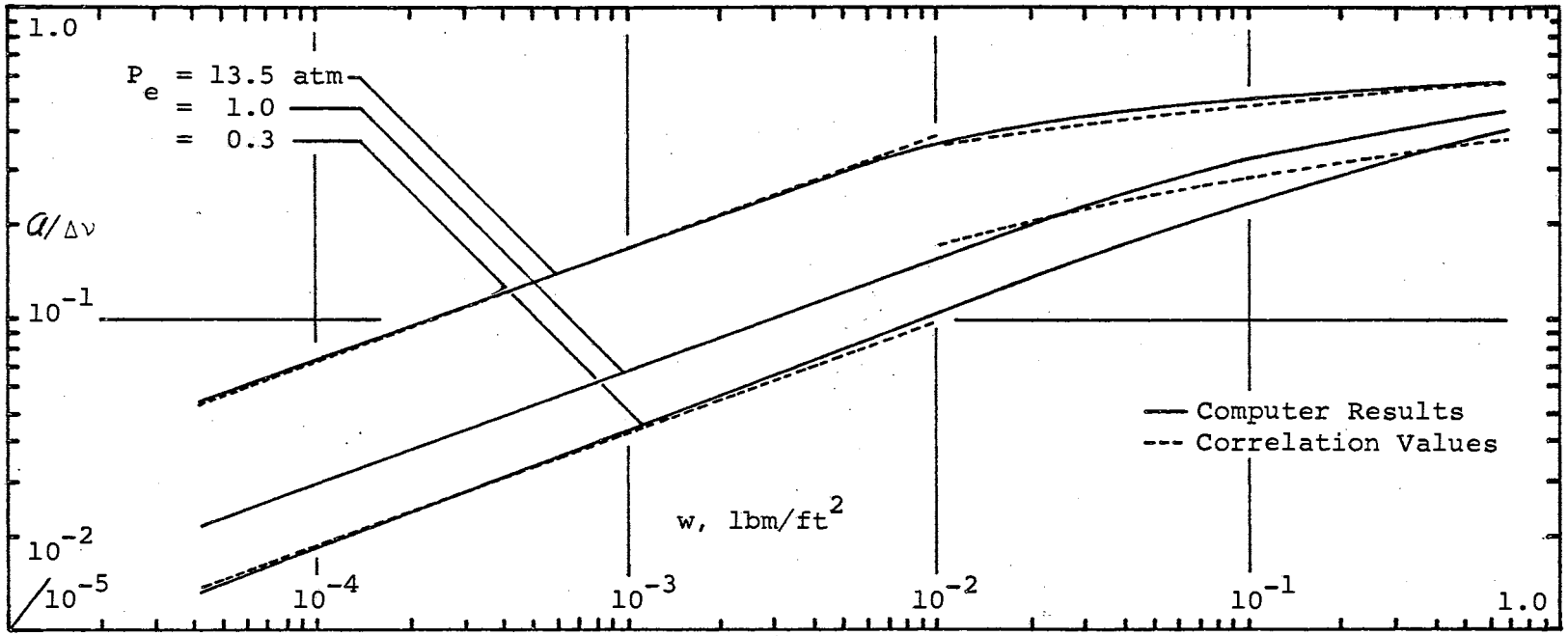

Figure 25. Variation of $a/\Delta\nu$ with Mass Path Length and Equivalent Pressure, 2.7μ - 535°R

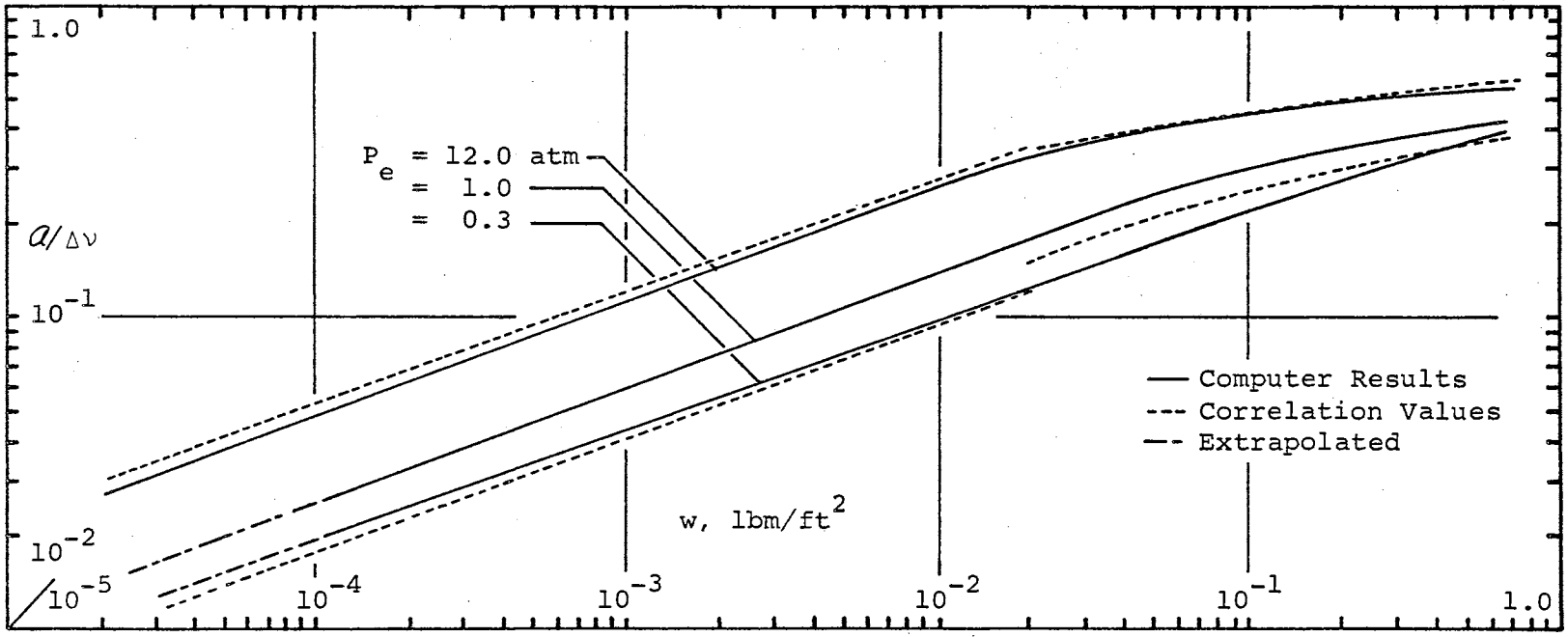

Figure 26. Variation of $a/\Delta\nu$ with Mass Path Length and Equivalent Pressure, 2.7μ- 1000°R

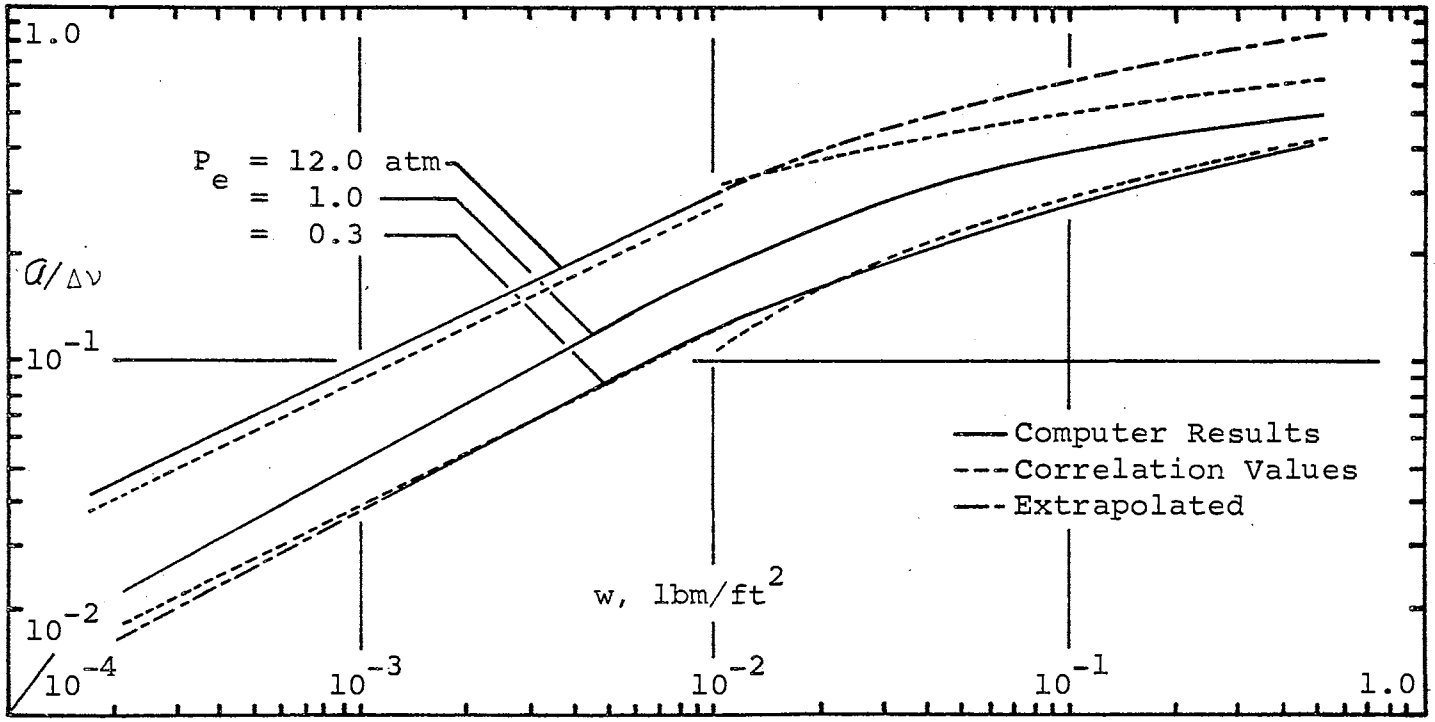

Figure 27. Variation of $a/\Delta\nu$ with Mass Path Length and Equivalent Pressure, 2.7μ - 1500°R

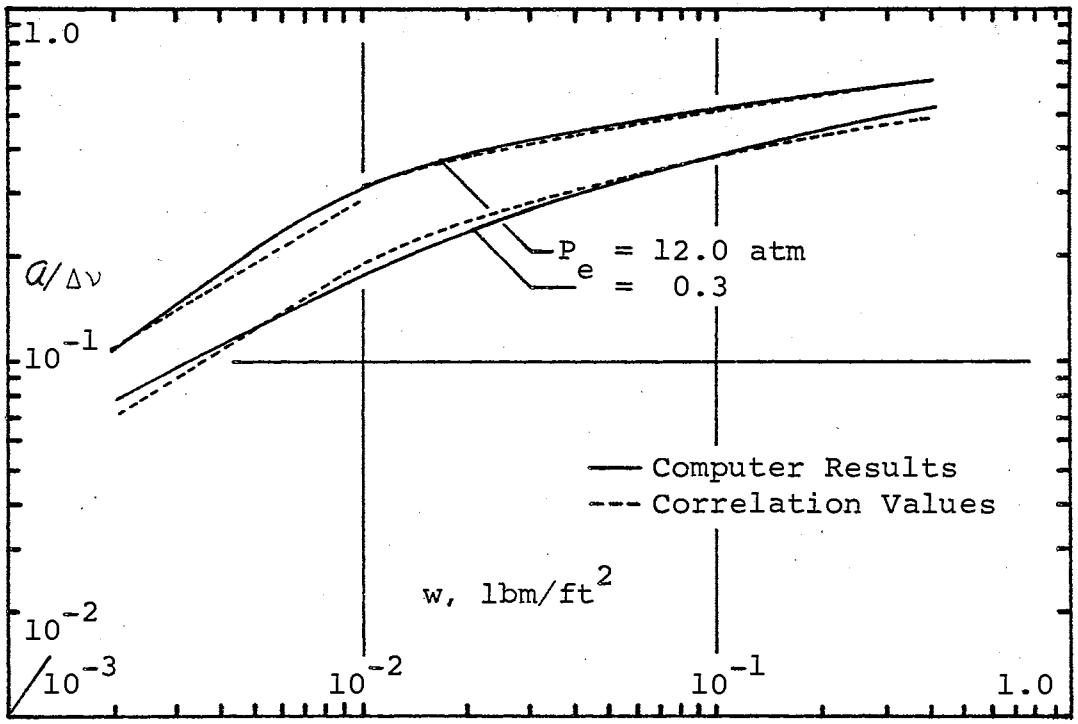

Figure 28. Variation of $a/\Delta\nu$ with Mass Path Length and Equivalent Pressure, 2.7μ - 2000°R

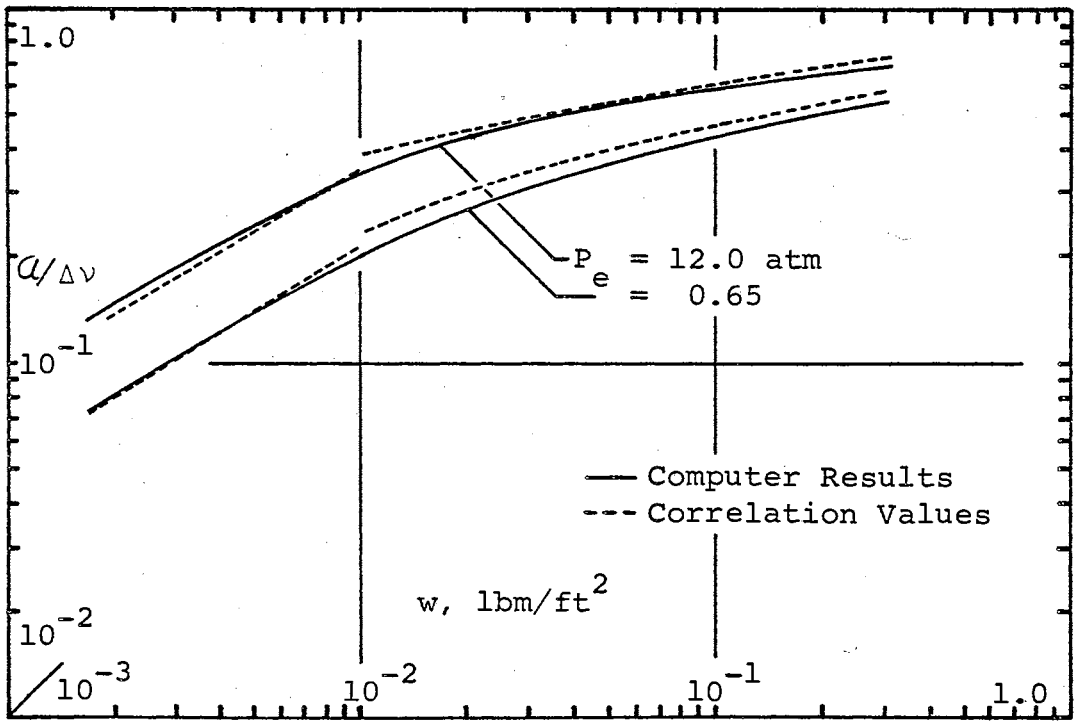

Figure 29. Variation of $a/\Delta\nu$ with Mass Path Length and Equivalent Pressure, 2.7μ - 2500°R

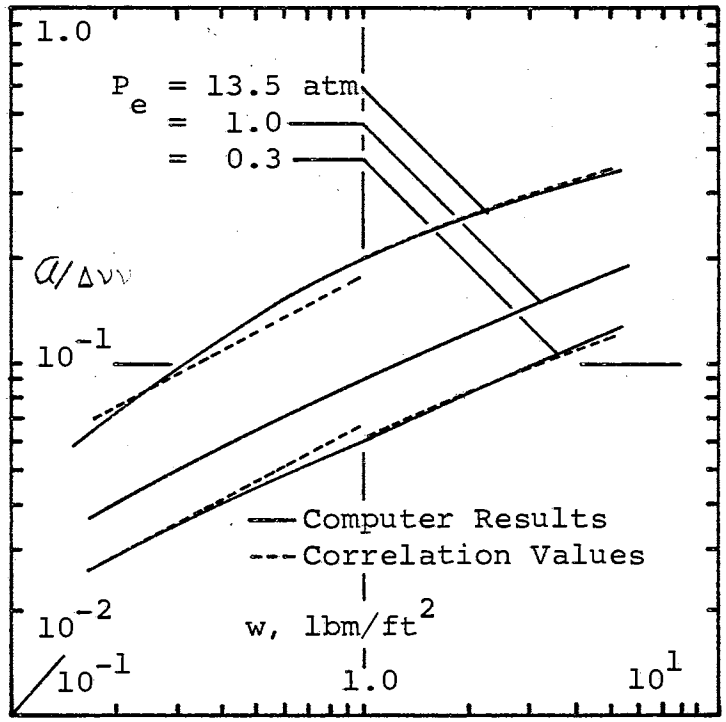

Figure 30. Variation of $a/\Delta\nu$ with Mass Path Length and Equivalent Pressure, 2.0μ - 535°R

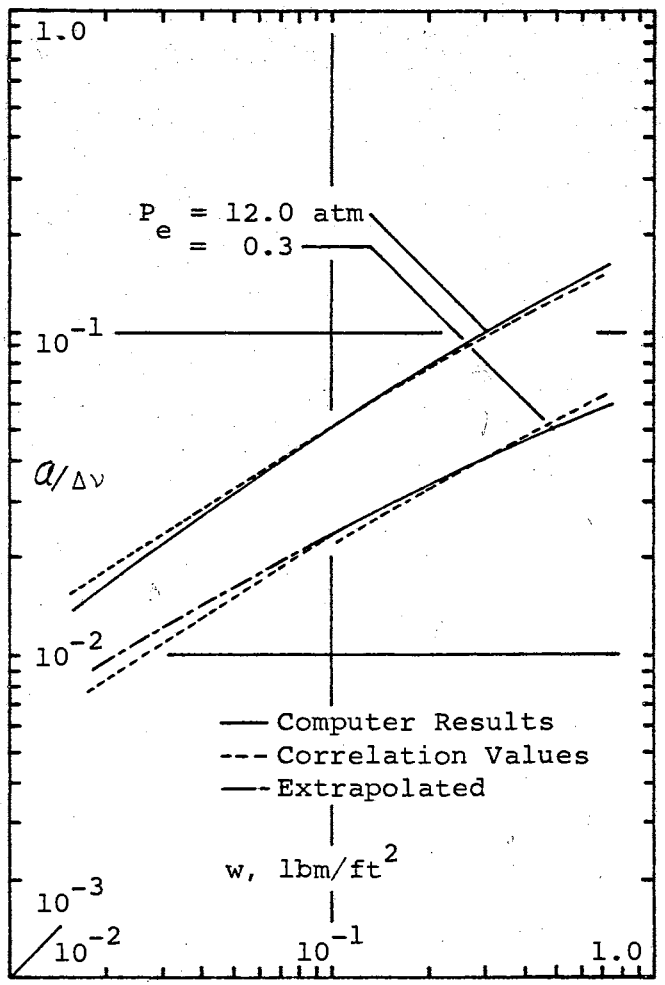

Figure 31. Variation of $a/\Delta\nu$ with Mass Path Length and Equivalent Pressure, 2.0μ - $1000^{\circ}R$

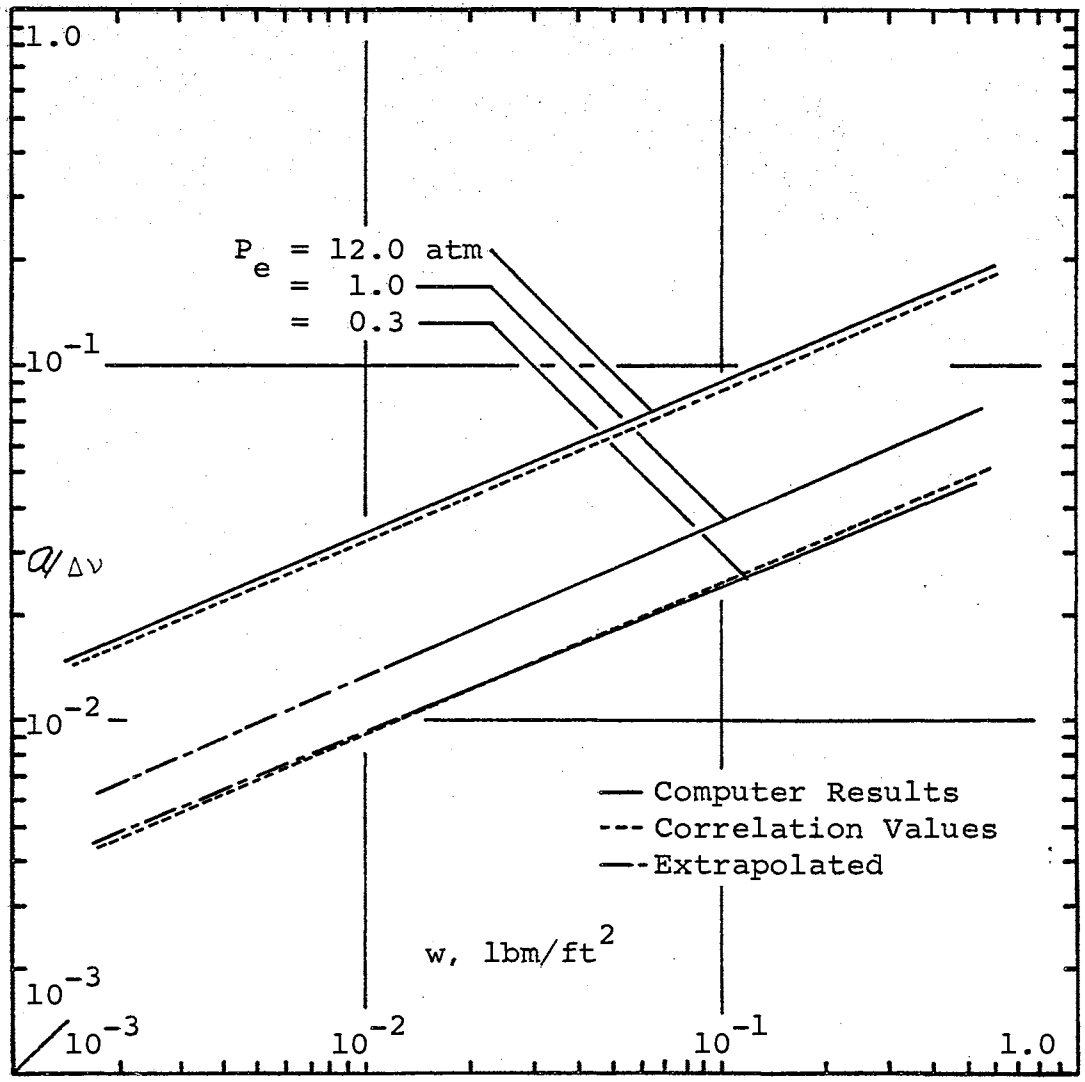

Figure 32. Variation of $a_{\Delta\nu}$ with Mass Path Length and Equivalent Pressure, 2.0μ - 1500°R

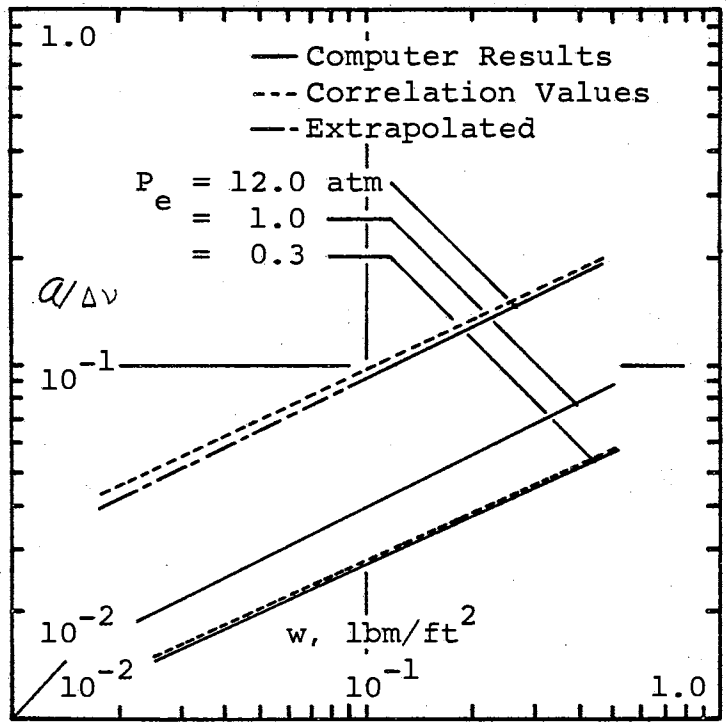

Figure 33. Variation of $a/\Delta\nu$ with Mass Path Length and Equivalent Pressure, 2.0μ - 2000°R

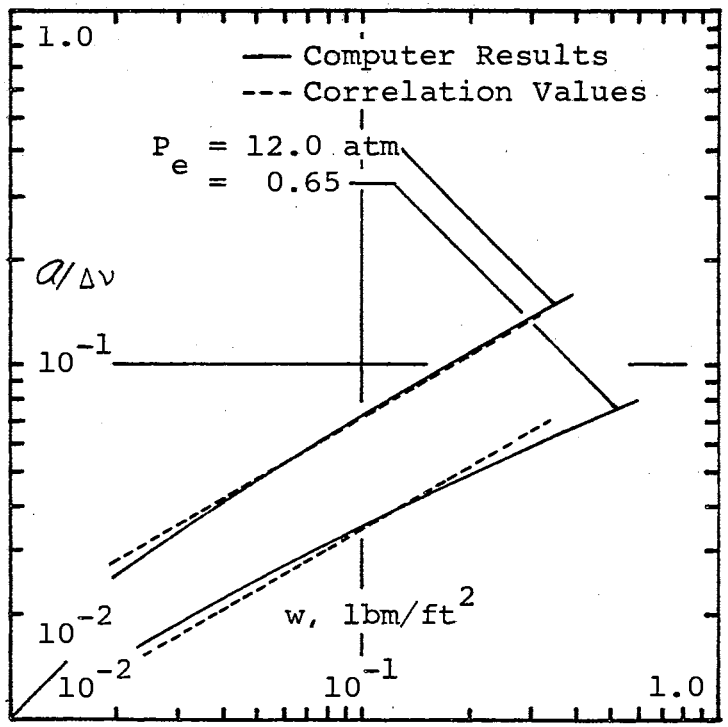

Figure 34. Variation of $a/\Delta\nu$ with Mass Path Length and Equivalent Pressure, 2.0μ - 2500°R

APPENDIX D

CURVES OF a VERSUS w

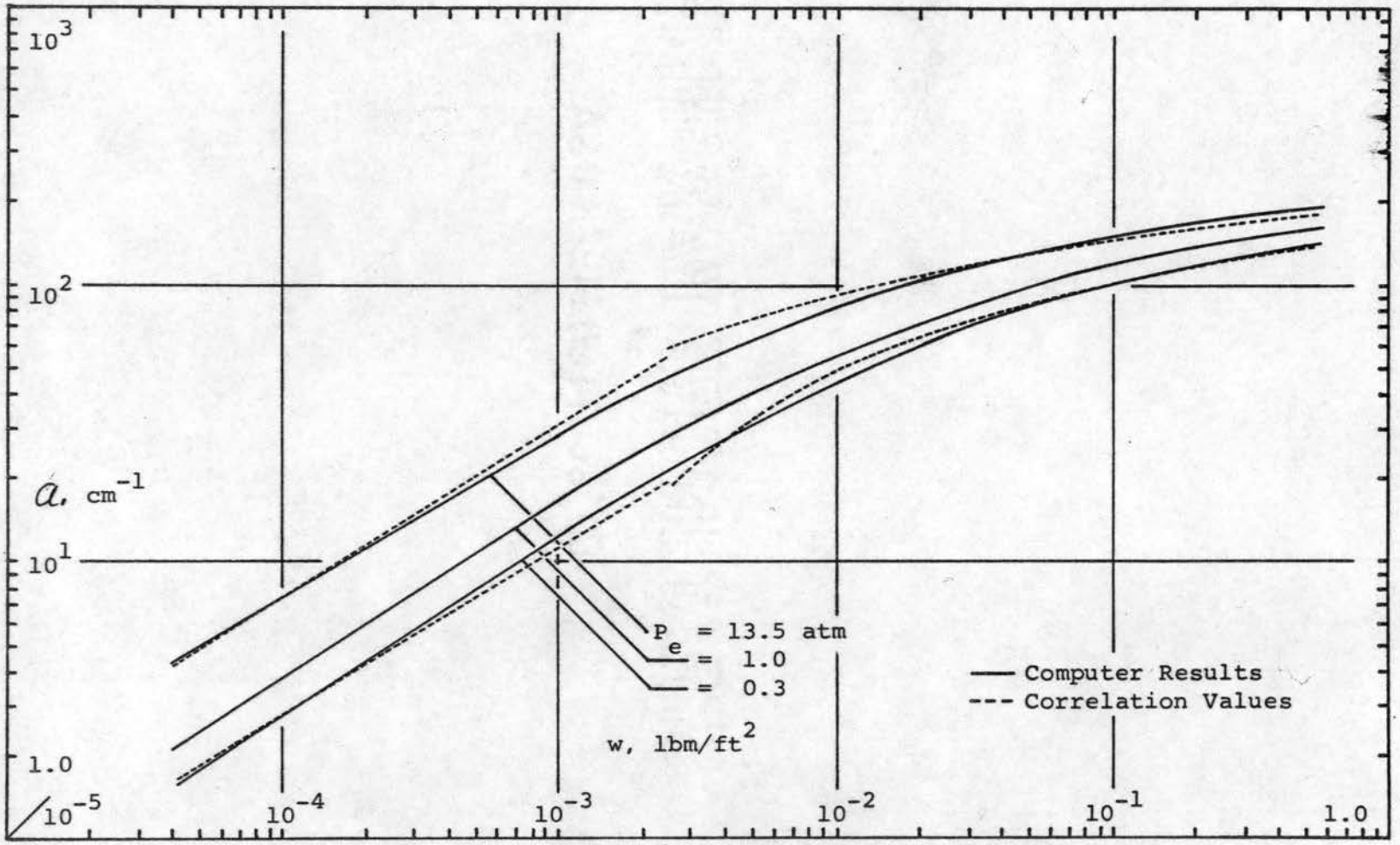

Figure 35. Variation of a with Mass Path Length and Equivalent Pressure, 15.0μ - 535°R

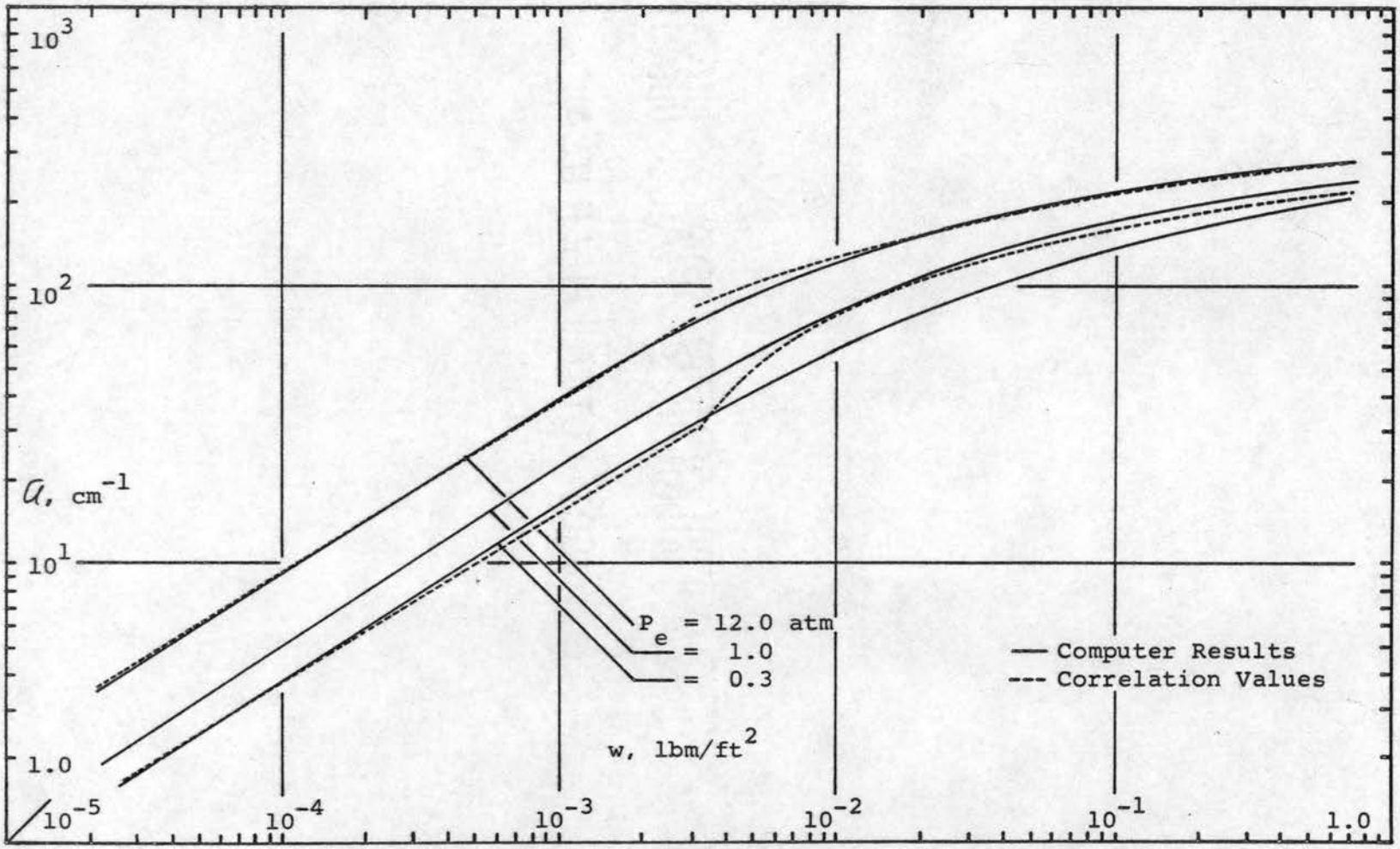

Figure 36. Variation of a with Mass Path Length and Equivalent Pressure, 15.0μ - 1000°R

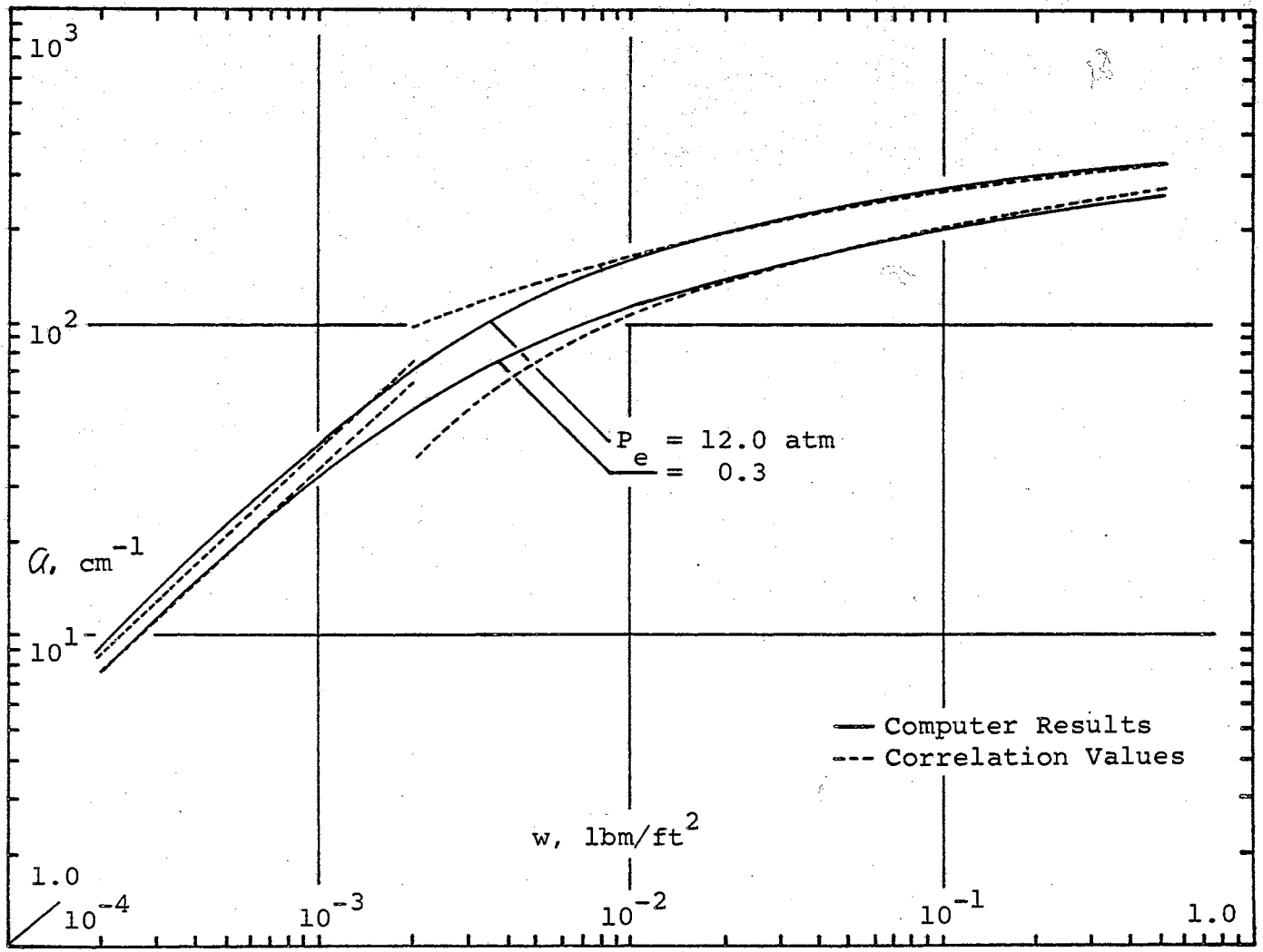

Figure 37. Variation of α with Mass Path Length and Equivalent Pressure, 15.0μ - 1500°R

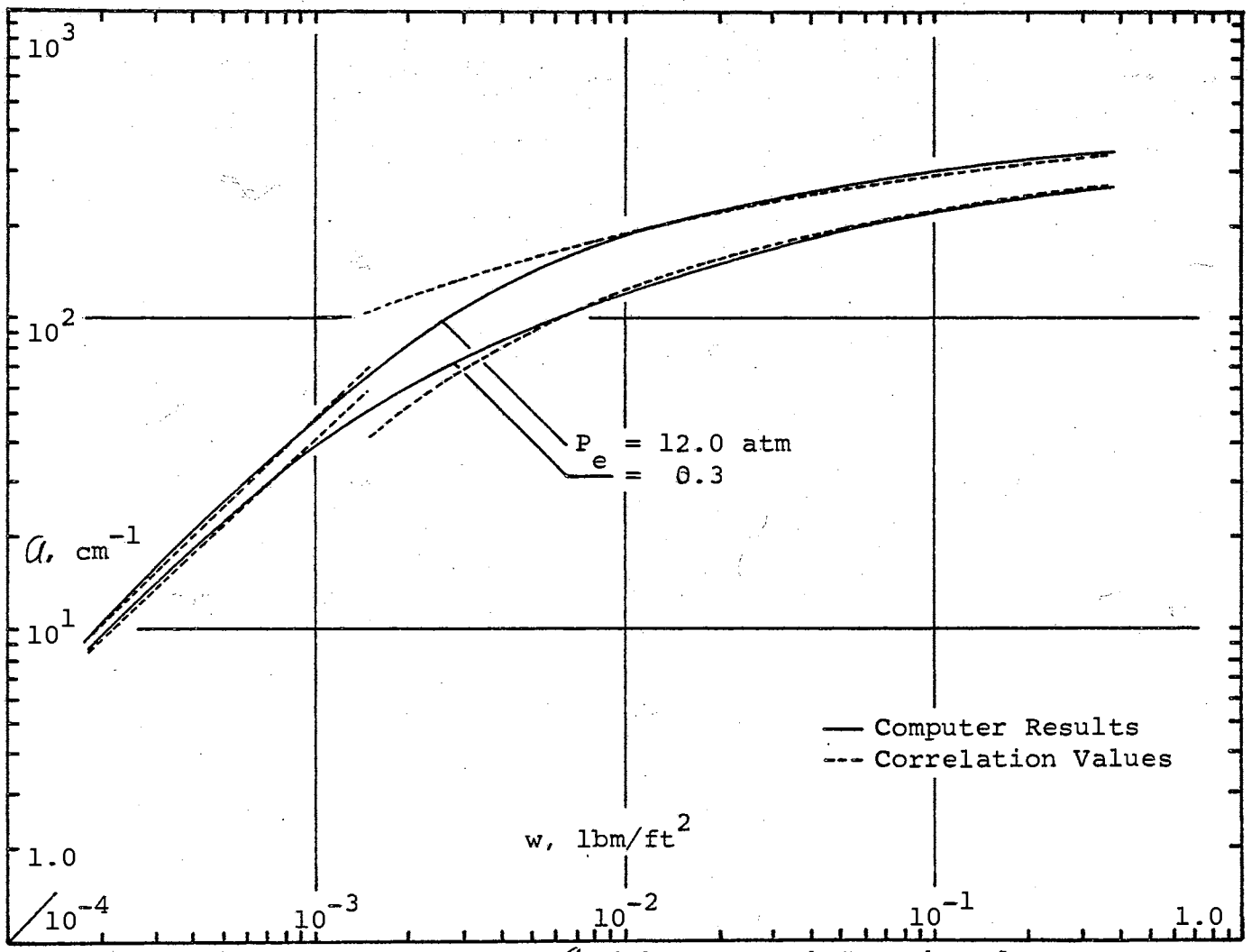

Figure 38. Variation of a with Mass Path Length and Equivalent Pressure, 15.0μ - 2000°R

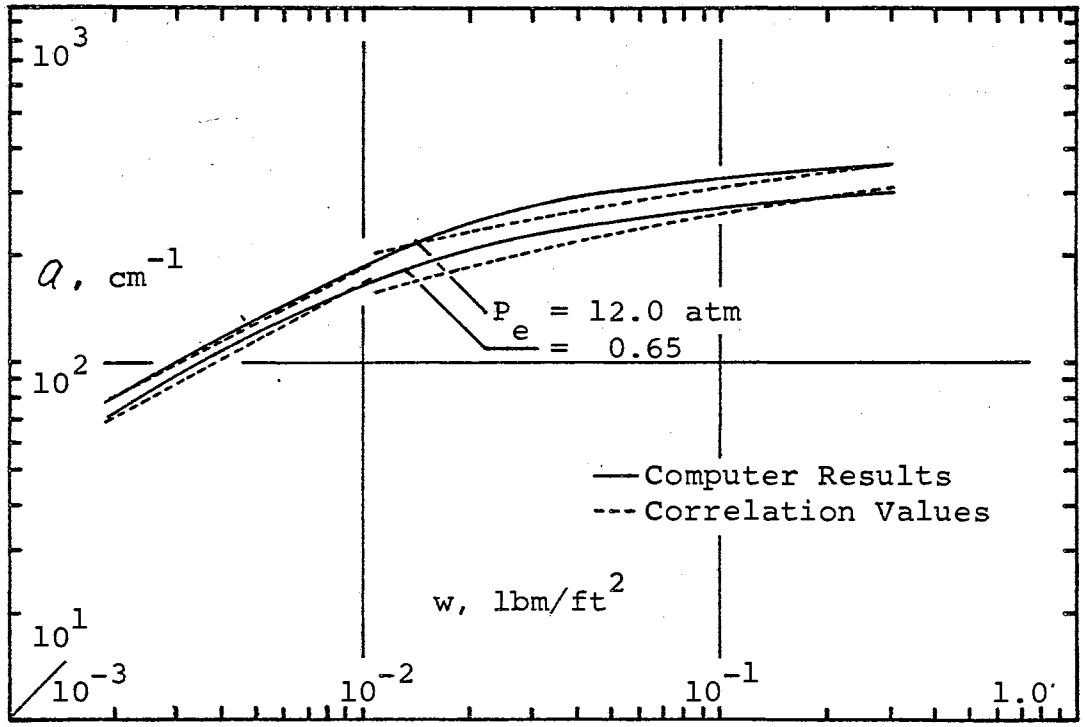

Figure 39. Variation of a with Mass Path Length and Equivalent Pressure, 15.0μ - 2500°R

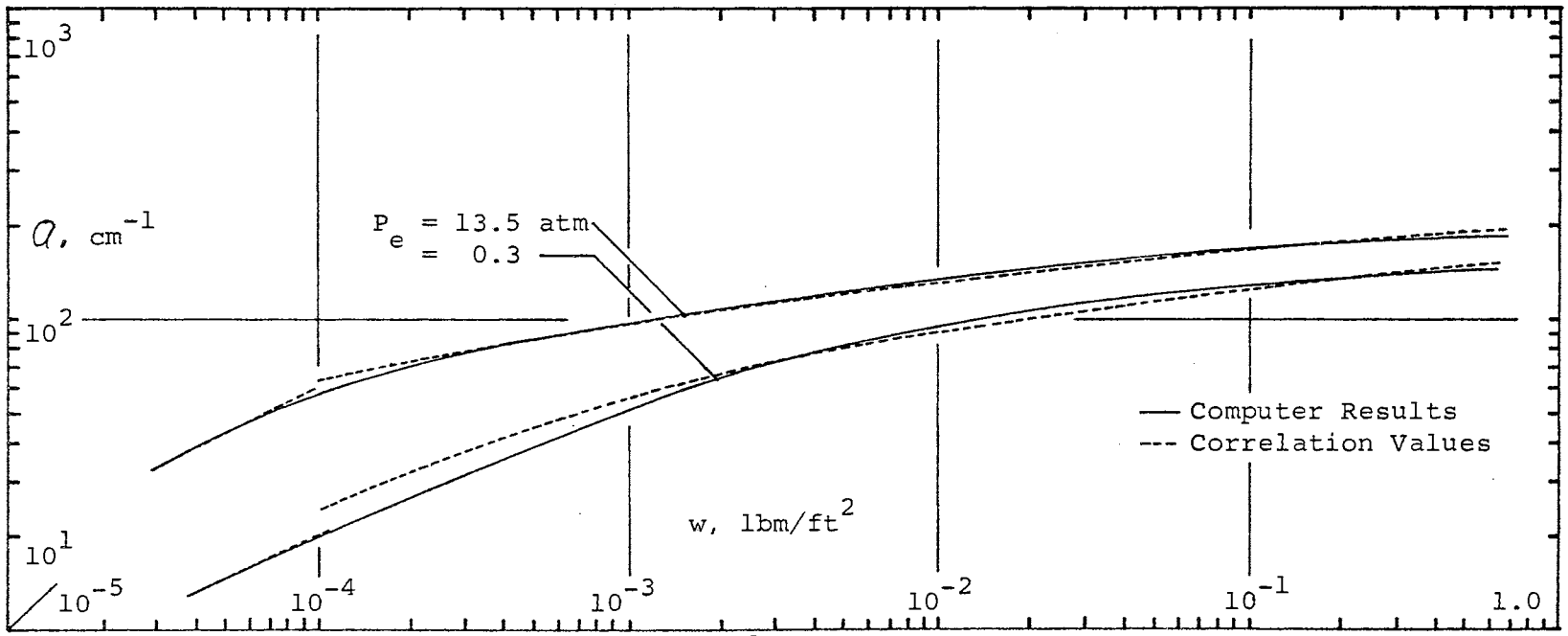

Figure 40. Variation of a with Mass Path Length and Equivalent Pressure, 4.3μ - 535°R

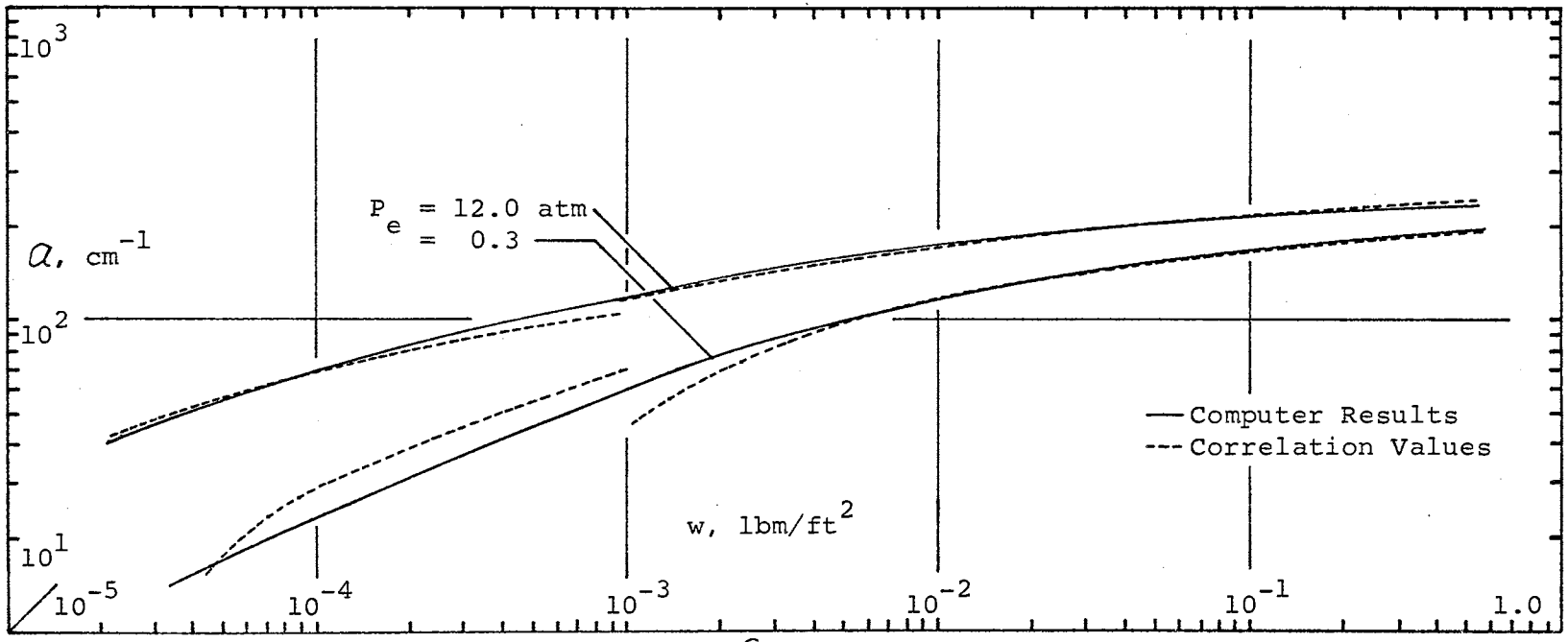

Figure 41. Variation of a with Mass Path Length and Equivalent Pressure, 4.3μ - 1000°R

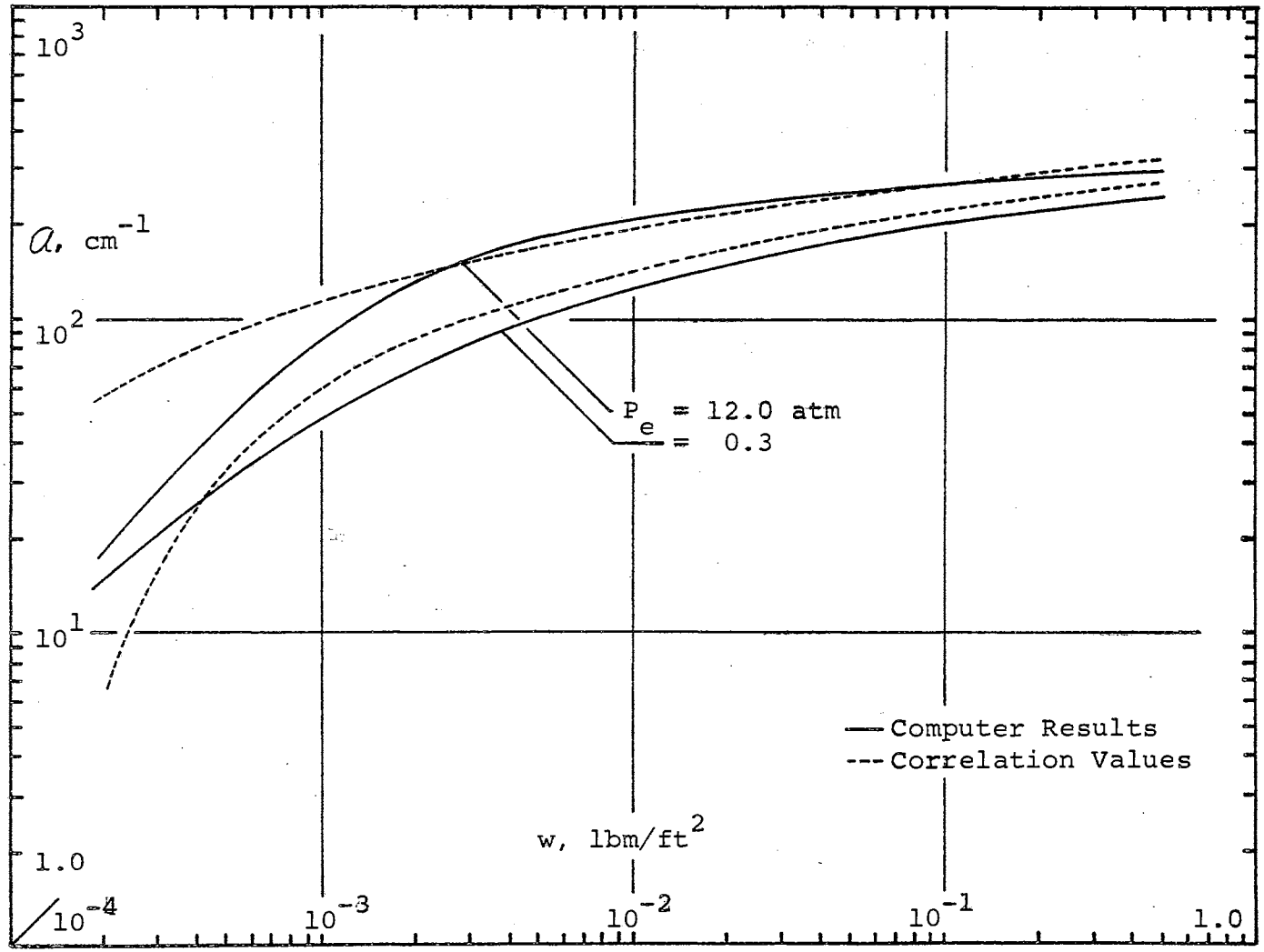

Figure 42. Variation of a with Mass Path Length and Equivalent Pressure, 4.3μ - 1500°R

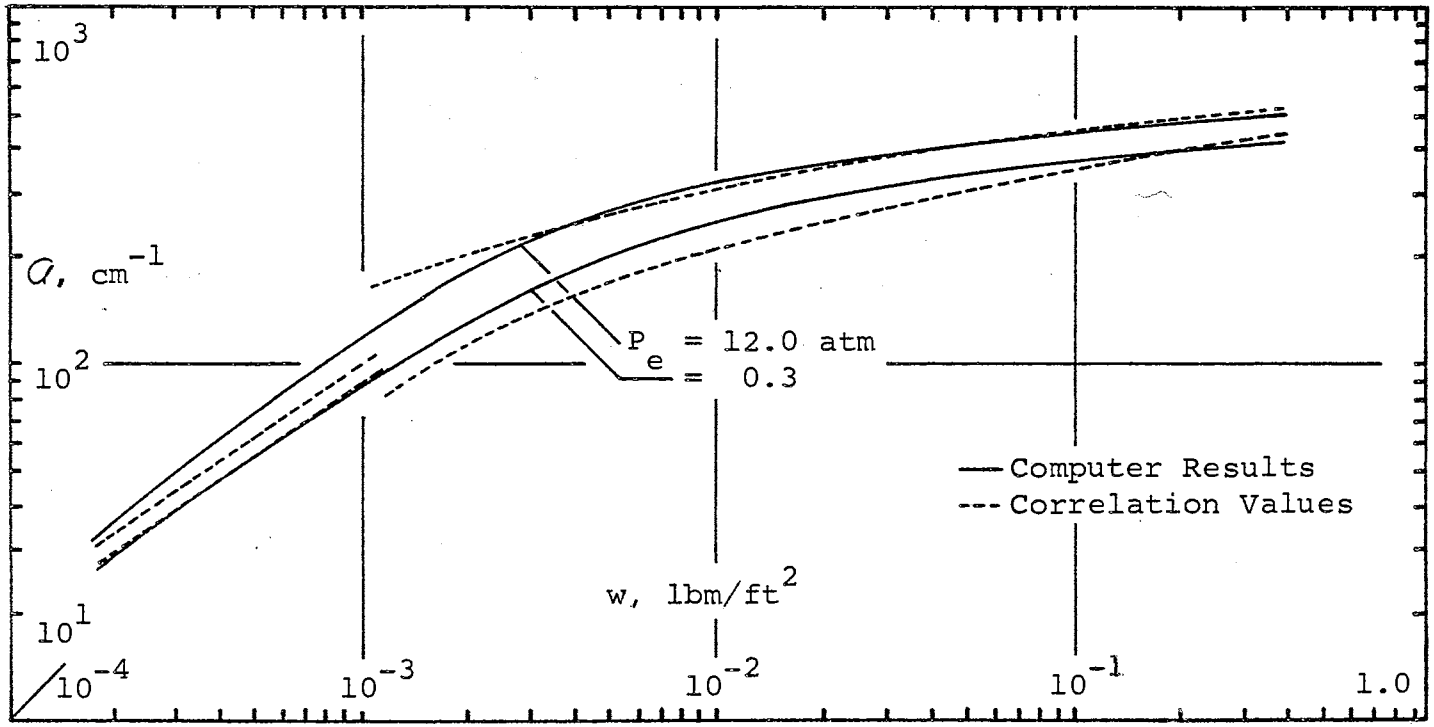

Figure 43. Variation of α with Mass Path Length and Equivalent Pressure, 4.3μ - 2000°R

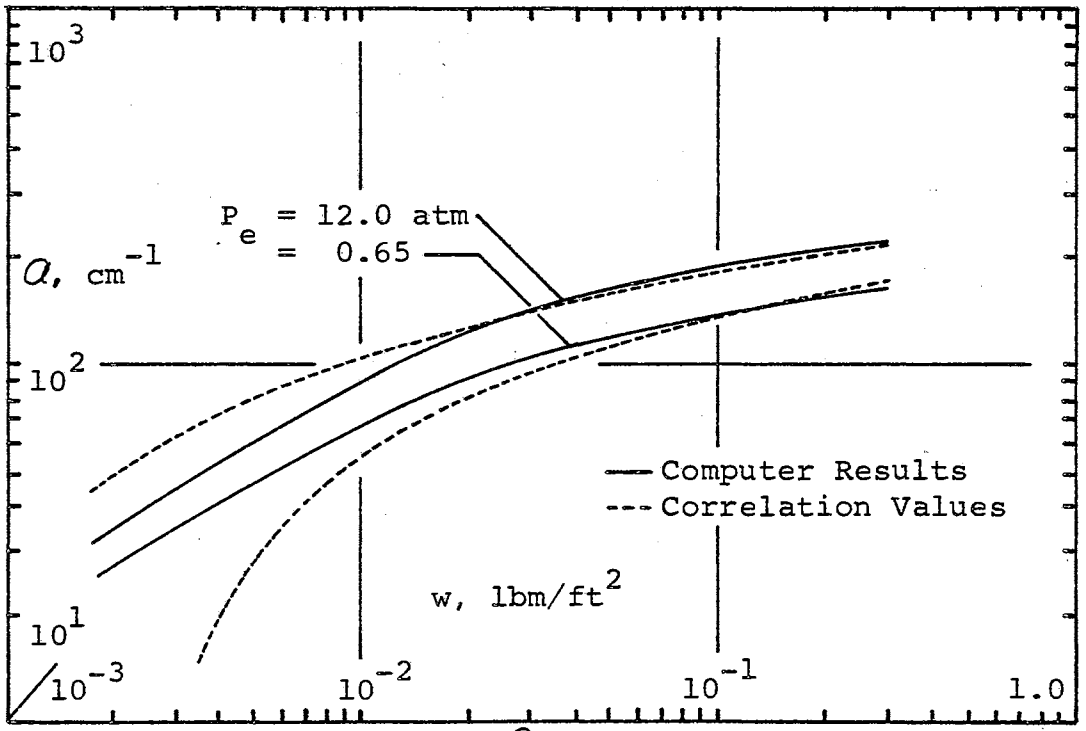

Figure 44. Variation of a with Mass Path Length and Equivalent Pressure, 4.3μ - 2500°R

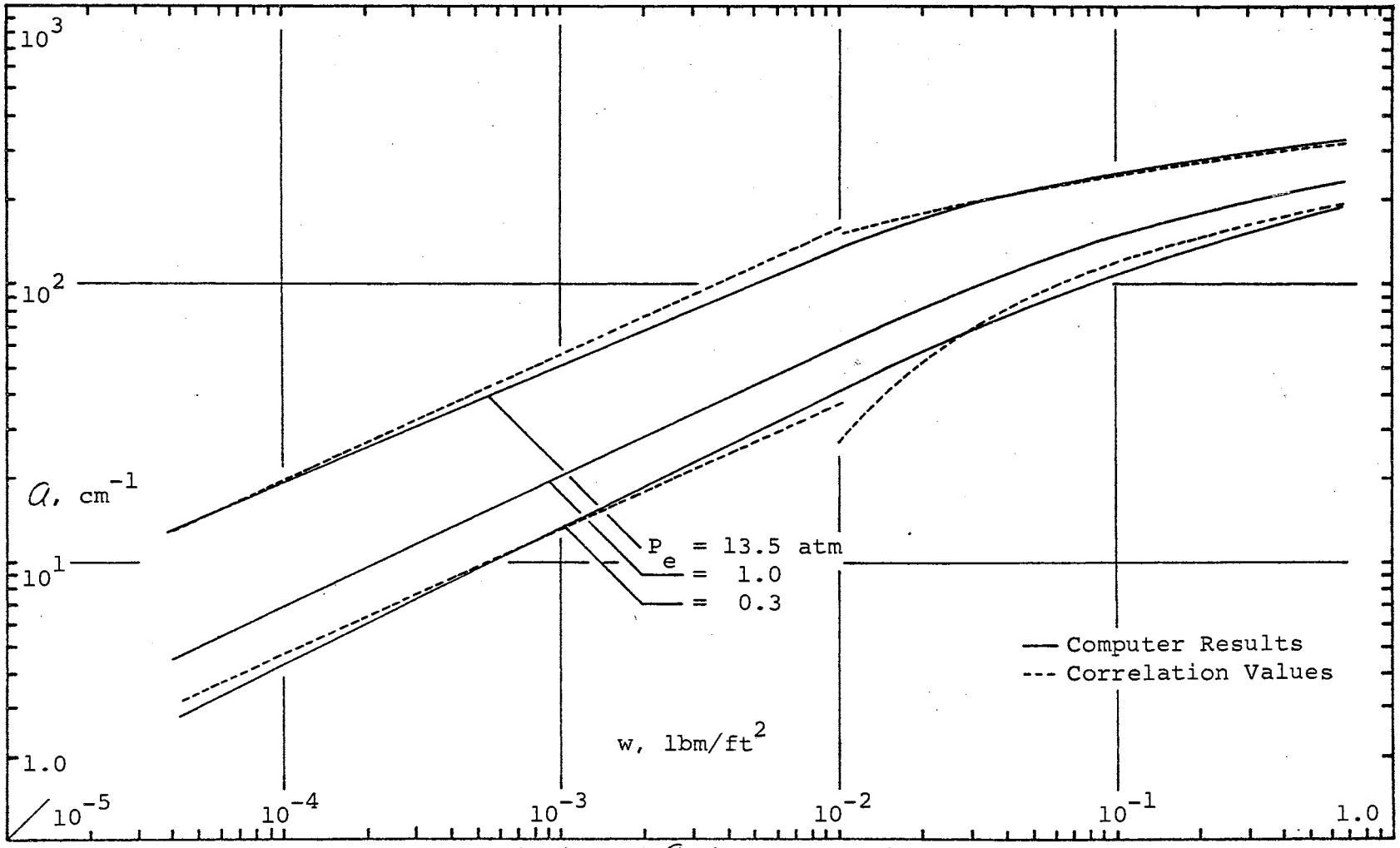

Figure 45. Variation of a with Mass Path Length and Equivalent Pressure, 2.7μ - 535°R

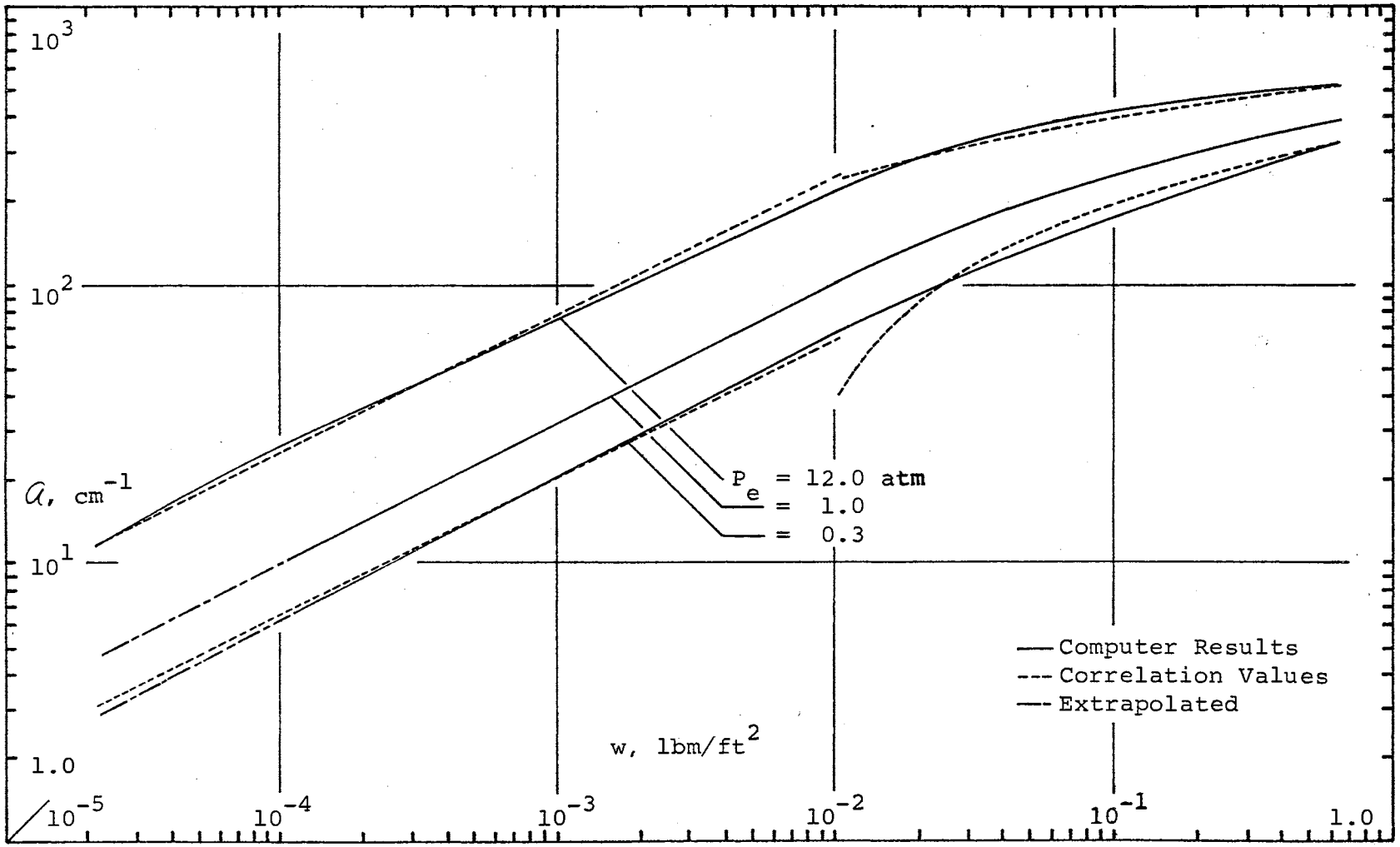

Figure 46. Variation of $\mathcal{A}$ with Mass Path Length and Equivalent Pressure, 2.7μ - 1000°R

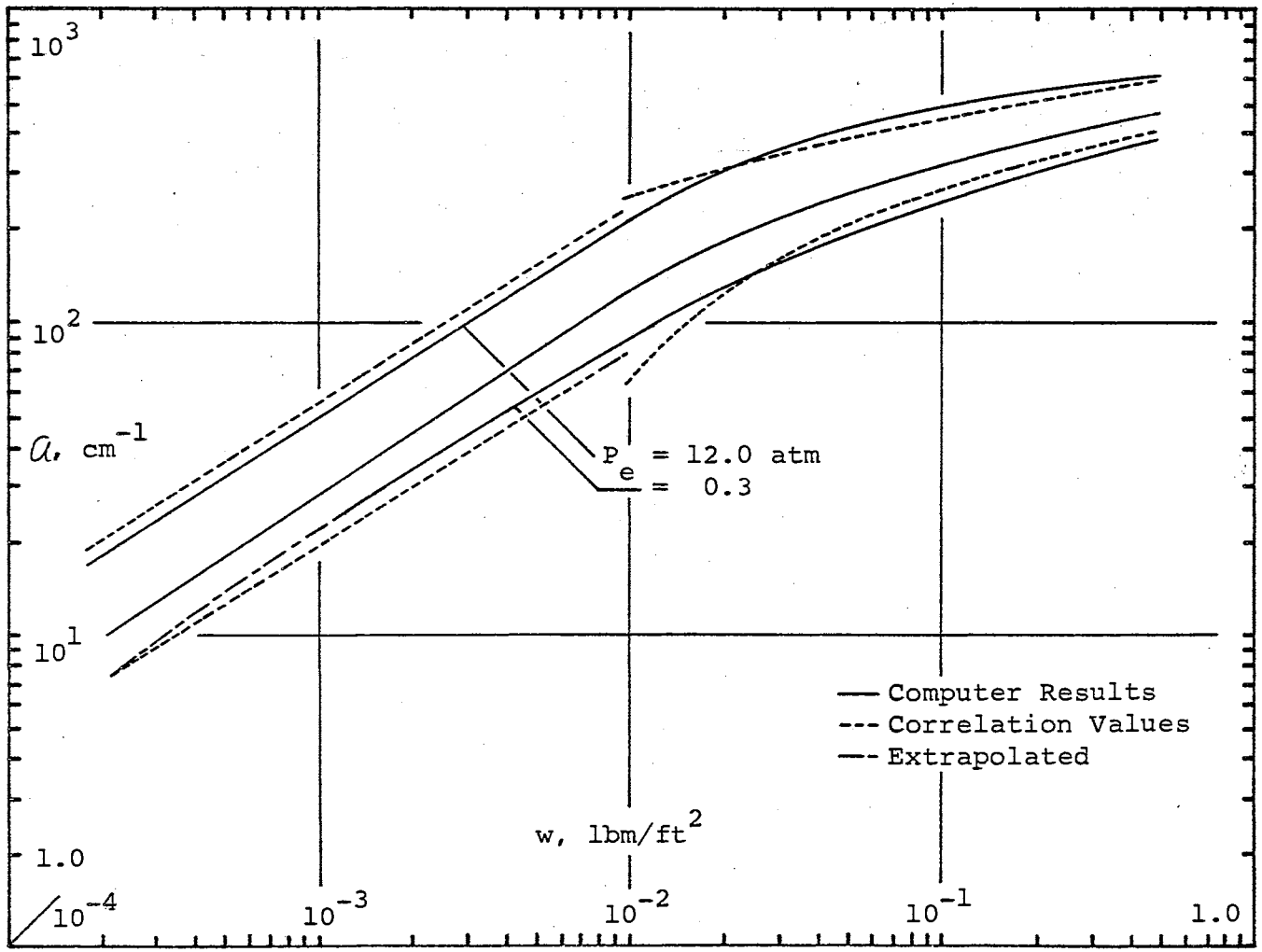

Figure 47. Variation of α with Mass Path Length and Equivalent Pressure, 2.7μ - 1500°R

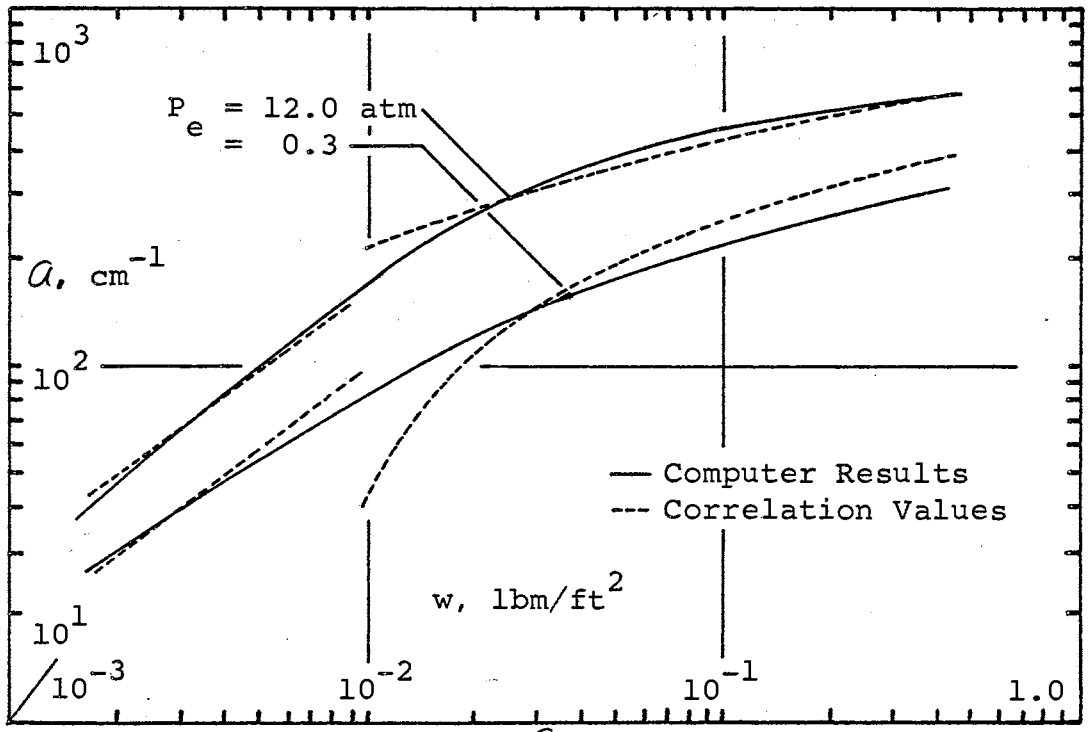

Figure 48. Variation of a with Mass Path Length and Equivalent Pressure, 2.7μ - 2000°R

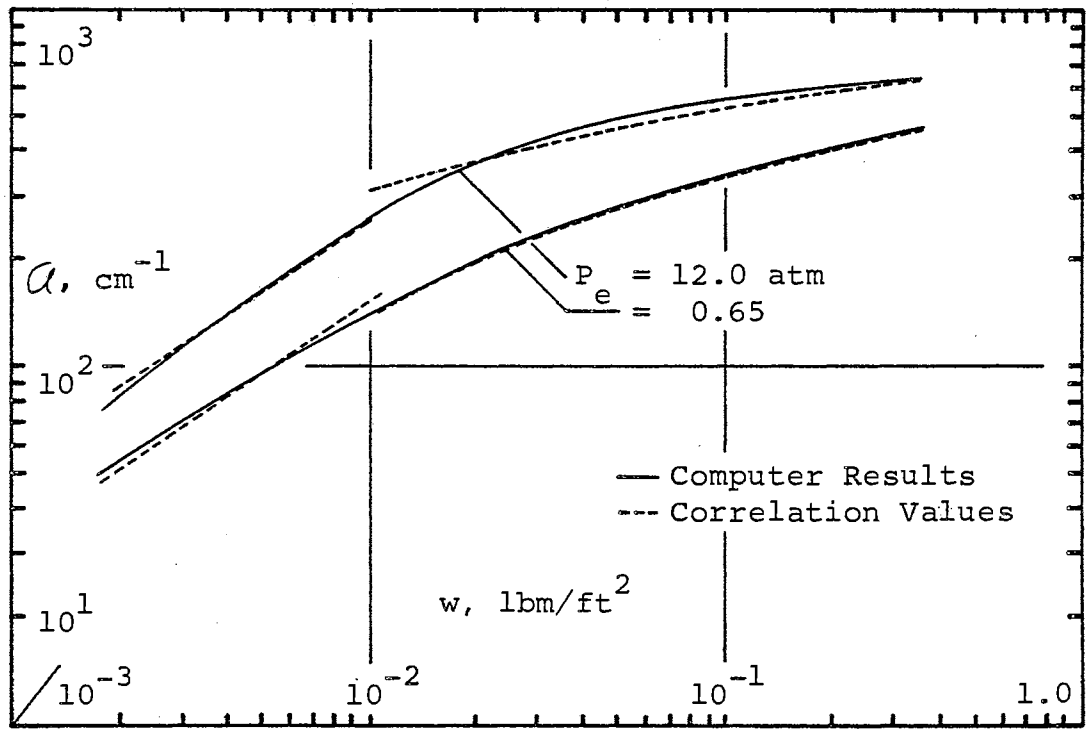

Figure 49. Variation of α with Mass Path Length and Equivalent Pressure, 2.7μ - 2500°R

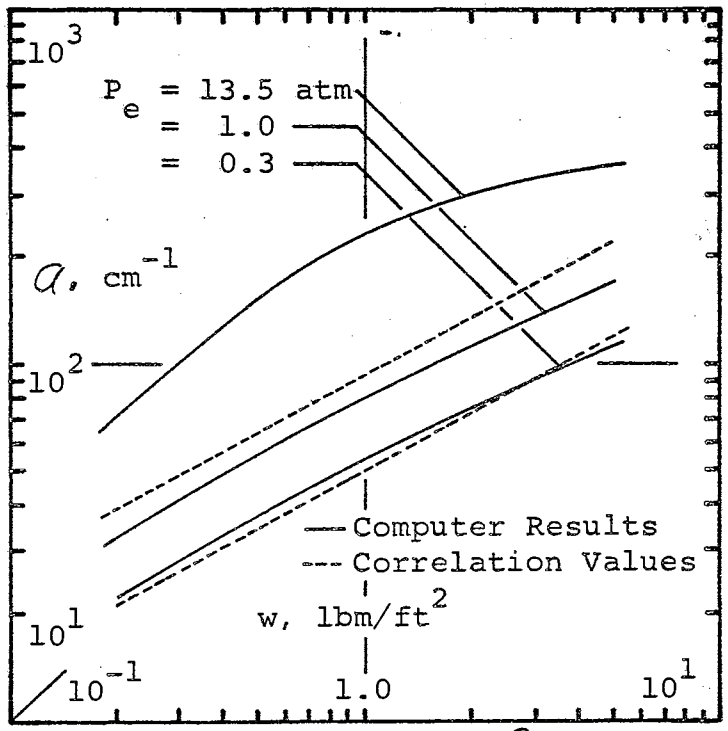

Figure 50. Variation of a with Mass Path Length and Equivalent Pressure, 2.0μ - $535^{\circ}R$

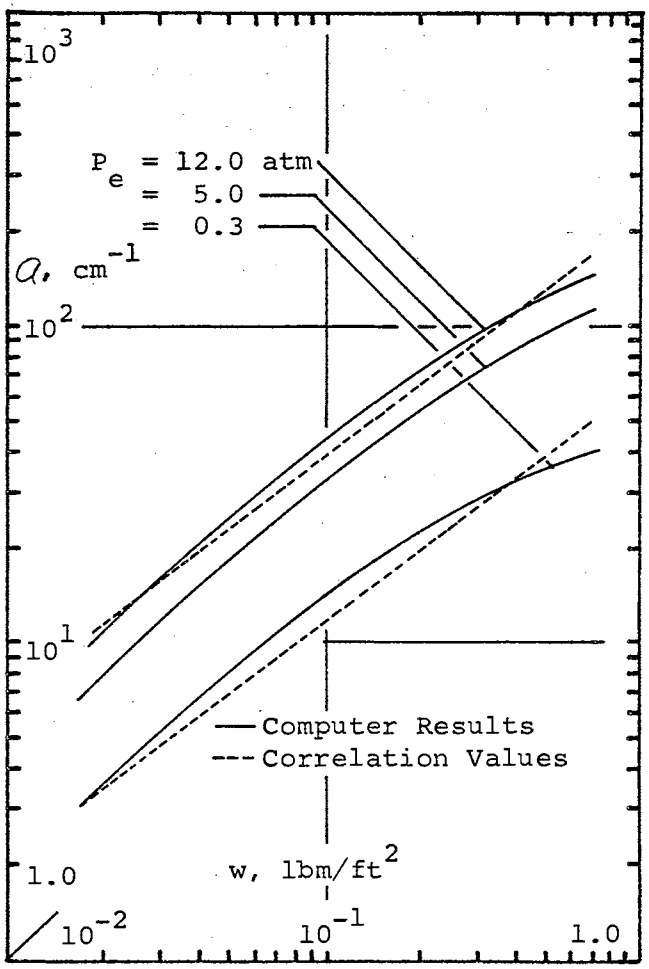

Figure 51. Variation of $\mathcal{Q}$ with Mass Path Length and Equivalent Pressure, 2.0μ - 1000°R

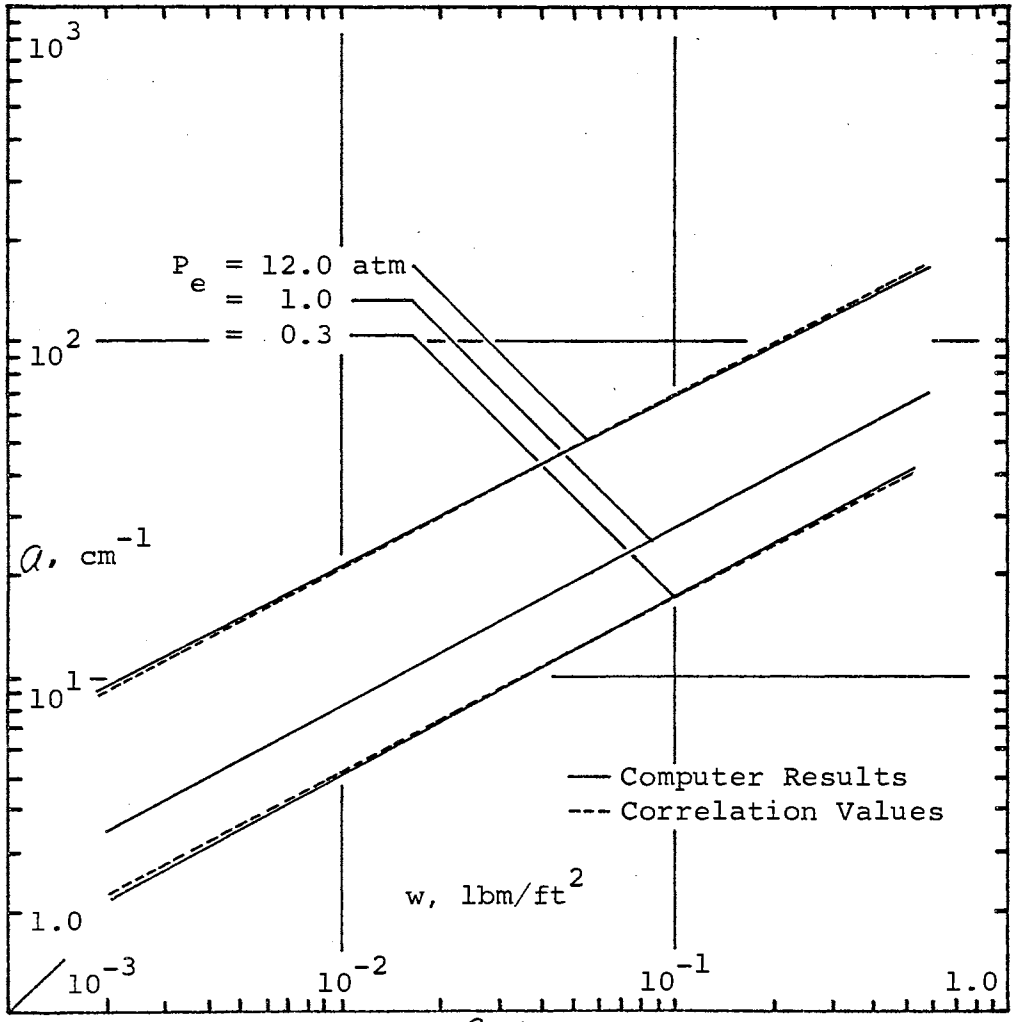

Figure 52. Variation of a with Mass Path Length and Equivalent Pressure, 2.0μ - 1500°R

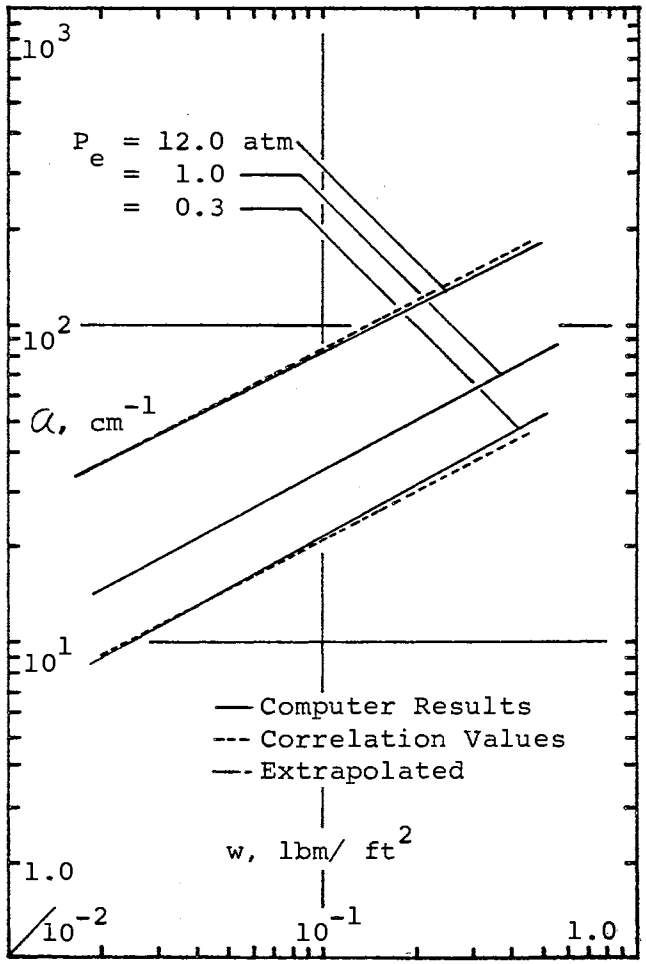

Figure 53. Variation of α with Mass Path Length and Equivalent Pressure, 2.0μ - 2000°R

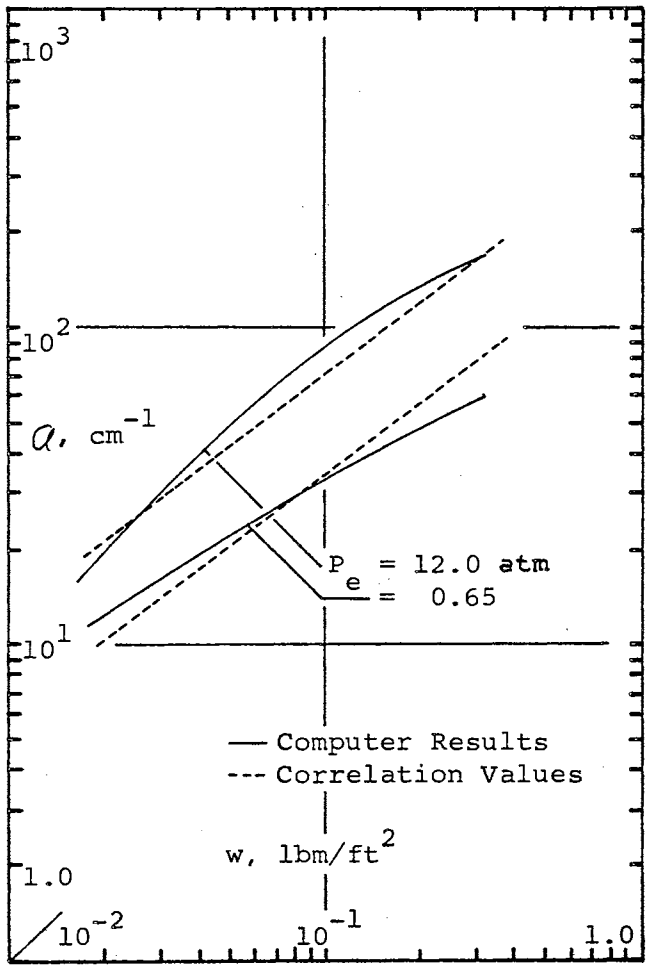

Figure 54. Variation of a with Mass Path Length and Equivalent Pressure, 2.0μ - 2500°R

APPENDIX E

MONOCHROMATIC SOLUTION OF EXAMPLE PROBLEM

Monochromatic values of radiant heat transfer to the surfaces of the duct enclosure may be calculated from Equations (I-1) and (I-8). Using the relation, $\epsilon_{j\nu}=\alpha_{j\nu}$, Equation (I-1) becomes

$$q_{j\nu} = \frac{\alpha_{j\nu}}{\rho_{j\nu}} (J_{j\nu} - E_{bj\nu}) \quad . \tag{E-1}$$

Equation (I-8) may be rewritten as

$$J_{j\nu}=\epsilon_{j\nu}E_{bj\nu}+\rho_{j\nu}\sum_{k=1}^{M}[\tau_{g\nu}(\bar{r}_{jk})J_{k\nu}+\alpha_{g\nu}(\bar{r}_{jk})E_{bg\nu}]F_{jk} \tag{E-2}$$

$$j = 1, 2, \ldots, M,$$

where the functional dependence of gas absorptance on $\bar{r}_{jk}$ is indicated.

One may expand Equation (E-2), letting j and k range from 1 to 4 for the duct enclosure. After expansion, the coefficients of the four unknown spectral radiosities may be collected and the resulting four algebraic equations may be expressed in matrix notation, as was done with the band method of solution. The results are shown in Equation (E-3).

$$
\begin{pmatrix}
1 & -\rho_{1\nu}\tau_{g\nu}(\bar{r}_{12})F_{12} & -\rho_{1\nu}\tau_{g\nu}(\bar{r}_{13})F_{13} & -\rho_{1\nu}\tau_{g\nu}(\bar{r}_{14})F_{14} \\
-\rho_{2\nu}\tau_{g\nu}(\bar{r}_{21})F_{21} & 1 & -\rho_{2\nu}\tau_{g\nu}(\bar{r}_{23})F_{23} & -\rho_{2\nu}\tau_{g\nu}(\bar{r}_{24})F_{24} \\
-\rho_{3\nu}\tau_{g\nu}(\bar{r}_{31})F_{31} & -\rho_{3\nu}\tau_{g\nu}(\bar{r}_{32})F_{32} & 1 & -\rho_{3\nu}\tau_{g\nu}(\bar{r}_{34})F_{34} \\
-\rho_{4\nu}\tau_{g\nu}(\bar{r}_{41})F_{41} & -\rho_{4\nu}\tau_{g\nu}(\bar{r}_{42})F_{42} & -\rho_{4\nu}\tau_{g\nu}(\bar{r}_{43})F_{43} & 1
\end{pmatrix}
$$

(E-3)

$$
= \begin{pmatrix}
\rho_{1\nu}E_{bg\nu}[\alpha_{g\nu}(\bar{r}_{12})F_{12} + \alpha_{g\nu}(\bar{r}_{13})F_{13} + \alpha_{g\nu}(\bar{r}_{14})F_{14}] + \epsilon_{1\nu}E_{b1\nu} \\
\rho_{2\nu}E_{bg\nu}[\alpha_{g\nu}(\bar{r}_{21})F_{21} + \alpha_{g\nu}(\bar{r}_{23})F_{23} + \alpha_{g\nu}(\bar{r}_{24})F_{24}] + \epsilon_{2\nu}E_{b2\nu} \\
\rho_{3\nu}E_{bg\nu}[\alpha_{g\nu}(\bar{r}_{31})F_{31} + \alpha_{g\nu}(\bar{r}_{32})F_{32} + \alpha_{g\nu}(\bar{r}_{34})F_{34}] + \epsilon_{3\nu}E_{b3\nu} \\
\rho_{4\nu}E_{bg\nu}[\alpha_{g\nu}(\bar{r}_{41})F_{41} + \alpha_{g\nu}(\bar{r}_{42})F_{42} + \alpha_{g\nu}(\bar{r}_{43})F_{43}] + \epsilon_{4\nu}E_{b4\nu}
\end{pmatrix}
$$

In order to check the calculations with an energy balance, one may calculate the energy from the j^{th} surface to the gas from the following expression:

$$q_{j\text{-}gas,\nu} = \sum_{k=1}^{M} [\alpha_{g\nu}(\bar{r}_{jk}) F_{jk} J_{j\nu} - \alpha_{g\nu}(\bar{r}_{jk}) F_{jk} E_{bg\nu}],$$

which simplifies to

$$q_{j\text{-}gas,\nu} = (J_{j\nu} - E_{bg\nu}) \sum_{k=1}^{M} \alpha_{g\nu}(\bar{r}_{jk}) F_{jk} \quad . \qquad \text{(E-4)}$$

A computer program was written to evaluate Equations (E-1, 3, 4) for the surface radiosities and spectral heat transfer. A listing of this program follows.

PROGRAM TO CALCULATE MONOCHROMATIC HEAT TRANSFER

INPUT

TG = gas temperature, T_g, $^\circ R$

PTOT = total gas mixture pressure, atm

XA = absorbing gas mole fraction

RA = gas constant of absorbing gas, $\frac{ft - lbf}{lbm - {}^\circ R}$

PB = partial pressure of broadening gas, atm

B = constant b in Equation (II-9)

EN = exponent n in Equation (III-1)

MM = number of surfaces in enclosure

T(I) = temperature of i^{th} surface, $^\circ R$

F(I,J) = configuration factor, F_{ij}

R(I,J) = geometric mean beam length, $\bar{r}_{ij}$

GNU = wavenumber, ν, cm^{-1}

CSQ, BSQ, BC = constants in Equations (III-1, 2)

OUTPUT

GNU = wavenumber, ν, cm^{-1}

Q(I) = monochromatic radiant heat transfer to the i^{th} surface,

$$q_{i\nu}, \frac{Btu}{hr - ft^2 - cm^{-1}}$$

QG(I) = monochromatic radiant heat transfer from the i^{th} surface to the gas,

$$q_{i-g,\nu'} \frac{Btu}{hr - ft^2 - cm^{-1}}$$

```
      DIMENSIONT(10),F(10,10),R(10,10),W(10,10),TAU(10,10),ALFAG(10,10),
     1EB(10),RHO(10),ALFA(10),A(10,11),Q(10),QG(10)
      COMMONA,N,M
  100 FORMAT(8F10.5)
  101 FORMAT(I3)
  102 FORMAT(1HL,4HGNU=,1PE20.7/(28X,2HQ(,I2,2H)=,1PE20.7,5X,3HQG(,I2,2H
     1)=,1PE20.7))
      READ(1,100)TG,PTOT,XA,RA,PB,B,EN
      READ(1,101)MM
      READ(1,100)(T(I),I=1,MM)
      DO1000I=1,MM
 1000 READ(1,100)(F(I,J),J=1,MM)
      DO1001I=1,MM
 1001 READ(1,100)(R(I,J),J=1,MM)
    9 READ(1,100)GNU,CSQ,BSQ,BC
      PA=XA*PTOT
      DO10J=1,MM
      DO10I=1,MM
   10 W(I,J)=(2116.224*PA*R(I,J))/(RA*TG)
      PE=PB+B*PA
      C1=1.1855E-8
      C2=2.5884
      IF(BC.NE.0.0)GOTO30
      DO20J=1,MM
      DO20I=1,MM
   20 TAU(I,J)=EXP(-(CSQ*W(I,J))/(SQRT(1.+(CSQ*W(I,J))/(BSQ*(PE**EN)))))
      GOTO41
   30 DO40J=1,MM
      DO40I=1,MM
   40 TAU(I,J)=EXP(-BC*SQRT(W(I,J)*(PE**EN)))
   41 DO50J=1,MM
      DO50I=1,MM
   50 ALFAG(I,J)=1.-TAU(I,J)
      EBG=(C1*(GNU**3.))/(EXP((C2*GNU)/TG)-1.)
      DO60I=1,MM
   60 EB(I)=(C1*(GNU**3.))/(EXP((C2*GNU)/T(I))-1.)
      READ(1,100)GNU,(RHO(I),I=1,MM)
      DO70I=1,MM
   70 ALFA(I)=1.-RHO(I)
      DO80I=1,MM
      MM1=MM+1
      DO80J=1,MM1
      IF(I.EQ.J)GOTO90
      IF(J.EQ.MM+1)GOTO91
      A(I,J)=-RHO(I)*TAU(I,J)*F(I,J)
      GOTO80
   90 A(I,J)=1.
      GOTO80
   91 SUM=0.
      DO92K=1,MM
   92 SUM=SUM+ALFAG(I,K)*F(I,K)
      A(I,J)=(RHO(I)*EBG*SUM)+ALFA(I)*EB(I)
   80 CONTINUE
      N=MM
      M=MM+1
      CALL INVERT
      DO93I=1,MM
   93 Q(I)=(ALFA(I)/RHO(I))*(A(I,MM+1)-EB(I))
      DO95I=1,MM
      SUM2=0.
      DO94L=1,MM
   94 SUM2=SUM2+(ALFAG(I,L)*F(I,L))
   95 QG(I)=(A(I,MM+1)-EBG)*SUM2
      WRITE(3,102)GNU,(I,Q(I),I,QG(I),I=1,MM)
      GOTO9
      END
     MON$$     EXEQ FORTRAN,SOF,SIU,10,03,,,
      SUBROUTINE INVERT                                                 0284
      COMMONX(10,11),N,M
      DO 30 I=1,N                                                       0294
      PIVOT1 = 1.0/X(I,I)                                               0295
      X(I,I) = PIVOT1                                                   0296
      DO 10 J=1,M                                                       0297
      IF(J.EQ.I) GO TO 10                                               0298
      X(I,J) = PIVOT1*X(I,J)                                            0299
   10 CONTINUE                                                          0300
      DO 20 K=1,N                                                       0301
      IF(K.EQ.I) GO TO 20                                               0302
      PIVOT2 = X(K,I)                                                   0303
      X(K,I) = -PIVOT2*PIVOT1                                           0304
      DO 20 L=1,M                                                       0305
      IF(L.EQ.I) GO TO 20                                               0306
      X(K,L) = X(K,L)-PIVOT2*X(I,L)                                     0307
   20 CONTINUE                                                          0308
   30 CONTINUE                                                          0309
      RETURN                                                            0310
      END                                                               0311
```

APPENDIX F

GRAY SOLUTION

Equations (II-16) and (II-20) were used to calculate the total radiant heat transfer to the surfaces of the infinitely long square duct. Assuming $\epsilon_j = \alpha_j$, Equation (II-16) becomes

$$q_j = \frac{\alpha_j}{\rho_j} (J_j - E_{bj}) \quad . \tag{F-1}$$

Rewriting Equation (II-20) to indicate the functional dependence of gas transmittance and emittance on mean beam length, one obtains

$$J_j = \epsilon_j E_{bj} + \rho_j \sum_{k=1}^{M} [\tau_g(\bar{r}_{kj}) J_k + \epsilon_g(\bar{r}_{kj}) E_{bg}] F_{kj} \quad . \tag{F-2}$$

Configuration factors and geometric mean beam lengths for use in Equation (F-2) are tabulated in Tables III and IV, respectively of Chapter IV. An average value of surface reflectance was calculated from

$$\rho_j = \frac{\int_0^{\infty} \rho_{j\lambda} E_{b\lambda}(T_w)\, d\lambda}{\sigma T_w^4} \quad . \tag{F-3}$$

Monochromatic reflectance data from Figure 12 were used in Equation (F-3) and computation was performed by an electronic computer. Surface emittance was approximated by the relation

$$\epsilon_j = 1 - \rho_j \quad .$$

The results of these calculations are:

surface temperature, °R	ρ	ϵ
800	0.665	0.335
1000	0.658	0.342

From Chapter 4 of McAdams' text, by Hottel (33), values of gas emittance and absorptance were calculated. The gas emittance results are:

for opposed rectangles . . . . . $\epsilon_g = 0.135$

for adjacent rectangles . . . . . $\epsilon_g = 0.123$

The gas absorptance results are:

for $T_w = 800°R$ . . . . $\alpha_g(T_g,w,T_w) =$ 0.147 for opposed rectangles; 0.132 for adjacent rectangles

for $T_w = 1000°R$ . . $\alpha_g(T_g,w,T_g) =$ 0.123 for opposed rectangles; 0.123 for adjacent rectangles

Substituting the above values into Equation (F-2) one may find:

$$J_1 = 1444. \text{ Btu/hr - ft}^2$$

$$J_2 = 1175. \text{ Btu/hr - ft}^2$$

From Equation (F-1) the heat transfer results are found to be:

$$q_1 = -140.\ \text{Btu/hr - ft}^2$$

$$q_2 = 238.\ \text{Btu/hr - ft}^2.$$

To check the energy balance, the heat transfer from each of the surfaces to the gas may be calculated from

$$q_{j\text{-gas}} = J_j \sum_{k=1}^{M} \alpha_{gjk} F_{jk} - E_{bg} \sum_{k=1}^{M} \epsilon_{gkj} F_{kj} \quad . \qquad \text{(F-4)}$$

The results of such calculations are:

$$q_{1\text{-gas}} = -41.6\ \text{Btu/hr - ft}^2$$

$$q_{2\text{-gas}} = -56.8\ \text{Btu/hr - ft}^2$$

The sum of these two values is -98.4 Btu/hr - ft^2. This is approximately numerically equal to the sum of q_1 and q_2, 98.5 Btu/hr - ft^2, thereby indicating conservation of energy, and completing the solution.

VITA

Charles Alfred Morgan, Jr.

Candidate for the Degree of

Doctor of Philosophy

Thesis: ABSORPTION BANDWIDTHS FOR CARBON DIOXIDE GAS

Major Field: Mechanical Engineering

Biographical:

Personal Data: Born in San Antonio, Texas, January 12, 1938, the son of Charles A. and Evonne Morgan.

Education: Bachelor of Science degree in Mechanical Engineering received from Southern Methodist University in 1961; Master of Science degree in Mechanical Engineering received from Oklahoma State University in 1963; completed requirements for the Doctor of Philosophy degree in May of 1966.

Professional Organizations: Member of the American Society of Mechanical Engineers; the American Society for Engineering Education.